COMPLEMENTING UREA HYDROLYSIS AND NITRATE REDUCTION METABOLISMS TO ENHANCE MICROBIAL SELF-HEALING PERFROMANCE IN CEMENTITIOUS COMPOSITES

BİRBİRİNİ TAMAMLAYAN ÜRE HİDROLİZİ VE NİTRAT İNDİRGENMESİ METABOLİZMALARI İLE ÇİMENTOLU KOMPOZİTLERİN MİKROBİYAL YOLLARLA KENDİNİ ONARMA PERFORMANSLARININ İYİLEŞTİRİLMESİ

BETÜL ÖZBAY

ASSOC. PROF. DR. YUSUF ÇAĞATAY ERŞAN

Supervisor

Submitted to

Graduate School of Science and Engineering of Hacettepe University

as a Partial Fulfillment to the Requirements for the Award of the Degree of Master of Science in Environmental Engineering

2023

Begüm Özbay için…

ABSTRACT

COMPLEMENTING UREA HYDROLYSIS AND NITRATE REDUCTION METABOLISMS TO ENHANCE MICROBIAL SELF-HEALING PERFORMANCE IN CEMENTITIOUS COMPOSITES

Betül ÖZBAY

Master of Science, Department of Environmental Engineering

Supervisor: Assoc. Prof. Dr. Yusuf Çağatay ERŞAN

September 2023, 156 pages

Concrete is a commonly used material in construction, but it tends to crack due to many reasons. When the size and number of cracks exceed a certain threshold, they threat concrete durability and shorten its lifespan. Since recycling of the concrete components is difficult, it leads to the accumulation of concrete waste worldwide. Researchers suggesting the use of bacteria and exploitation of biomineralization to repair concrete cracks and to extend the service life of structures. This phenomenon is known as "bioconcrete."

In this study, the use of biogranules, non-axenic microbial granules capable of urease hydrolysis and nitrate reduction, is proposed for the improvement of concrete crack healing. These granules were produced in a cylindrical sequencing batch reactor (SBR) at laboratory scale. The granules were then harvested, and their resuscitation performance was tested after drying. The study showed that biogranules can be stored in a dried form and reactivated when needed. Biogranules efficiently consumed urea and NO_3-N. The study determined that biogranules had the capacity to consume 1 g/L of urea in 6 hours

and 200 mg/L of NO_3-N in 3 hours. Furthermore, the study revealed that the granule production process can be adapted to minimal nutrient conditions (Phase I) and alkaline pH conditions (Phase 2) as well as enables regular granule harvesting (Phase 3). The analyses and granule samples obtained from the reactor demonstrated its ability to adapt to these conditions effectively.

After the resuscitation and confirmation of the activity of the dried biogranules, they were added to cementitious composites. The cementitious composites were cracked in a controlled manner to obtain crack widths ranging from 100±20 μm to 600±30 μm in the samples. These cracks were observed weekly under a light microscope. By adding these biogranules to the cementitious composites, biogranules contained bacteria capable of consuming nutrients that entered the cracks with water, such as urea and nitrate, and producing calcium carbonate, which is a natural mineral that can fill and repair cracks.

This research explores the crack healing performance of biotic samples in diverse environmental conditions. Notably, crack healing thresholds reaching 90% recovery were highest in rainwater, tap water, and seawater, measuring at 156, 230, and 253 μm, respectively. Further analysis revealed varying closure percentages within specific crack width ranges, with rainwater, tap water, and seawater exhibiting distinct behaviors. Additionally, a 70 μm disparity between biotic and abiotic samples in marine water signifies the extent of microbial healing, while rainwater showed no significant advantage for both abiotic and biotic healing at higher percentages. In tap water, microbial healing was observed at 55 μm. In particular, in rainwater, microbial healing at the 80% healing threshold was approximately 70 μm. These findings shed light on the environmental factors influencing biomortar crack healing and constitute a study on the application of granular bacterial concrete.

Keywords: Biogranules, biomineralization, $CaCO_3$ precipitation, self-healing of concrete, nitrate reduction (denitrification), urea hydrolysis, SBR bioreactor.

ÖZET

BİRBİRİNİ TAMAMLAYAN ÜRE HİDROLİZİ VE NİTRAT İNDİRGENMESİ METABOLİZMALARI İLE ÇİMENTOLU KOMPOZİTLERİN MİKROBİYAL YOLLARLA KENDİNİ ONARMA PERFORMANSLARININ İYİLEŞTİRİLMESİ

Betül ÖZBAY

Yüksek Lisans, Çevre Mühendisliği Bölümü

Tez Danışmanı: Dr. Öğr. Ü. Yusuf Çağatay Erşan

Eylül 2023, 156 sayfa

Beton, inşaatta sıkça kullanılan bir malzemedir ancak birçok nedenden dolayı çatlamaktadır. Çatlakların boyutu ve sayısı belirli bir eşiği aştığında, betonun dayanıklılığı için tehdit oluşturmakta ve kullanım ömrünü kısaltmaktadır. Beton bileşenlerinin geri dönüşümü zor olduğundan, dünya genelinde beton atığı birikmesine neden olur. Bu sorunu çözmek için araştırmacılar, bakterilerin ve biyomineralizasyon sürecinin beton çatlaklarının onarımında kullanılmasını önermektedir. Bu konsept "biyobeton" olarak bilinmektedir.

Bu çalışmada, üre hidrolizi ve nitrat indirgeme yeteneğine sahip non-aksenik mikrobiyal biyogranüller, beton çatlakların kendini onarmasının daha da geliştirilmesi için önerilmiştir. Bu granüller laboratuvar ölçeğinde silindirik ardışık kesikli reaktörde (AKR) üretildi. Granüller daha sonra hasat edildi ve kurutulduktan sonra canlandırma

performansları test edildi. Çalışma, biogranüllerin kurutulmuş bir formda saklanabileceğini ve ihtiyaç duyulduğunda yeniden etkinleştirilebileceğini gösterdi. Biogranüller, üre ve NO_3-N'yi verimli bir şekilde tüketti. Çalışma, biogranüllerin 6 saatte 1 g/L üre ve 3 saatte 200 mg/L NO_3-N tüketebilecek kapasiteye sahip olduğunu belirledi. Ayrıca, çalışma reaktörün granülasyon performansını yapılan modifikasyonlar sonrasında dikkatli bir şekilde değerlendirdi ve granül üretim sürecinin minimum besin kullanımı (faz1) ve alkali pH koşullarına (Faz 2) uyum sağlayabildiği ve düzenli granül hasatına (Faz 3) imkan tanıdığı belirlendi. Reaktörden elde edilen analizler ve granül örnekleri, reaktörün bu koşullara etkili bir şekilde uyum sağlama yeteneğini gösterdi.

Kurutulmuş biogranüller, canlandırılması ve kuru formdaki aktivitelerinin onaylanmasından sonra, çimentolu kompozitlere eklenmiştir. Çimentolu kompozitler kontrollü olarak çatlatılıp örneklerde 100±20 ila 600±30 mikron aralığında çatlak genişlikleri elde edildi. Bu çatlaklar haftalık olarak bir ışık mikroskobu altında gözlemlendi. Biogranüller, çatlaklardan içeri giren su dolayısıyla çözünen besinlerle birlikte, çatlakları kapatabilen doğal bir mineral olan kalsiyum karbonat üretebilen bakteriler içeriyordu.

Bu araştırma, çeşitli çevresel koşullarda biyotik örneklerin çatlak iyileştirme performansını incelemektedir. Özellikle, çatlak iyileştirme eşiklerinin %90 iyileşmeye ulaşması, sırasıyla 156, 230 ve 253 mikron ölçülen yağmur suyunda, musluk suyunda ve deniz suyunda en yüksek olduğunu göstermektedir. Daha fazla analiz, belirli çatlak genişlik aralıklarında değişen kapanma yüzdeliklerini ortaya çıkardı, yağmur suyu, musluk suyu ve deniz suyu farklı davranışlar sergiledi. Ayrıca, deniz suyundaki biyotik ve abiyotik örnekler arasındaki 70 µm fark, mikrobiyal iyileşmenin boyutunu göstermektedir, yağmur suyu hem abiyotik hem de biyotik iyileşme açısından yüksek yüzdeliklerde önemli bir avantaj göstermedi. Musluk suyunda mikrobiyal iyileşme 55 µm gözlendi. Fakat yağmur suyunda, mikrobiyal iyileşme %80 iyileşme eşiğinde yaklaşık olarak 70 µm oldu. Bu bulgular, biomortar çatlak iyileştirmeyi etkileyen çevresel faktörleri aydınlatmaktadır ve granül içeren bakteriyel betonun uygulanmasına yönelik çalışmadır.

Anahtar Kelimeler: Biogranüller, biyomineralizasyon, $CaCO_3$ çökelmesi, betonun kendi kendini tamir etmesi, nitrat indirgeme (denitrifikasyon), üre hidrolizi, SBR biyoreaktörü

ACKNOWLEDGEMENTS

First of all, I would like to thank and express my deepest gratitude to my supervisor Assoc. Prof. Dr. Yusuf Çağatay ERŞAN for his guidance, precious advice, and endless support throughout my thesis studies. My thesis was greatly enhanced by his extensive knowledge, patience, and motivation. This master thesis was supported by The Scientific and Technological Research Council of Turkey (TUBITAK) under project number 120Y291 and by the Hacettepe University Scientific Research Projects Coordination Unit under project number 20394.

I would also like to thank the thesis committee members Prof. Dr. Selim SANİN, Prof. Dr. Okan Tarık KOMESLİ, Assoc. Prof. Dr. İlknur Durukan TEMUGE and Assist. Prof. Dr. Cihan ÇİFTÇİ for their valuable contributions.

I would like to thank Beyza KARDOĞAN for her assistance in my laboratory studies and Merve SÖNMEZ for her help in preparing my cementitious composite samples in the Department of Civil Engineering. Additionally, I would like to express my gratitude to Rabia KONAKCI for her friendship and positivity.

Additionally, I would like to express my gratitude to Assoc. Prof. Dr. Orkun ERSOY, who generously opened his microscopy lab during my research, as well as to my professors in the Geological Engineering Mineralogy-Petrography Department. Also, I have to give thanks to Prof. Dr. Mustafa ŞAHMARAN for giving me the opportunity to work in his laboratory in the Department of Civil Engineering.

I want to extend my heartfelt gratitude and deepest appreciation to my family; Nihal ÖZBAY, Murat ÖZBAY, and my lovely sister Begüm ÖZBAY for their unwavering support, encouragement, and love throughout my life. Having this wonderful family has been a source of strength and motivation for me in my studies. Finally, I owe a special thanks to my dear sister Begüm. I am grateful for your endless love and for being there for me at every moment. Your presence means everything to me. Thank you for always being by my side.

CONTENTS

LIST OF FIGURES

LİST OF TABLES

ABBREVIATIONS

ACDC	Activated Compact Denitrifying Core
BNMP	Bentonite Nano/micro-Particles
$CaCO_3$	Calcium Carbonate
$CaSO_4$	Calcium Sulfate
CO_3^{2-}	Carbonate
CCS	Cemented Coral Sand
CERUP	Cyclic Enriched Ureolitic Powder
COD	Chemical Oxygen Demand
EPS	Extracellular Polymeric Substances
HCO_3^-	Bicarbonate
INMP	Iron oxide Nano/micro-Particles
FT	Frezzing Temperature
LWA	Light Weight Aggregate
MICP	Microbially- Induced Calcium Carbonate Precipitation
OPC	Portland Cement
SBR	Sequencing Batch Reactor
SVI	Sludge Volume Index
TSS	Total Suspended Solid
VSS	Volatile Suspended solid

1. INTRODUCTION

Cracks in cement-based composites are significant factors affecting the strength and durability of these materials. Macro-cracks are visible to the naked eye and can occur due to several reasons such as shrinkage, thermal stresses, and mechanical loading. On the other hand, micro-cracks are not visible to the naked eye and are typically caused by the development of tensile stresses within the material. Both macro-cracks and micro-cracks can facilitate liquid and gas penetration to the concrete matrix, leading to various durability problems such as reinforcement corrosion due to chloride penetration and carbonation, sulfate attack, alkali-silica reaction, and freeze-thaw damage [1], [2]. Cracks wider than 0.1 mm can be controlled and eliminated by incorporating proper design and placement of steel reinforcement or by utilizing known repair methods such as epoxy injection. However, cracks that are smaller than 0.1 mm, referred to as microcracks, are more challenging to detect and control[3].

Conventional crack repair methods in cementitious composites often involve the use of synthetic agents such as epoxy, resin, and polymers[4]. However, these methods can have negative environmental and health impacts, as well as being costly and providing only temporary solutions to the underlying durability issues. Alternative and more sustainable approaches are being researched, including self-sensing, self-healing concrete, and bio-based repair materials[5]. One such innovative method is microbial self-healing concrete developed by Jonkers (2007) using bacteria capable of producing calcium carbonate ($CaCO_3$)[6]. When cracks occur, the bacteria are activated and produce $CaCO_3$, effectively filling in the cracks and healing the concrete. Bacteria based healing process relies on a ubiquitous natural phenomenon so called microbial-induced calcium carbonate precipitation (MICP). This biomineralization based crack healing process showed promising results in terms of functionality regain [7]–[11].

Previous studies have shown that $CaCO_3$ precipitation can occur through the activities of several types of microorganisms, including ureolytic bacteria, nitrate-reducing bacteria, sulfate-reducing bacteria[12] and aerobic heterotrophs[7], [9], [10], [13]. Among these, urea hydrolysis is the most commonly used metabolic pathway in so far conducted MICP studies[14]. Researchers prefer urea hydrolysis as the preferred method for $CaCO_3$ precipitation due to its straightforward and easily controllable process [15] .Urea hydrolysis is characterized by its simple hydrolysis mechanism and the high yield of $CaCO_3$[15], [16]. It offers exceptional benefits, including a rapid reaction speed and the potential for up to 90% chemical conversion efficiency of precipitated $CaCO_3$ in less than 24 hours[16]. While urea hydrolysis offers several advantages, it also comes with significant drawbacks. Factors such as pH, initial cell number, oxygen concentration, and cell damage can all influence urease activity performance and need to be optimized for successful MICP[12], [17]. Additionally, from an environmental perspective, urea hydrolysis's production of toxic ammonia as a by-product raises concerns about its ecological impact[13], [17].

In order to overcome certain drawbacks of ureolytic based MICP, researchers also focused on the use of nitrate-reducing bacteria as an alternative to ureolytic bacteria in the MICP process. Nitrate-reducing bacteria can function under anoxic conditions, thus eliminates the dependence on oxygen that ureolytic bacteria strictly require for growth and urease production. Denitrification's compatibility with oxygen-deficient environments and its minimal nutrient requirements, as demonstrated in research by Ersan et al.[18], further enhance its attractiveness for MICP applications. Moreover, denitrification exhibits superior thermodynamic properties compared to other metabolic pathways [19], [20]. Denitrification process also has the ability to generate its own alkalinity, eliminating the need for external alkaline sources [21], and produces non-toxic, chemically inert byproducts, in contrast to other pathways that may pose environmental and health risks due to the production of gases like ammonia and hydrogen sulfide [21], [22]. The adoption of nitrate-reducing bacteria and denitrification metabolism offers a sustainable and promising alternative for MICP applications in various in situ scenarios, including soil consolidation and projects related to concrete [23]. One advantage lies in the abundance of denitrifying bacteria in subterranean environments, allowing for the

utilization of indigenous denitrifying populations without the need for introducing external microbial cultures[20], [24] .Additionally, the use of nitrate-reducing bacteria in the MICP process can also have the additional function of inhibiting rebar corrosion. The use of denitrifying cultures in self-healing concrete, as demonstrated by Ersan et al.[25], provides a notable advantage by preventing steel rebar corrosion during the natural crack-healing process. This benefit arises from the production of NO_2^-, a well-known corrosion inhibitor, as a metabolic byproduct during MICP through denitrification within the concrete [25].

Denitrification-based MICP has shown promise but faces substantial challenges in scaling up for practical applications[23]. One significant disadvantage is the potential generation of harmful intermediates during incomplete microbial nitrate reduction, including nitrite, nitric oxide, and nitrous oxide[20]. Additionally, in applications like soil improvement, issues related to gas bubble retention may arise, affecting the degree of saturation and potentially leading to cracks, especially in shallow-depth conditions[26], [27]. Furthermore, MICP through denitrification exhibits a slower $CaCO_3$ precipitation rate compared to ureolysis-based MICP. While ureolysis can produce 6% $CaCO_3$ (w/w) in a few days[28], [29], denitrification-based MICP typically generates only 1–3% $CaCO_3$ (w/w) within weeks to months[20], [27], [30]. Slower precipitation rates, although seemingly a drawback, help maintain microbial activity without occluding microbial cells with precipitated $CaCO_3$ crystals, potentially making it advantageous over ureolysis in the long term[23].Recent studies have shown that using MICP through denitrification can heal cracks by causing $CaCO_3$ to precipitate within them[7], [25], [31]–[33].

Numerous bacterial strains possess the capacity to hydrolyze urea, with bacterial strains closely related to *Bacillus sphaericus* exhibiting notably high urease activity, thereby enabling more extensive $CaCO_3$ precipitation [34]. However, the axenic (pure) cultures of ureolytic bacteria production comes at a considerable cost, rendering it impractical for the concrete industry [35]. Consequently, the cultivation of non-axenic (mixed) cultures of ureolytic bacteria emerges as a viable alternative. Surprisingly, non-axenic cultures have demonstrated comparable ureolytic activity and $CaCO_3$ precipitation capabilities to those exhibited by the axenic culture of *B. sphaericus* spores, which is often used as the

benchmark. Moreover, non-axenic cultures offer distinct advantages, such as cost-effectiveness, ease of cultivation, and the potential for enhanced robustness in complex environments, making them a promising solution for various practical applications in industries like construction[36].

After considering both the advantages and disadvantages of urea hydrolysis and denitrification, it is clear that there is a critical need for their improvement or alternative utilization. Furthermore, the adoption of non-axenic cultures serves to enhance the MICP process and promote self-healing in cracks.

1.1.Aim and Scope

This research study aimed at developing microbial self-healing concrete using a non-axenic granular community that is capable of both urea hydrolysis and nitrate reduction. Previous research has shown that these two pathways can be useful individually for crack healing. However, combining these two pathways in a single non-axenic granular culture can further enhance the effectiveness of crack healing. By incorporating biogranules into the concrete mix, it is expected that the cementitious composites will be able to heal themselves when cracks occur, leading to increased durability and reduced maintenance costs over time. The study can be broadly divided into three main phases. Firstly, desired biogranules were produced with analyzing and controlling the activities under laboratory conditions. The second phase of the study involved the incorporation of the obtained biogranules into cementitious composites to develop microbial self-healing mortar. Then the crack healing performance of the samples were evaluated. The latter initially required the casting of concrete samples and the induction of controlled cracking to simulate the types of cracks that could commonly occur in concrete structures. Finally, in the third phase, the self-healing concrete samples were subjected to three different aquatic environments to assess their ability to heal cracks under different exposures. Ultimately, obtained crack healing performances in various aquatic environments were compared among each other.

2. LITERATURE REVIEW

2.1.Environmental Impact of Concrete Production and Maintenance

Concrete is the most widely used construction material globally and plays a significant role in building infrastructure, including roads, bridges, and buildings [37], [38].With an estimated annual production of approximately 6 million cubic meters worldwide [39], concrete's environmental impact needs attention to ensure sustainability in the construction industry.

Despite its high compressive strength, concrete is weak in tension and prone to cracking due to loads and various environmental factors such as chemical attacks and freeze-thaw cycles. Cracks exceeding critical thresholds can increase permeability which allows moisture and aggressive substances, such as chloride ions, sulfate ions, and acids, to penetrate into and further cause corrosion of the reinforcement, degradation of the concrete matrix and decline of load bearing capacity [40]. This increased permeability related issues reduce the durability and service life of concrete structures [37], [40]. Hence, minimizing and preventing cracking in concrete is vital for its long-term durability and increasing the sustainability of concrete structures.

Cracks in concrete structures, while often micron (μm) scale and not immediately cause collapse, can still have a negative impact on the structural health, the service life, and the sustainability of structures. When cracks widen, they create pathways for water, moisture, and air to penetrate into the concrete and change the chemical or physical state of the surroundings. This can further lead to the corrosion of the reinforcement, degradation of the matrix which weakens the overall structure [38]. As a result, service life of the structures can significantly decrease which arise a need for renovation, restoration or rebuilding of the structure and related additional environmental burden.

Concrete production has significant direct and indirect environmental impacts. Direct impacts result from the production process itself, such as the release of greenhouse gases

like carbon dioxide (CO_2) during cement manufacturing. As a composite material, concrete is typically made by combining aggregates (such as sand and gravel) with cement, water, and optional additives[41]. The production of cement requires a large amount of energy, primarily for the calcination process and the heating of the kiln. Unfortunately, this energy-intensive cement production process, primarily from burning fossil fuels like coal or natural gas, releases substantial amounts of CO_2 into the atmosphere. One metric ton of cement production can emit anywhere from 0.73 to 0.99 metric tons of CO_2 [42], contributing to approximately 8% of the global emissions, as estimated by the International Energy Agency (IEA). Reducing the carbon footprint of cement production is essential to address climate change and foster sustainability.

Furthermore, cement production can release other greenhouse gases like NOx and SOx [43], [44], contributing to the greenhouse effect and acid rain, which harm the ecosystems. The process also generates particulate matter and noise pollution, adversely affecting air quality and human health. Dust emissions during cement manufacturing, including PM10 and PM2.5, can arise from extracting, crushing, grinding raw materials, as well as loading and transporting cement [44]. Indirect impacts on the environment include land use changes leading to the loss of vegetation and wildlife habitats, along with environmental consequences resulting from construction and demolition waste generated during the lifecycle of concrete structures. In repair work and for the improvement of the durability of concrete structures, various chemicals can be used. Traditional methods using synthetic agents like epoxy, resin, polymers, and repair mortars are not considered sustainable anymore [45]–[47]. Moreover, this approach only offers a short-term solution due to the low compatibility of the used repair agents with the concrete matrix, and thus in the long term the utilization of extra chemicals results in increased pollution and higher treatment expenses[46].

2.2.Microbial-Induced Calcium Carbonate Precipitation (MICP)

The concept of self-healing materials, initially focused on polymers, gained significant attention and interest among researchers in various fields following the publication of the article by White et al. in 2001[25]. Since then, there has been an increasing focus on

developing self-healing materials, including self-healing concrete using MICP phenomenon[35].

Concrete healing processes can be categorized into two types: autogenous healing and autonomous healing. Autogenous healing is an inherently occurring physical or chemical process that can occur in concrete cracks, particularly in early age cracks. It involves the hydration of non-reacted cement particles within the concrete matrix, where moisture penetrates into the cracks and reacts with the unhydrated cement particles to form additional calcium silicate hydrate (C-S-H) gel that fills the cracks[48], [49]. Another chemical reaction leading to autogenous healing is the $CaCO_3$ formation due to the reaction between the $Ca(OH)_2$ in the crack zone and the dissolved CO_2 in water or moisture. In commonly used ordinary portland cement (OPC) concrete, small cracks, typically up to 0.2 mm wide, can be healed through chemical autogenous healing[50], [51]. Other physical mechanisms such as swelling of the crack walls and accumulation of fine particles inside the crack can also provide autogenous healing at some extent [52], [53], [54]. Conventional crack repair methods in cementitious composites often involves the use of synthetic repair agents like epoxy, resin, polymers, and repair mortars. However, these agents offer only temporary solutions, and their application introduces additional chemicals, leading to increased pollution and treatment costs. Moreover, chemical injection can seal the cracks, but it often entails labor-intensive work and can disrupt regular services, indirectly imposing an economic burden. The materials used in these methods may not always be compatible with the concrete matrix and may not be suitable for repairing cracks below a certain size. As a result, in some cases, when conventional repair methods are applied to fix cracks, they may inadvertently lead to hidden damage. These issues represent the primary challenges associated with conventional repair methods[53] .

Another approach for concrete self-healing is chemical autonomous self-healing, which involves the use of various chemical agents and compounds to repair cracks. Microcapsules are a common type of chemical self-healing method used in concrete. These microcapsules are typically filled with healing agents, such as polyurethane or epoxy resins, and are embedded in the concrete mix during production. When the concrete

experiences a crack, the microcapsules break and release the healing agent into the crack. The healing agent then reacts with the environment, such as air or moisture, and forms a solid material that fills the crack and restores the structural integrity of the concrete[54], [55].

Bio concrete also known as bacterial concrete, however, has the potential to solve this problem by providing a continuous self-healing mechanism that can repair cracks as soon as they form, preventing further damage to the structure[56].

Self-healing in bio concrete mainly relies on MICP. Bacteria specifically selected for MICP are introduced into the concrete mix as healing agents. The CO_2 produced by bacteria turns into carbonate (CO_3^{2-}) and bicarbonate ions (HCO_3^-), in the presence of alkalinity and in Ca-rich environments this further leads to the formation of $CaCO_3$, which precipitates and forms solid mineral deposits. This overall process can effectively seal the concrete cracks. Studies have demonstrated the successful repair of concrete cracks using MICP in bio concrete, with the self-healing capacity extending to crack widths of up to 300-500 µm on average [7], [8], [10], [11], [56], [57], and even up to 970 µm depending on the microbial agent used [58].

During the casting of concrete, bacterial spores, nutrients, and mineralization precursors are added to the mixture. These spores remain dormant until cracks form, and their activation is triggered by the presence of moisture and/or oxygen[59]. Bacterial metabolic processes then cause the precipitation of $CaCO_3$, effectively sealing the cracks in the concrete. Refer to Figure 2.1 for a visual representation of this process[53].

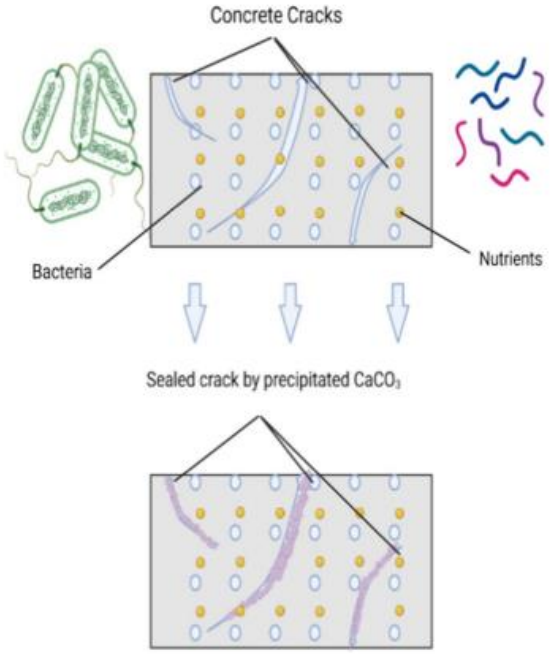

Figure 2.1 $CaCO_3$-producing bacteria and nutrients in the concrete mix assist in repairing the microcracks [55].

2.2.1. Microbial Metabolisms Used in Self-Healing Concrete

Calcium carbonate ($CaCO_3$) can be formed through a process known as biologically induced mineralization, which occurs when there is a source of calcium ion present in the environment. This process of calcification and biomineralization involving $CaCO_3$ can occur through two major types: autotrophic and heterotrophic $CaCO_3$ precipitation [47], [60], [61].

Microorganisms play a crucial role in this process by producing CO_3^{2-} extracellularly through various metabolic pathways. These pathways allow microorganisms to generate CO_3^{2-} outside of their cells. Examples of these metabolic pathways include non-methylotrophic methanogenesis, oxygenic and anoxygenic photosynthesis, utilization of organic acids, reduction of calcium sulfate ($CaSO_4$), urea hydrolysis, and dissimilatory nitrate reduction [62]. Fig. 2.2 provides a visual representation of the different methods utilized for biomineralization [47].

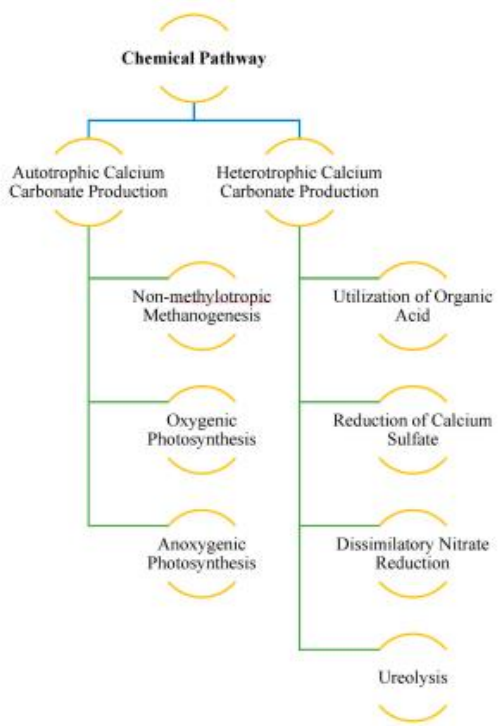

Figure 2.2 Pathways of $CaCO_3$ precipitation [47].

Autotrophic organisms are capable of producing their own organic compounds from inorganic carbon sources such as CO_2, using either light or chemical energy. Non-methylotrophic methanogenesis[63], oxygenic photosynthesis, and anoxygenic photosynthesis [51], [64] are all examples of autotrophic pathways that can lead to the production of $CaCO_3$[47]. In non-methylotrophic methanogenesis, certain types of bacteria use CO_2 and hydrogen gas as a source of carbon and energy, respectively. The process results in the production of methane gas and water, with some of the CO_2 reacting with calcium ions to form $CaCO_3$. Oxygenic photosynthesis is another autotrophic pathway that can lead to the production of $CaCO_3$. During oxygenic photosynthesis, cyanobacteria[65] use light energy to convert CO_2 and water into organic compounds. Some of these organic compounds, particularly those containing HCO_3^-, can react with calcium ions to form $CaCO_3$. Anoxygenic photosynthesis, employed by certain bacteria, is a less common form of photosynthesis that does not produce oxygen. Similar to oxygenic photosynthesis, anoxygenic photosynthesis can also lead to $CaCO_3$ formation, as some of the organic compounds produced can react with calcium ions to generate the mineral[47].

Regarding $CaCO_3$ production, heterotrophic pathways can also lead to the production of $CaCO_3$. For example, some bacteria can use organic acids, such as citric acid, as a carbon source and produce $CaCO_3$ as a byproduct. Reduction of $CaSO_4$ [66]–[68] is another process that can lead to the formation of $CaCO_3$ by heterotrophic organisms. In this process, bacteria reduce $CaSO_4$ to hydrogen sulfide, which reacts with CO_2 to form $CaCO_3$. Finally, dissimilatory nitrate reduction[69], [70] is a process employed by some bacteria to derive energy by reducing nitrate to nitrogen gas. During this process, bacteria can generate alkalinity and carbonate ions (CO_3^{2-}), which induces the precipitation of $CaCO_3$ in a calcium rich environment. It's important to note that various bacteria can be involved in $CaCO_3$ precipitation, and the specific reactions and mechanisms can vary depending on the bacterial species and environmental conditions. Table 2.1 presents commonly known MICP pathways.

Table 2.1 $CaCO_3$ precipitation processes, reactions, and the bacteria involved.

Bacterial Activity	**Mechanism and process**	**Bacteria**
Non-methylotrophic methanogenesis	$CO_2 + 4H_2 \rightarrow CH_4 + 2H_2O$ $CH_4 + SO^{2-} \rightarrow HCO^{-} + HS^{-} + HO$ $Ca^{2+} + 2HCO^{-} \leftrightarrow CaCO_3 + CO_2 + H_2O$	*Methanobacterium species* [71]
Oxygen Photosynthesis	$CO_2 + H_2O \rightarrow CH_2O + O_2$ $2HCO_3^{-} \leftrightarrow CO_2 + CO_3^{2-} + H_2O$ $CO_3^{2-} + H_2O \rightarrow HCO_3^{-} + OH^{-}$	*Synechococcus Bacterium species*[65], [72]
Anoxygenic Photosynthesis	$CO_2 + 2H_2S + H_2O \rightarrow CH_2O + 2S + 2H_2O$ $2HCO_3^{-} \leftrightarrow CO_2 + CO_3^{2-} + H_2O$ $CO_3^{2-} + H_2O \rightarrow HCO_3^{-} + OH^{-}$	*Halobacterium* and *the Heliobacterium cyanobacteria species*[65]

Bacterial Activity	**Mechanism and process**	**Bacteria**
Utilization of organic acid	$CH_3COO^- + 2O_2 \rightarrow 2CO_2 + H_2O + OH^-$ $2CO_2 + OH^- \rightarrow CO_2 + HCO^-$ $Ca^{2+} + 2HCO_3^- \leftrightarrow CaCO_3 + CO_2 + H_2O$	*Anthrobacter species*[73], [74], *Rhodococcus species*[73], [74]and *Bacillus species*[73]
Reduction of $CaSO_4$	$CaSO_4 + 2(CH_2O) \rightarrow CaS + 2CO_2 + 2H_2O$ $CaS + 2H_2O \rightarrow Ca(OH)_2 + H_2S$ $CO_2 + H_2O \rightarrow H_2CO_3$ $Ca(OH)_2 + H_2CO_3 \rightarrow CaCO_3 + 2H_2O$	*Desulfovibrio*[75], [76],*Desulfobulbus,* [76]*Desulfobacter species*[76]
Ureolysis	$NH_2COOH + H_2O \rightarrow NH_3 + H_2CO_3$ $2NH_3 + 2H_2O \rightarrow 2NH^+ + 2OH^-$ $2OH^- + H_2CO_3 \rightarrow CO^{2-} + 2H_2O$ $Ca^{2+} + Cell \rightarrow Cell\text{-}Ca^{2+}$ $Cell\text{-}Ca^{2+} + CO^{2-} \rightarrow Cell\text{-}CaCO_3$	*Sporosarcina pasteurii*[77] *Bacillus sphaericus*[78]*Bacillus cereus*[79] *Bacillus subtilis*[80] *Bacillus megaterium* [81], [82]
Nitrate reduction	$NO_3^- + H^+ \rightarrow$ complete reduction $\rightarrow CO_2 + H_2O + N_2$ $CO_2 + 2OH^- \rightarrow CO_3^{2-} + H_2O$ $Ca^{2+} + CO^{2-} \leftrightarrow CaCO_3$	*Denitobacilus, Thiobacilus, Alcaligenes, Pseudomonas, Spirilium, Achromobacteri,* and

		Micrococcus species[74]. *Diaphorobacter nitroreducens* [83]

2.2.2. Bacteria's Involvement in MICP

The success of MICP in concrete depends on the type and concentration of bacteria used, as well as the availability of nutrients in the culture media. The culture media should contain nitrogen sources, such as urea, ammonium, or nitrate, to support bacterial growth and metabolic activity. Calcium sources, such as calcium chloride ($CaCl_2$) or calcium nitrate ($Ca(NO_3)_2$), are also added to the culture media to promote the formation of $CaCO_3$[84]. The selection of bacterial strains and nutrient sources is crucial for optimizing the rate and efficiency of MICP. The concentration of nutrients in the culture media should also be optimized to support bacterial growth and activity.

Concrete is a highly alkaline, with a pH ranging from 12 to 14, which can be harmful to many microorganisms[9], [83], [85]. However, the bacteria used for MICP in concrete are specially selected for their ability to withstand the alkaline environment. They are expected to be resilient and dormant at highly alkaline pH conditions and activate when the pH drops below 10.5 in the crack environment [86].

The behavior of bacteria in mortar and their crack healing process can be explained as follows; once a crack occurs, water can enter into the crack and dissolve the nutrients as well as decreasing the local pH. Increasing nutrient availability and the pH drop activate the bacterial spores. The activated bacteria conduct their metabolic activities which induces the precipitation of $CaCO_3$. Accumulation of the $CaCO_3$ minerals in the crack seals/heals the crack. Once the cracks are filled, the bacteria may enter a dormant or "stagnant" state until another crack forms [87], [88]. This is because the bacteria require a source of nutrients and moisture to remain active, and these resources are not available once the cracks have been filled.

Bacteria can be classified based on several characteristics, including their shape, which can be categorized as spherical (cocci), rod-shaped (bacilli), or spiral-shaped (spirilla), as well as their gram stain reaction and oxygen requirements[48]. Gram-positive and gram-negative bacteria are classified based on their cell wall structure; Gram-positive bacteria have a thick layer of peptidoglycan in their cell wall. In contrast, gram-negative bacteria have a thinner layer of peptidoglycan and an outer membrane composed of lipopolysaccharides[53]. Some of the Bacillus species are alkaliphilic and non-pathogenic, which makes them a safe and effective option for concrete production. They are also able to grow at moderate temperatures and can remain dormant for extended periods under extreme conditions. Various strains of Bacillus genus, including *Bacillus megaterium, Bacillus Mucilaginous, Bacillus Halodurans, Bacillus subtilis, Bacillus Licheniformis, Bacillus Cohnii, Bacillus Sphaericus, Bacillus Pseudofirmus, Bacillus cereus*, and *Bacillus Pasteurii*, have been successfully used in concrete production. Different bacterial dosages ranging from 10^3 to 10^9 CFU/ml have been tested, and a dosage of more than 10^5 CFU/ml was found to be suitable for improving the physical and mechanical properties of concrete through biomineralization[9], [88]–[90].

2.2.3. Recorded MICP Activities in Literature

Understanding the role of oxygen in the process is crucial for determining the optimal conditions for efficient and reliable MICP in practical applications, such as strengthening and repairing concrete structures in the construction industry. Researchers have designed experiments with varying oxygen levels, ranging from aerobic to anaerobic conditions, to observe the response of microorganisms and the efficiency of the MICP process under different oxygen availabilities. In the literature, experiments comparing the behavior of *S. pasteurii* bacteria with other microbial communities under various environmental conditions have been commonly conducted. However, these studies have reported various observations and interpretations regarding the impact of anoxic conditions on the ureolytic activity of *S. pasteurii.*

For instance, Mortensen et al. (2011) [91] and Tobler et al. (2012) [92] observed significant ureolytic activity in *S. pasteurii* under anoxic conditions, suggesting that the absence of oxygen does not inhibit the activity of urease. These findings indicate that

ureolytic activity can still occur effectively even in the absence of oxygen. On the other hand, Martin et al. (2012) [93] reported limited cell growth and poor ureolysis in *S. pasteurii* under anoxic conditions. They proposed that the observed ureolytic activity was primarily attributed to the urease enzyme already present in the cells, rather than active de novo synthesis of urease under anoxic conditions.

In a selected study [94], the kinetics of urea hydrolysis (ureolysis) and induced $CaCO_3$ precipitation were investigated for *S. pasteurii* and *Bacillus sphaericus* 21776 and 21787 strains. The study compared the rate constants for ureolysis (k_{urea}) and $CaCO_3$ precipitation (k_{prepic}) among the different bacterial strains. *Bacillus sphaericus* strains 21776 and 21787 exhibited slightly higher rate coefficients for ureolysis (k_{urea} = 0.10 ± 0.03 h^{-1}) and $CaCO_3$ precipitation (k_{prepic} = 0.60 ± 0.34 h^{-1}) compared to *S. pasteurii* (k_{urea} = 0.07 ± 0.02 h^{-1}, k_{prepic}= 0.25 ± 0.02 h^{-1}).The kinetics of ureolysis and $CaCO_3$ precipitation with *S. pasteurii* were also analyzed under anaerobic conditions in the study. The results showed that the rate constant for $CaCO_3$ precipitation (k_{prepic}) under anaerobic conditions (0.25 h^{-1}) was comparable to that observed under aerobic conditions (0.19 h^{-1}). These findings suggest that, in the short term, anaerobic conditions did not significantly affect urea hydrolysis. However, further research is needed to investigate the long-term effects and sustainability of both ureolysis and $CaCO_3$ precipitation in anaerobic environments.

In another study [95] , researchers explored the use of facultative and anaerobic haloalkaliphilic bacteria as an alternative to *S. pasteurii* in MICP. The researchers enriched and identified microbial communities capable of ureolysis, with dominant populations of *Sporosarcina*- and *Clostridium*-like organisms. The obligate anaerobic communities exhibited the highest cell-specific urea hydrolysis rates, ranging from 3.05 $\times 10^{10}$ to 2.40 $\times 10^{11}$ moles of urea hydrolyzed per cell per hour. The urea hydrolysis rates for *S. pasteurii* and the facultative enrichment cultures were similar, ranging from 1.05 $\times 10^{10}$ to 1.95$\times 10^{10}$ moles of urea hydrolyzed per cell per hour. This study highlights the potential of obligate anaerobic enrichment communities for achieving high urea hydrolysis rates, suggesting their suitability for efficient biomineralization processes. Additionally, the study demonstrates that ureolysis can occur across a wide

range of NaCl concentrations (0 to 100 g/L) and at high pH values up to 11, indicating the potential of ureolytic haloalkaliphilic organisms to thrive in challenging environments such as anoxic, high-pH, and high-salinity conditions found in deep saline aquifers.

Furthermore, one different study [96] focused on the impact of oxygen availability on MICP, specifically investigating the growth rate of *S. pasteurii*, urease enzyme activities, and $CaCO_3$ precipitation. The researchers compared three environments: aerobic, anoxic, and anaerobic. In aerobic conditions, appropriate aeration was provided, while in anoxic conditions, dissolved oxygen was present, and in anaerobic conditions, oxygen was completely removed using a reducing agent called sodium thioglycolate. After 72 hours, the mass of precipitated carbonate minerals was measured. The results showed that in aerobic conditions, 32.24 ± 3 mg of $CaCO_3$ were precipitated, while in anoxic conditions, the amount decreased to 17.38 ± 3 mg. In anaerobic conditions, the amount further decreased to 7 ± 2 mg, with negligible biomineral precipitation.

In related another study [13], three bacterial strains (*Bacillus sphaericus* LMG, *Ralstonia eutropha* H16, and *Diaphorobacter nitroreducens* M5) were investigated. LMG and H16 strains exhibited rapid urea hydrolysis under anaerobic conditions, while no urea reduction was observed in the M5 strain. Observations revealed that both the LMG and H16 strains hydrolyzed nearly all the urea within the first 8 hours of the experiment under anaerobic conditions. Subsequently, no further hydrolysis occurred. The presence of additional urea in the culture medium slowed down the rate of nitrate reduction, taking 7 days to achieve complete decomposition of NO_3^-. Elevated Ca^{2+} ion concentration in the media significantly restricted H16 strain's nitrate reduction capability. Optimization of metabolic pathways improved $CaCO_3$ precipitation yield by 20 to 30%, with the highest total yield achieved at 14 g/L in an orthogonal experiment.

Overall, understanding the influence of oxygen availability on MICP is crucial for tailoring the process to specific environmental conditions and achieving efficient and reliable concrete repair and strengthening. Further research is needed to explore the potential of different bacterial strains and optimize the biomineralization process for practical applications in the construction industry.

2.3. Bacteria Protection Methods and Protective Carriers

The mixing process and mechanical forces can harm the bacteria[97], and direct addition of bacteria to concrete can cause their destruction due to cement hydration[58] and the reduction of pore diameter in concrete. Bacteria added directly to concrete remains viable for up to 4 months, but their number decreases rapidly within 22 days, and none are alive after 135 days[61].

Most researchers believe that the continuous hydration of concrete causes the colloidal pores to gradually shrink, leading to the destruction of bacterial cells or spores during the cement hydration stage[10], [36], [58], [61]. Hence, it is generally accepted that adding bacteria to concrete requires a carrier with a "shell or carrier" function to protect the bacteria.

There are several methods of incorporating bacteria into the concrete mixture, including direct incorporation, encapsulation, and spraying or direct injection[47]. The Figure 2.3 illustrates the methods of incorporating bacteria into concrete. Direct incorporation involves mixing the bacteria into the concrete mixture, while encapsulation protects the bacteria from the high pH levels of the concrete. Spraying or direct injection involves applying a solution of bacteria to the surface of the concrete or directly into the cracks. In all cases, the bacteria produce $CaCO_3$, which fills cracks and voids in the concrete and strengthens the material.

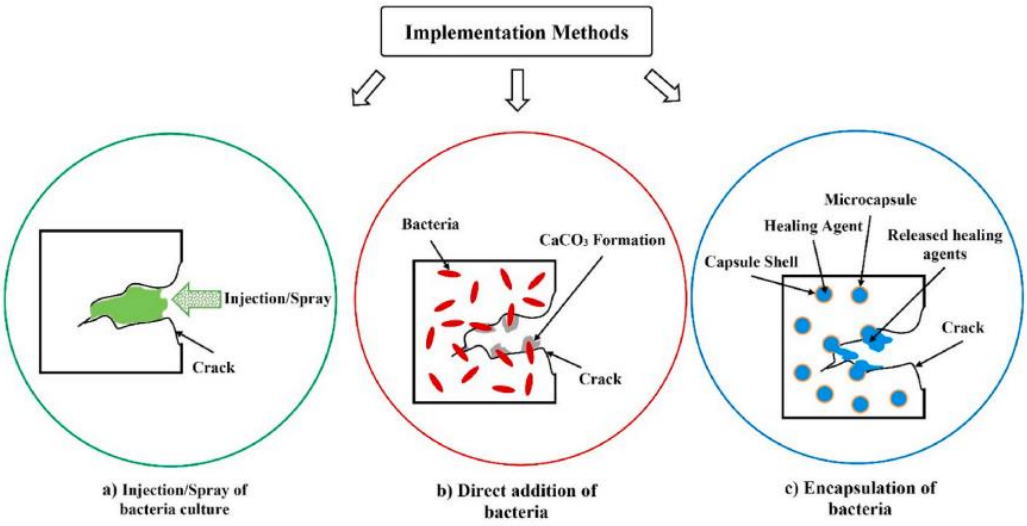

Figure 2.3 Incorporating bacteria into the concrete mixture[47]

Different types of carriers are used to add bacteria to concrete, including nano and micro particles like nano iron oxide, diatomaceous earth [98]–[100], expanded clay[101], [86], [102] coarse and lightweight aggregate[103], [104], and various alternative carriers[105]. These carriers help protect the bacteria and provide a suitable environment for their growth and activity within the concrete matrix.

2.3.1. Effect of Protection Strategies on Microbial Activity, Resuscitation Performance and Concrete Properties

The application of protection strategies in self-healing concrete can have significant effects on microbial activity and resuscitation performance, which can ultimately impact the effectiveness of the self-healing process. The viability of microorganisms in cementitious materials is highly dependent on the internal and external environmental factors of concrete, including temperature, pressure, salinity, oxygen availability, and pH[106].

The" temperature" is a critical factor that affects bacterial growth and viability, as most bacteria have an optimum temperature range for growth. Most bacteria will die outside their optimal temperature range, except for spore-forming bacteria. Studies have shown that the growth of *Bacillus sphaericus* LMG 22257 was slow at low temperatures (10°C), and spore activation occurred after six days[107]. Similarly, the highest growth of *Sporosarcina saprophyticus* and *Sporosarcina pasteurii* was observed at 30°C, and 30-

40% dosage of $CaCO_3$ was formed at the optimal temperature of 50°C[108].Therefore, the appropriate selection of bacteria should consider their growth and metabolism with respect to temperature to ensure optimal self-healing performance in concrete.

“Salinity” is another significant factor that can affect the inherent metabolism of bacteria. Studies have shown that an increase in salinity inhibits the production of $CaCO_3$ and self-healing ability due to the increase in ionic strength[109]. Therefore, it is essential to evaluate the bacterial metabolism under different environmental factors, such as salinity, before applying them as a self-healing agent in cementitious materials. For instance, the growth and biological $CaCO_3$ precipitation metabolism of *Sporosarcina pasteurii* were observed to be equally effective in soil-type environments and seawater. However, the growth and biological $CaCO_3$ precipitation metabolism of *Sporosarcina pasteurii* were observed to be the same from a soil-type environment to seawater[110]. Therefore, it is necessary to characterize the bacterial metabolism based on environmental factors before applying bacteria to cementitious materials as a self-healing agent.

“Bacterial types” can be classified based on their oxygen demand for growth and that the oxygen availability can vary depending on the location of the concrete structure, which can affect bacterial viability and metabolic performance[8]. Ureolysis, the process by which ureolytic bacteria precipitate $CaCO_3$, is a well-studied self-healing mechanism. However, it can be difficult to apply ureolytic bacteria to underwater structures due to the difficulty of supplying sufficient oxygen in an aquatic environment. The passage suggests that denitrifying bacteria, which use nitrate to produce carbonate ion in an anaerobic condition, may be more useful than ureolytic bacteria for self-healing in underwater or marine concrete structures[111].

The internal environmental factors of concrete, such as "changes in pressure and “pH levels” during curing, can impact the viability and metabolic activities of bacteria that are essential for self-healing properties[112]. During the curing process, these factors have the potential to break down microbial cells, destroy endospores, and weaken concrete structures. The high temperature and pH levels occurring during cement hydration can also reduce viability of vegetative cells and inhibit microbial activity. Therefore, some

studies strongly suggest the use of spore-forming alkaliphilic bacteria for reliable long-term self-healing properties [61]. Some other studies showed that vegetative cells can also be used for healing of early age cracks [113]. Degradation of the nutrients incorporated into concrete mixtures due to the high temperatures occurring during hydration was reported to be another issue which resulted in a lack of essential nutrients for bacterial viability and self-healing performance[112], [114]. Additionally, direct mixing of nutrients together with the spores might cause reactivation of some spores and decrease in the number of viable cells. Therefore, most of the studies suggest encapsulation of either nutrients or the bacteria or separate encapsulation of both depending on their properties and resilience [86] .

It is preferable to protect the microorganisms by encapsulating or immobilizing them in a carrier material before adding them to cementitious materials[8]. In the study by Wang et al. (2014)[115], "bio-hydrogels" were proposed as protective agents to protect bacterial spores. By using urea hydrolysis as a metabolic pathway and bio-hydrogel as a bacterial carrier agent, it was reported that a crack width of 500 µm could be closed and water permeability could be reduced by 68%. In the study by Gupta et al. (2018)[116], the bacterium *B. sphaericus* was immobilized using biochar prepared from food and wood waste and used as a healing agent in cement mortar. The results of the study showed that through the metabolic pathway of urea hydrolysis, cracks with a width of 700 µm could be completely closed. Furthermore, the compressive strength was increased by 38% and the water absorption capacity was reduced by 70%. This research demonstrates the potential for using immobilized bacteria as a sustainable and effective approach for improving the performance and durability of cementitious materials. Shaheen et al. (2019)[117] used the *Bacillus subtilis* bacterium that performs urea hydrolysis in their study of self-healing concrete using microbial pathways. Iron oxide nano/micro particles (INMP) and bentonite nano/micro particles (BNMP) were used for immobilizing the bacteria. The results showed that through immobilization using INMP media, cracks with a width of 1200 µm could be healed and the compressive strength could be recovered by 85% after processing the cracked samples. On the other hand, through immobilization using BNMP media, cracks with a width of 400 µm could be healed, and the compressive strength could be recovered by 65% after processing the cracked samples.

Diatomaceous earth (DE) can be used as an encapsulation material to protect bacteria from the high pH environment of the concrete matrix. When bacteria are immobilized with DE, they have higher ureolytic activity compared to bacteria that are not immobilized in a cement matrix. In a study by Wang et al. (2012)[118], the urea decomposition rate at three days was 12-17 g/l for bacteria immobilized with DE, compared to 1 g/l for non-immobilized bacteria in a cement matrix.

In their study, Jonkers and Wiktor [10] used light weight aggregate (LWA) for the bacterial protection and healing of cracks up to 0.46 mm in width. The LWA was used as a carrier material for the bacteria, which were able to colonize and produce $CaCO_3$ to heal the cracks. The study found that the addition of LWA increased the compressive strength of the concrete samples, and the cracks were successfully healed with the help of the bacteria immobilized in the LWA.

According to Wang et al. [9], polymeric microcapsules based on melamine were used to encapsulate *Bacillus sphaericus* spores. These microcapsules were then incorporated into concrete. The healing ratio of the encapsulated spores was found to be between 48 and 80%, while the healing ratio for samples without spores was only 50%. This suggests that the use of encapsulated spores can improve the healing properties of concrete. It appears that in the study being described, samples of concrete were subjected to wet and dry cycles using a water-hydrated medium, and the crack region was closely examined. However, it is mentioned that the wet cycle was unusually lengthy, lasting around 16 hours. The largest crack that was successfully healed had a width of 970 μm [9]. The Table 2.2 presents detailed studies on the impact of protection strategies on the performance of self-healing concrete as reported in the literature.

Table 2.2 Impact of protection strategies on the performance of self-healing concrete

Type of bacteria	**Concentration**	**Nutrient**	**Technique using bacteria**	**Crack healing**	**Reference**
Bacillus pseudofirmus	2.54×10^5 cells/cm^3	Calcium chloride	Encapsulation in calcium alginate chitosan	1 mm	[60]
Bacillus cohnii	1.7×10^5 cells/g	Calcium lactate	Immobilizing in expanded clay	0.15 mm	[10]
Bacillus cohnii	3.6×10^9 cells/ml	Calcium lactate and yeast extract	Immobilizing in perlite Immobilizing in expanded clay Direct	0.79 mm 0.45 mm 0.25mm	[119]
Bacillus cohnii	1.1×10^9 cells/ml	Calcium lactate, yeast extract, and inosine	Immobilizing in perlite	1.24 mm	[105]

Type of bacteria	Concentration	Nutrient	Technique using bacteria	Crack healing	Reference
Bacillus sphaericus	10^9 cells/g	Urea, calcium nitrate, and yeast extract	Melamine-based microcapsule	970 µm	[58]
Bacillus sphaericus	10^9 cells/ml	Urea, calcium nitrate, and yeast extract	Encapsulation in hydrogel	0.5 mm	[97]
Bacillus sphaericus	10^{10} cfu/ml	Urea, calcium nitrate, and yeast extract	Immobilizing in biochar Direct	550–700 µm 400–700 µm	[120]
Bacillus sphaericus	10^9 cells/ml	Urea, calcium nitrate, and yeast extract	Encapsulation in chitosan-based hydrogel	200–300 µm	[121]
Bacillus sphaericus	10^9 cells/ml	Urea, calcium nitrate, and yeast extract	Immobilizing in diatomaceous earth	0.15–0.17 mm	[122]

Type of bacteria	Concentration	Nutrient	Technique using bacteria	Crack healing	Reference
Bacillus sphaericus	*NA	Liquid medium, Tryptose, Yeast extract	Direct	0.1–0.5 mm	[87]
Sporosarcina pasteurii	10^9 cells/ml	Urea and calcium nitrate	Encapsulation in calcium sulphoaluminate cement	417 µm	[123]
Sporosarcina pasteurii	2.8×10^9 cells/ml	Calcium lactate	Immobilizing in recycled coarse aggregates Immobilizing in diatomaceous earth	0.28 mm 0.32 mm	[124]
Bacillus mucilaginous	10^9 cells/ml	Sucrose, yeast extract, and calcium nitrate	Immobilizing in ceramsite	0.4–0.5 µm	[125]

Type of bacteria	Concentration	Nutrient	Technique using bacteria	Crack healing	Reference
Bacillus mucilaginous	10^9 cells/ml	Calcium nitrate	Direct	0.4 mm	[126]
Bacillus subtilis	2.8×10^8 cells/ml	Calcium lactate	Direct Lightweight aggregates Graphite nano platelets	0.15 µm 0.52 µm 0.38 µm	[127]
Bacillus subtilis	1.9×10^7 cells/cm^3	Calcium lactate	Immobilizing fine aggregates Immobilizing in recycled coarse aggregates Direct	1.1 mm 0.7 mm 0.6 mm	[128]

Type of bacteria	Concentration	Nutrient	Technique using bacteria	Crack healing	Reference
Bacillus subtilis	10^7 cells/ml	*NA	Direct	1.2 mm	[129]
Bacillus subtilis	2.3×10^8 cells/cm^3	Calcium lactate	Immobilizing in iron-oxide nano-particle Immobilizing in bentonite Direct	1.2 mm 0.2 mm 0.45 mm	[99]
Bacillus alkalinitrilicus	1.7×10^5 cells/g	Calcium lactate and yeast extract	Immobilizing in expanded clay	0.46 mm	[10]
Deinococcus radiodurans	2.41×10^8 cells/ml	Calcium lactate	Direct	1.5mm	[130]
Bacillus halodurans	*NA	*NA	Spray bacteria	80–270 µm	[131]

Type of bacteria	Concentration	Nutrient	Technique using bacteria	Crack healing	Reference
Bacillus cereus	3.52×10^{7} cells/m	Urea, calcium lactate, and yeast extract	Direct	100-800 µm	[88]
Bacillus strain B2-E2-1	*NA	Calcium lactate, Calcium carbonate	Expanded clay particles, Organic compounds	0.15 mm	[10]
*NA: No information available.					

2.3.2. Self-Protected Granular Cultures and Powders

Self-protected cultures and powders are novel approaches that have been proposed to improve the effectiveness and efficiency of microbial self-healing concrete. These methods involve the use of non-axenic cultures, which provide protection to the bacteria against environmental stresses such as desiccation and nutrient deprivation. Non-axenic cultures refer to cultures that contain multiple different microorganisms, rather than a single, isolated strain. By providing the appropriate conditions for growth and metabolism, such as the right temperature, pH, and nutrient availability, non-axenic cultures are able to protect themselves from harsh conditions and avoid the need for additional protection materials[83]. This approach can reduce costs and improve the efficiency and sustainability of various processes.

An example of a self-protected culture is the Cyclic Enriched Ureolitic Powder (CERUP), developed by Silva et al. [36]. CERUP contains a non-axenic bacterial culture with ureolytic activity and is composed of spores that protect the bacteria from environmental stresses. In experiments using mortars containing CERUP, cracks up to 400 µm in width were completely sealed in 28 days. The use of non-axenic cultures, such as CERUP, has demonstrated promising results in terms of self-healing capabilities in bio concrete. In one study, CERUP was dried, ground to a particle size below 500 µm in diameter and mixed with mortar samples at a specific ratio. The study found that CERUP closed cracks up to 0.5 mm in width after a healing period of four weeks, which was higher than the maximum closure of 0.4 mm obtained with axenic culture in the same period[132]. One significant advantage of using CERUP is that there is no need for the addition of highly nutritious compounds to activate the bacteria. Furthermore, CERUP is not only composed of bacterial spores but also some carbonate salts that appear to shield the spores from aggressive agents. The production of CERUP also has lower CO_2 emissions compared to the cultivation of axenic cultures such as *B. sphaericus* and *B. cohnii*. The study [36] found that the CO_2 emissions from CERUP production were 2.7 and 40 times lower than the cultivation of *B. sphaericus* and *B. cohnii*, respectively. This suggests that non-axenic cultures like CERUP are more environmentally friendly and sustainable for the production of bio concrete.

Another example of a self-protected culture is the Activated Compact Denitrifying Core (ACDC), developed by Ersan et al.[7]. ACDC is a granular culture composed of a compact denitrifying core community that is mainly composed of nitrate-reducing bacteria. The granules protect the bacteria from environmental stresses, and in experiments using mortars containing ACDC, cracks up to 500 µm in width were closed more than 90% at the end of 28 days. This resulted in an 80% decrease in water permeability of the cracks.

The use of ACDC granulated culture in bio concrete has shown promising results in terms of its effectiveness and cost-effectiveness. In a study, it was found that ACDC had a higher NO_3^- reduction rate compared to axenic cultures, especially at pH 9.5. Additionally, ACDC was compatible with concrete up to the addition of 1% w/w of

cement, and it showed a significant increase in crack closure potential and watertightness regain compared to axenic cultures[132].

One of the most significant findings of the study was that the use of ACDC granulated culture reduced the cost of bio concrete production by about ten times compared to traditional maintenance and repair methods such as epoxy resin reinforcing grouting or cementitious material filling. This brings the bio concrete technology closer to practical application and makes it a more viable solution for maintaining and repairing concrete structures.

2.4.Self-Healing Performances Under Different Environmental Conditions

To evaluate the effectiveness of methods utilizing water ingress as a trigger mechanism, samples are either submerged in water or subjected to wet/dry cycles throughout the entire healing process. To activate the bacterial self-healing concrete proposed by Jonkers et al. [112], both water and O_2 must be present inside the crack. Many of the studies conducted to explore self-healing efficiency have been carried out under ideal or controlled laboratory conditions. In contrast, only a small number of studies have examined self-healing in harsh, real-world environments [133]. The majority of studies on self-healing have been conducted in tap water. In real situations, structures may come in contact with rain or other sources of liquid water, so the effects of different water environments on the self-healing process should be evaluated.

In some literature, the term "fresh water" is used instead of "tap water." Although these terms have similar meanings, "tap water" typically refers more specifically to a source of drinking water, while "fresh water" is a more general term that encompasses freshwater sources such as rivers, lakes, and groundwater. Literature does not clearly specify whether the water used in the immersion process is rainwater or drinking water and is only referred to as "fresh water." However, based on literature studies, it has been observed that bacteria-based self-healing concrete is effective only under room temperature freshwater conditions[7], [10], [58], [61], [97], [118], [134]. In one selected article[135] discusses the effect of different curing environments on the self-healing capacity of mortars

containing crystalline admixture. The study found that wet curing led to higher self-healing capacity compared to dry curing, and immersion in water resulted in the highest self-healing capacity followed by moist curing and air curing.

The effect of temperature on self-healing has also been investigated, and it has been observed that self-healing bacteria can survive at low temperatures. In marine environments, a bacterium that can survive in seawater needs to be selected. Skevi et al. [136] investigated the viability of self-healing bacteria at low temperatures (7.5 ± 2°C), using a *psychrotrophic* species (Psy39) and *Bacillus cohnii*. Mortar specimens with cracks ranging from 400-500 μm, created at 28 days of age, were exposed to semi-submerged conditions at both 7.5 ± 2°C and 20°C for over 28 days. While *Bacillus cohnii* had better performance at 20°C, Psy39 showed the greatest efficiency at both temperatures. Palin et al. [137] developed a bacteria-based self-healing cementitious composite that can almost completely heal cracks in low-temperature (8°C) marine environments. The healing capacity was 95% for cracks up to 400 μm in width and 93% for 600 μm wide cracks.

Seawater or marine water is rich in Cl^-, SO_4^{2-}, Mg^{2+}, and Na^+ ions, which can undergo reactions with cement to generate various products such as brucite, ettringite, aragonite or calcite form of $CaCO_3$, magnesium silicate hydrate, Friedel's salt, gypsum, $CaCl_2$, $Ca(HCO_3)_2$, and more[138], [139]. According to Liu et al. [140]the rate of crack closure in specimens cured with seawater is 2.5 times faster than those cured with water. Seawater has a significant effect on promoting crack healing. Through TGA testing, it was discovered that in a seawater curing environment, Mg^{2+} ions were the primary reaction ion, rather than Cl^- ions which have the highest concentration. The main products of healing are brucite and $CaCO_3$, and very little chlorine is present in the healing products.

In one research, Palin et al.[139], [141] discovered that cracked specimens cured in seawater mainly produced brucite and aragonite as healing products. Brucite layer formation occurred rapidly within two days, followed by a slow formation of aragonite precipitation on the brucite layer. The maximum crack widths of OPC mortar specimens cured in seawater and tap water were 0.592 mm and 0.168 mm, respectively. However,

the compressive strength of cracked specimens after 56 days of seawater curing was about 30% lower than that of tap water curing specimens. Thus, while corrosive ions could promote crack healing, they could also lead to significant mechanical property losses in specimens. This piece of work serves as a guide towards the development of bacteria-based self-healing concrete that can be utilized in the marine environment.

Erşan et al. [25] studied the tolerance of a nitrate reducing ACDC microbial culture to osmotic stress in the marine environment and found that the ionic strength (μ) of the solution was the major influential parameter, rather than a change in specific ion concentrations. Results showed that the ACDC culture demonstrated adequate resistance in typical seawater conditions ($\mu \sim 0.7$ and $[Cl^-] \sim 0.5$ M).

Khan et al. [248] conducted an experiment to test the efficacy of *Sporosarcina halophila* bacteria, calcium lactate, and expanded perlite aggregate as a carrier in mortar subjected to submerged and tidal marine environments for a period of 90 days. They found that the combination of these materials resulted in the formation of aragonite and brucite within the cracks of the mortar. The presence of bacteria, water, and oxygen within the crack enhanced the mineralization process, resulting in the closure of the cracks by 50% for cracks up to 800 μm in depth. Cappellesso et al. [142] studied self-healing bacterial concrete exposed to freezing temperatures (FT) associated with chlorides. They found that the addition of *Bacillus cohnii* bacteria improved the concrete's performance by reducing scaling by 90% and chloride ingress by 46% under FT compared to reference concrete without bacteria. The bacterial addition had an air-entraining effect that may have contributed to the improvements. However, it was unable to block chloride ingress through a pre-defined crack of 170 ± 50 μm that had been healed during 28 days of water immersion prior to exposure. The healing products formed by the bacteria before exposure to FT were damaged by scaling due to freezing during the subsequent exposure period. The same authors [253] also tested two types of healing agents (a water repellent agent and sodium silicate) by injecting them into 100 μm wide cracks and subjecting them to FT. After a healing regime of 14 days in a layer of water, sodium silicate was able to prevent chloride ingress through the crack even after 56 freezing-thawing cycles with 3 wt-% NaCl.

River water and deicing salt environments are known to have high concentrations of Cl^-. In recent years, researchers[138], [139], [143]–[145] have focused on studying the healing properties of cement-based materials in these Cl^--rich environments. For example, Xue et al. [146]conducted a study on the self-healing process of concrete cracks and found that chloride ions (Cl^-) react with cement compounds to promote self-healing. The reaction initially consumes AFm (alumina, ferric oxide) and $3CaO{\cdot}Al_2O_3{\cdot}CaCO_3{\cdot}12H_2O$, producing Friedel's salt, CO_3^{2-}, and OH^-. This reaction promotes the formation of $CaCO_3$ and increases the pH value of the crack solution. This study discovered that Cl^- ions can react with certain cement compounds to promote self-healing of concrete cracks. In another study, the effective and efficiency of microcapsules in self-healing cemented coral sand (CCS) under various water environments were investigated[147]. The experimental results suggest that the healing efficiency of microcapsules is affected by different water environments. Specifically, the healing efficiency in freshwater was found to be higher compared to seawater, with healing efficiencies of 75% and 59.56%, respectively. This could be attributed to the presence of salt and other minerals in seawater, which can affect the performance of the microcapsules.

Overall, the literature suggests that the self-healing efficiency of cementitious materials under different water environments depends on several factors, including the chemical composition of the material, the duration of immersion, and the environmental conditions. Further research is needed to develop more effective self-healing materials that can withstand different water environments and maintain their self-healing efficiency.

2.5.Added Benefits of Microbial Self-Healing

Traditional maintenance and repair methods for concrete structures such as epoxy resin reinforcing grouting, gravity filling using cementitious materials, or epoxy injections can be costly, especially for repairing cracks with a width of 400 μm, which can cost approximately $\$250/m^2$. In contrast, the estimated cost of producing new concrete is $\$44/m^2$[148]. Therefore, there is a significant cost difference between repairing and maintaining concrete structures versus producing new concrete. Microbial self-healing is an emerging technology that has the potential to significantly reduce the cost of concrete maintenance and repair.

In addition to cost savings, there are other added benefits of microbial self-healing that make it an attractive option for concrete repair. One benefit is increased durability. Microbial self-healing can help to extend the lifespan of concrete structures by repairing cracks and preventing the spread of damage. This can ultimately lead to a more sustainable and cost-effective infrastructure.

Another benefit is environmental sustainability. Microbial self-healing uses natural bacteria to repair cracks, which can reduce the need for harsh chemicals and synthetic materials that may be harmful to the environment. Additionally, the use of microbial self-healing can reduce the carbon footprint associated with concrete maintenance and repair, as it requires less energy and resources compared to traditional repair methods[38], [56], [61], [148].

Overall, the added benefits of microbial self-healing make it a promising technology for the future of concrete maintenance and repair. While it is still a relatively new technology, ongoing research and development will likely lead to more widespread adoption in the construction industry.

2.6.Added Benefits of Non-Axenic Cultures

Non-axenic cultures offer several benefits over axenic cultures, including:

1. Lower Cost: Non-axenic cultures can be produced at a lower cost as compared to axenic cultures. This is because they can be cultivated using minimal nutrient media or even industrial waste, which reduces the cost of production. Furthermore, non-axenic culture has been shown to significantly reduce the cost of bio concrete production[36], [149].
2. Environmental Friendliness: The production of non-axenic cultures typically generates lower CO_2 emissions compared to the cultivation of axenic cultures. This makes them more environmentally friendly and sustainable for bioconcrete production, contributing to the overall goal of reducing the environmental impact of construction materials[150].

3. Protection from Aggressive Agents: Non-axenic cultures, such as CERUP, contain not only bacterial spores but also some carbonate salts, which shield the spores from aggressive agents. The formation of biogranules involves the aggregation of microorganisms within a matrix of extracellular polymeric substances (EPS). This matrix, along with the microbial community structure, contributes to the resilience of biogranules against harmful environmental factors[7], [36].

4. Compact Form: Non-axenic cultures can be cultivated in a compact form, such as microbial granules, which protect the bacterial core and make them easier to store and transport. Furthermore, the granulated culture can be dried, stored, and resuscitated as needed, which adds to its versatility and ease of use. This is particularly useful for situations where the granulated culture needs to be transported or stored for an extended period of time[151].

5. Selective Enrichment: Selective enrichment of particular species can be done by altering the cultivation process, making it possible to cultivate specific bacteria for a particular application. This compact form allows for the growth of different types of bacteria, including aerobic heterotrophs, denitrifiers, polyphosphate accumulating bacteria, and nitrifiers, all at the same time. Additionally, the cultivation process can be altered to selectively enrich particular species of bacteria within the granulated culture[7].

6. Higher effectiveness: non-axenic cultures, like ACDC or CERUP, have been found to exhibit higher rates of NO_3^- reduction and ureolytic activity compared to axenic cultures. This indicates that they are more efficient in their metabolic activities, leading to improved performance in terms of crack closure potential and watertightness regain[132], [152].

2.7.Techniques for Evaluation of Self-Healing

The assessment of self-healing in concrete can be categorized into three groups of assessment techniques: visualization and determination, assessment of regained resistance, and assessment of regained mechanical properties[153]. Each group includes various test methods that can be used to evaluate the effectiveness of the self-healing

process. Here is a brief overview of the three groups of assessment techniques and the relevant test methods.

2.7.1. Visualization and Determination

The methods of visualization and determination for the assessment of self-healing capability of cementitious materials can be further categorized into microscopy, imaging, and spectroscopy[153]. Note that, Thermal gravimetric analysis (TGA) is also another less popular test method that can be used to characterize the post-healing products in self-healing concrete. TGA is a thermal analysis technique that measures the change in weight of a material as it is heated or cooled under controlled conditions. TGA is not as commonly used as other test methods for assessing self-healing in concrete[154], [155].

2.7.1.1.Microscopy

Microscopic methods are widely used for the evaluation of cementitious materials, including the assessment of self-healing capability. These methods involve the use of microscopes to visualize the microstructure of the concrete and identify any healed cracks. Optical microscopy, scanning electron microscopy (SEM), and environmental scanning electron microscopy (ESEM) are among the major test methods for the evaluation of self-healing capability in cementitious materials. In optical microscopy, a digital microscope can be used to observe the crack surface, measure the crack width, and measure the crystalline products formed during the healing process. SEM and ESEM can provide high-resolution imaging of the microstructure of the concrete, allowing for the observation of the morphology and distribution of the rehydrated products[156]. These techniques can be used to analyze the crystallographic structure of the products using techniques such as electron diffraction or X-ray diffraction.

Several authors have conducted experimental studies involving microscopic investigations on cementitious composites to evaluate the efficiency of the improved autogenous crack healing mechanism[157]–[161]. Microscopic examination has provided valuable information on the autonomous crack healing mechanism of bacteria-based concrete[9], [10], [134], [155], [162].

2.7.1.2.Imaging

Imaging techniques can be used to quantify the degree of healing in the concrete. Imaging techniques such as backscattered electron imaging (BSEI), X-ray radiography/tomography, neutron radiography/tomography, and digital image correlation provide a variety of methods for analyzing the structure and properties of concrete. BSEI and SEM are often used together to examine the microstructure of concrete and identify different phases and regions within the material. X-ray and neutron imaging techniques create images of the internal structure of the concrete, with tomography producing 3D images by combining multiple 2D images taken from different angles[153]. Digital image correlation analyzes deformation and strain in the material by processing a series of images to quantify displacement of individual pixels. These imaging techniques provide valuable information for evaluating the effectiveness of different materials and techniques for repairing and strengthening concrete[153].

Mihashi et al. used X-ray radiography to investigate autonomous self-healing in concrete containing encapsulated two-component epoxy with urea formaldehyde formalin (UFF)[163]. Van Tittelboom et al. used X-ray tomography to examine the efficiency of self-healing in connected capsules filled with a two-component healing agent[164]. Neutron radiography/tomography was utilized to visualize and quantify capillary water uptake in healed cracks due to capsule-based autonomous healing mechanism[165], [166].

2.7.1.3. Spectroscopy

Spectroscopic testing techniques are namely X-ray spectroscopy, infrared spectroscopy, Raman spectroscopy, and X-ray diffraction analysis. X-ray spectroscopy is used to analyze the X-ray spectrum, while infrared analysis utilizes light beams in the infrared region of the electromagnetic spectrum. Both techniques are helpful in detecting and determining precipitated products in a healed specimen. Raman spectroscopy, on the other hand, relies on the scattering of monochromatic light to provide information on the chemical composition of crystallization products. Raman spectroscopy has recently become a preferred technique for evaluating the self-healing performance of materials[167]. It has been used in many studies to monitor and characterize the healing process in self-healing materials[168]–[171]. Raman spectroscopy relies on scattering of monochromatic light to provide information on the chemical composition of

crystallization products, while X-ray diffraction analysis produces 3D images of the atomic structure of the specimen, allowing for determination of the composition of the rehydrated product in the self-healing zone[172], [173]. Overall, these techniques are valuable tools for analyzing the self-healing behavior of materials.

2.7.2. Assessment of Regained Resistance

The transport properties, resistivity, and continuity of the healed concrete are major indicators of its regained resistance. These are important parameters to evaluate the effectiveness of the self-healing process.

2.7.2.1. Transport Properties

Transport properties of concrete refer to its ability to resist the penetration of fluids such as water and air. These properties are important because the penetration of fluids can cause damage to the concrete and affect its mechanical properties. Common test methods used to evaluate transport properties include water and air permeability, sorptivity, chloride diffusivity, and osmotic pressure in the healed concrete specimen. Water and air permeability tests are widely used non-destructive testing methods. These tests measure the rate of water or air flow through the concrete specimen and provide valuable information about the concrete's resistance to fluid penetration[174]. Transport properties have been used to investigate the effectiveness of capsule-based autonomous self-healing[100], [134], [175] and tubular based autonomous self-healing[176] in bacteria-based concrete.

2.7.2.2. Resistivity and continuity

Ultrasonic measurements (UT), corrosion tests, and frost/salt scaling are among the popular test methods in this category. During UT, a transducer is used to send ultrasonic waves into the concrete, and the waves are then reflected back to the transducer from the internal boundaries of the material. UT is a valuable tool for evaluating the quality and integrity of concrete structures, and is widely used in construction, maintenance, and repair projects. Corrosion testing is commonly used to evaluate the vulnerability of reinforced concrete structures to corrosion, which can lead to structural damage and failure over time. Pelletier et al. conducted a study to investigate the potential autonomous healing effect of encapsulated sodium silicate in concrete, and corrosion testing was utilized as a method to evaluate its effectiveness[177]. Frost/salt scaling is another

common issue that can affect concrete structures, particularly those exposed to freeze-thaw cycles or de-icing salt. When water inside the concrete freezes, it expands and can cause cracking, spalling, and scaling of the surface. Testing for frost/salt scaling can help evaluate the durability of concrete and identify areas that may require additional protection or maintenance to prevent deterioration. Note that, Resistivity and continuity examinations test methods are not as widely used as some other methods such as mechanical testing or visual inspections.

2.7.3. Assessment of regained mechanical properties

2.7.3.1. Mechanical Tests

To evaluate the regained mechanical properties of self-healed concrete, common test methods include a variety of mechanical tests such as 3-point and 4-point bending tests, compression tests, tensile tests, horizontal deformation tests, and impact loading tests. The bending test method has been widely used to assess the regained mechanical properties to differentiate between healed and unhealed cracks after the healing process has taken place in concrete. In the context of healed concrete, compression test can be used to investigate the regain in tensile strength, stiffness, and ductility of the healed specimen after a crack has been introduced and then allowed to heal[153]. [177], [178]. According to the horizontal deformation test, a horizontal load is applied to the top of a column-shaped concrete specimen to create cracks. After the self-healing mechanism occurs, the test is repeated to assess the healing efficiency. The test can provide valuable information on the load-displacement relationship and quantify the regained tangent stiffness of the healed concrete sample[153]. In the impact loading test, a weight is dropped onto a concrete slab specimen from a fixed height and the impact energy is measured. This test can determine the regained static stiffness of the healed concrete specimen [178], [179]. However, it's important to note that microbial self-healing studies typically do not focus on the regain of mechanical properties. Previous research, as highlighted in[31] has indicated that microbial self-healing primarily closes the crack mouth to a depth of approximately 1 cm from the surface, without completely filling the cracks. As a result, significant mechanical property regain is not expected in microbial self-healing concrete.

2.7.3.2. Non-Mechanical Tests

In addition, Acoustic emission (AE) analysis and resonance frequency analysis (RFA) are two non-mechanical test methods that can be used for the assessment of self-healing in concrete[153]. Acoustic emission (AE) analysis involves analyzing the brief elastic waves produced by a sudden stress distribution in a material. Micro-cracks that appear in the concrete matrix can release energy in the form of stress waves that are recorded by sensors. This technique can provide detailed data on the healing process and allow for evaluation of the regained internal energy in the healed concrete. Van Tittelboom et al. utilized the AE technique to record the breakage of capsules in capsule-based autonomous healing[180]. By using RF analysis, it is possible to quantify the degree of damage and recovery in the concrete structure, as well as the rate of self-healing. The healing process can be monitored using RF analysis by measuring changes in the resonance frequency of the structure as it heals[153]. Resonance frequency (RF) analysis has been used for the characterization of microcapsules in many self-healing studies[167].The frequently used methods and devices for visualizing crack closure in the literature and advantages and limitations are provided in the Table 2.3 [133].

Table 2.3 An overview of methods to measure the performance of healing agents.

Test method	**Purpose**	**Advantages**	**Limitations**
Optical microscopy	✓ Measuring crack closing at the surface. ✓ Quantification of the change in crack width or area.	✓ Simple and easy working principle. ✓ Monitoring of crack closure over time and in different locations along the crack.	✓ Can not provide a volumetric crack closing ratio. ✓ Can not monitor closure of the crack in deeper part.

Test method	Purpose	Advantages	Limitations
Scanning electron microscope (SEM)	✓ Combine the high-resolution images with the EDX results. ✓ Provide a comprehensive analysis of the sample's healing products and chemical composition.	✓ it's possible to obtain a more comprehensive understanding of the sample's composition and structure, surface topography.	✓ Small samples or limited test areas may exhibit more variability than larger samples
Energy-dispersive X-rays (EDX)	✓ To identify the chemical composition of self-healing products and perform both qualitative and quantitative analyses.	✓ it's possible to identify the chemical composition of self-healing products.	✓ Small samples or limited test areas may exhibit more variability than larger samples
X-ray computed microtomography (μCT)	✓ The damage or failure can be defined, and also the geometry of the crack can be characterized.	✓ It gives evidence of the damage, and quantification of crack closure by self-healing processes.	✓ Only applied for small sample sizes and restricted to mortars.

Test method	Purpose	Advantages	Limitations
X-ray computed tomography (CT)	✓ To understanding the internal self-healing capabilities of a material and phase ✓ To obtain phase identification and density analyses .	✓ Can be applied to concrete and provide high quality of data analysis.	✓ Larger equipment
X-ray radiography	✓ To visualization of rebar corrosion in cracked and moisture uptake over time.	✓ high-spatial resolution images can be obtained.	✓ Obtaining a perfect overlap of images before and after healing in concrete can be challenging
Nuclear magnetic resonance (NMR)	✓ to provide a comprehensive understanding of water transport in concrete.	✓ Non-destructive testing (NDT) and allowing a detailed study over time	✓ Equipment is not accessible.

2.8. Scope and Objective of the Thesis

The use of bacteria for the healing of concrete cracks (bio concrete, biomineralization) has been an increasingly researched topic in recent years, with positive results motivating further investigation and experimentation. Previous studies have shown that ureolytic and nitrate-reducing bacteria, when tested separately, can promote the precipitation of $CaCO_3$ through their microbial metabolisms. However, most studies in the literature have used axenic bacterial cultures containing a single type of bacterial strain and a single metabolic

pathway for concrete crack healing applications. A few studies have shown that non-axenic nitrate-reducing biogranules can be used for the development of microbial self-healing cement composites. Nevertheless, no studies exist in both national and international literature that explore the use of non-axenic biogranules containing both ureolytic and nitrate-reducing bacteria for the development of microbial self-healing cement composites. In such application, MICP can occur under both oxic and anoxic conditions which can be considered advantageous over commonly investigated microbial self-healing concrete. Sekercioglu (2021) has already developed biogranules that can conduct urea hydrolysis and nitrate reduction under neutral pH conditions. Therefore, in this thesis study, these non-axenic biogranules will be further processed to achieve microbial activity under alkaline pH conditions and then tested for the first time for development of self-healing concrete.

There have been only a few studies in the literature that have addressed the impact of the aqueous environment on the self-healing ability of concrete. Although tap water has been studied mostly, it is necessary to test the other aquatic environments such as marine or rainwater conditions that the self-healing performances can be more comparable to possible realistic conditions. Therefore, further research is needed to address this gap by studying the healing mechanisms and durability of cementitious composites in these environments. By examining the healing performance of cementitious composites in seawater and rainwater, researchers can gain insights into the effectiveness of self-healing mechanisms in these materials and how they can be improved to better withstand harsh environmental conditions.

Considering the needs in the literature, within the scope of the thesis, biogranules were produced, dried, and after testing their ability to perform urea hydrolysis and nitrate reduction, they were added to cementitious composites at a specific dose previously determined by Sonmez (2021)[181]. The microbial self-healing performances of the cementitious composites were assessed. The effect of marine, rain, and tap water aquatic environments on crack healing was determined separately.

3. MATERIALS AND METHODS

This section provides a detailed account of the production of biogranules, preparation of mortar samples, and their self-healing capacity. Additionally, the section focuses on the crack formation and healing process in the mortar samples tested in different aquatic environments.

3.1. Production of Biogranules Containing Both Nitrate-Reducing and Urea Hydrolyzing Bacteria

In accordance with the method described by Sekecrioglu (2022)[182], the biogranules were produced in a cylindrical sequential batch reactor (SBR) with a volume of 1.2 L, a length of 76 cm, and a diameter of 4.5 cm. Furthermore, while preparing the mortar samples, the production was continued. The biogranules were formed as a result of the microbial activity and the environmental conditions within the SBR. Sequential anoxic/aerobic periods were set to operate a single SBR cycle. SBR was operated with 4 identical cycles in a day as described in previous granular sludge production studies[86], [183]–[185]. This method involves alternating anoxic and aerobic conditions. There is no dissolved oxygen during the anoxic period, which is suitable for denitrifying bacteria to convert nitrate to nitrogen gas. In contrast, during the aerobic period, the dissolved oxygen level is increased to support the growth of aerobic bacteria, which perform urea hydrolysis This approach allows for the coexistence of both nitrate-reducing bacteria and urea-hydrolyzing bacteria, with the majority of urea-hydrolyzing bacteria typically being aerobic in nature [186]. During the aerobic period, the dissolved oxygen level is increased to support the growth of these aerobic bacteria, enabling them to perform urea hydrolysis as a primary function. In the aerobic period, air supply in the reactor was provided by using an aquarium aeration pump, which ensured a certain level of dissolved oxygen at approximately 0.76 L/min. Additionally, a peristaltic pump was used to provide necessary chemicals via nutrient solution. Nutrient solution was fed through the bottom of the reactor at a rate of 10 ml/min for an hour. This period was called anoxic feeding/withdrawal period and repeated at each cycle. During this feeding period, 600

mL of reactor content was collected from the top to maintain a 50% volume exchange ratio. The aeration and feeding periods were automated using a time controller.

The composition of the nutrient solution used for the production of granules is given in Table 3.1. The reactor was supplemented with nutrients providing final nutrient concentrations of 1 g/L urea, 200 mg/L NO_3-N and 1544 mg/L COD. The specific composition of this nutrient solution and the requirements of the microorganisms being used in the experiment was likely selected based on previous studies as described in one new thesis study[182]. The nutrient solution was formulated with specific components to support microbial activity in the granular biomass. It consisted of 1 g/L of urea and 0.24 g/L of yeast extract, which are sources to promote the growth and enrichment of urea-hydrolyzing microorganisms. In addition to that, the nutrient solution also included 200 mg/L of NO_3-N (nitrate nitrogen), providing a substrate for denitrification by denitrifying microorganisms. Yeast extract contains amino acids, vitamins, and other nutrients that can support microbial growth[187]. In urea hydrolysis, urea is included as an essential component in the nutrient feed, and bacteria serve as agents for the enzymatic hydrolysis of urea into ammonia and CO_2[188]. Yeast extract (YE) is frequently employed as a carbon source for the urea hydrolysis pathway[189]. In synthetic nutrient solutions, COD (Chemical Oxygen Demand) quantifies organic content. COD is a standardized parameter to quantify oxygen consumption during the oxidation of organic and inorganic substances in water. It's vital for assessing water quality and pollution levels, typically expressed as mg O_2/L, and determined using strong chemical oxidants like potassium permanganate or potassium dichromate. It's widely recognized as the standard for assessing oxygen consumption in water oxidation.[190]. The selection of these materials is crucial because they must be compatible with concrete, particularly when it is in its hardened state, and should not contribute to its deterioration[187]. The composition of the nutrient solution is available in Table 3.1.

Table 3.1 Composition of the nutrient solution used in production of biogranules.

Chemical	**Amount**
Urea	1 g/L
Yeast extract	0.24g/L

$NaNO_3$	1.02 g/L
$Ca(NO_3)_4.H_2O$	0.15 g/L
KH_2PO_4	0.6 g/L
$MgSO_4.7H_2O$	0.9 g/L
NaCl	1.8 g/L
CH_3OH	1.3 ml/L

The initial seed used for this process was a granular culture that had been previously grown by Sekercioglu (2023)[182]. The reactor operated continuously for approximately 70 days before the pH change. Subsequently, it continued to operate for an additional 120 days during the harvesting process until a sufficient amount of granules was collected for use in cementitious composites. Beginning on the 71st day, the granular culture was maintained at a pH level of 9.5 to cultivate and promote the growth of microorganisms capable of thriving in an alkaline pH environment within the concrete. After 124 days of operation for production of the desired granules, the granules were periodically harvested from the reactor, either once or twice a week, and then dried at 60°C for 48 hours.

The dried granules were then used to make self-healing cementitious composites, using only those granules with dry particle sizes ranging from 0.45 to 2.00 mm. Granules with particle sizes less than 0.45 mm were returned to the granule cultivation reactor for further growth and cultivation. The schematic view and the lab setup the granule production reactor is shown in Figure 3.1.

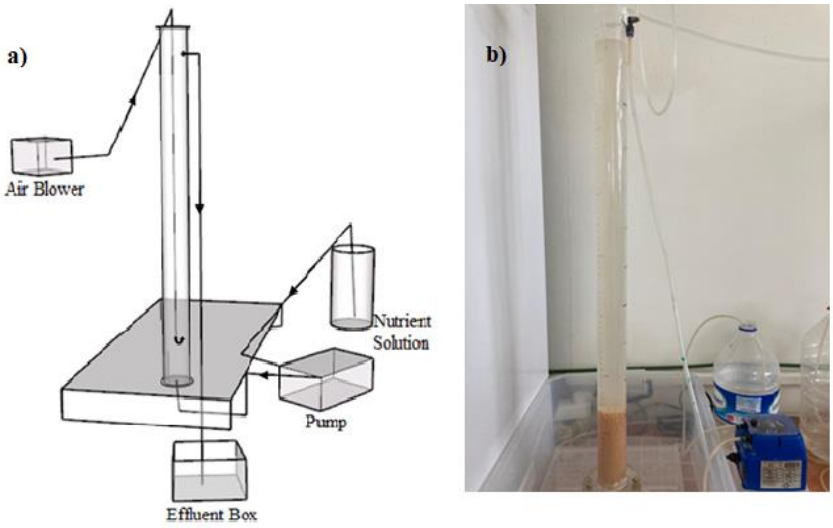

Figure 3.1 Representation of a) reactor setup b) photo of a biogranules production reactor.

3.1.1. Biogranulation Performance and Microbial Activity Analyses

During the continuous operation of the SBR, measurements were taken using initial and effluent samples from each period to assess the granule properties and microbial activity. Samples were analysed for Total Ammonia Nitrogen (TAN), Volatile Suspended Solids (VSS), Total Suspended Solids (TSS), and Sludge Volume Index (SVI).

The equation below illustrates the hydrolysis of urea, resulting in the production of 2 moles of ammonia (NH_4^+), along with bicarbonate (HCO_3^-) and hydroxide (OH^-) ions. This process leads to an elevated pH of the solution and an increase in ionic strength, as neutral urea is transformed into charged compounds[191].

$$NH_2(CO)NH_2 + 3H_2O \rightarrow 2NH_4^+ + + HCO_3^- + OH^- \text{ [191]} \quad \text{Equation (1)}$$

Since urea hydrolysis was responsible for the TAN generation in the bioreactor (Eqn (1)), TAN analyses were conducted regularly to determine the efficiency of urea hydrolysis and microbial activity in the bioreactor. In TAN analysis, urea ($CO(NH_2)_2$) can be regarded as a natural ammonia source that can be converted into the ammonium form (NH_4^+)[192]–[194]. The TAN analyses were performed twice a week on filtered samples according to standard methods (coded as 4500-NH_3 Step-B, C). A titration process was carried out using 0.02 N sulfuric acid[195], [196].

VSS and TSS are measures of the suspended solids in the samples, which can indicate the biomass amount and the inorganic content in the granulation reactor. VSS measures the amount of organic matter that is present in the suspended solids. TSS, on the other hand, measures the total amount of solids in the sample, including both organic and inorganic solids. A higher VSS/TSS ratio indicates a higher percentage of organic matter in the sample and thus can be interpreted as a higher concentration of bacteria. Changes in these parameters over time can provide insight into the activity and composition of the microbial community, the efficiency of the granulation process.

SVI is a measure of the settleability of the granules, with lower values indicating better performance[197]. SVI_{30}/SVI_5 ratio is a useful indicator for estimating the percentage of granules in the reactor[198]. By comparing the SVI values at 30 minutes (SVI_{30}) and 5 minutes (SVI_5), it is possible to determine the settling characteristics of the sludge, which can provide information about the presence and distribution of granular microbial culture in the reactor[198]–[200] . The higher the ratio, the higher the percentage of granules present in the sludge. This ratio is commonly used in biogranulation investigations because it provides a quick and easy way to estimate the percentage of granules without the need for more complex analysis techniques[197], [200]. The SVI_{30} limit value of 50 ml/g [198] is being continuously checked to ensure that the granular microbial culture remains within acceptable levels. This can help prevent problems such as bulking or foaming, which can disrupt the operation of the reactor[199].

Microscopic images of bio-granules were routinely acquired using a light microscope (LEICA DM EP Leitz Wetzlar Co., Germany) at 40x magnification and a 10-megapixel camera. Samples were collected during the fully mixed aerobic phase within the reactor and were carefully deposited onto a glass surface using a dropper. Approximately 15-20 photographs were taken for analysis. To determine their size distribution, these images were processed using ImageJ software (NIH and LOCI, University of Wisconsin Co. v3, USA), which provides detailed insights into the physical characteristics of the granules.

3.1.2. Harvesting and Drying the Granules from the Reactor

The process of harvesting and drying granules constitutes a critical step in the integration of biogranules into mortar, and this study closely adheres to a methodology consistent with previous research supervised by the co-advisor [201], [202]. This comprehensive process involves several key stages carefully designed to prepare the granules for their subsequent applications.

Firstly, the process begins with harvesting the granules from the reactor. This entails extracting a 200 ml sample from the reactor full mixed reactor with samples taken from approximately equal levels of reactor height, specifically 60 cm as the upper point, 40 cm as the middle point, and 20 cm as the lowest point, similar to the approach used during the VSS analysis. Subsequently, the granules are allowed to naturally settle in the liquid medium for a duration of approximately 2-3 minutes. Once settled, the settled granules are meticulously separated from the liquid portion. Following this separation, the granules undergo a thorough washing process using tap water. This step is importance in eliminating any residual liquid and impurities.

Once the washing process is completed, the granules are subjected to controlled drying conditions at a temperature of around 60°C for a period of roughly 48 hours. This precise drying process plays a critical role in eliminating any remaining moisture content, thereby preserving the granules in an optimal state for subsequent analysis or utilization. The selection of a drying temperature at 60°C is informed by the biology of the microorganisms within the granules. Bacteria, being microorganisms, have an "optimum growth temperature," and most cannot thrive at temperatures exceeding 60 degrees Celsius[203]. This is because high temperatures denature the enzymes essential for their growth and reproduction, making 60°C an effective choice for drying while maintaining the integrity of the granules[203], [204]. Following the drying phase, a comprehensive analysis is undertaken to assess size and density properties of the granules. Any granules falling below the 0.5 mm threshold or exceeding 2 mm are promptly returned to the bioreactor, underscoring the significance of maintaining a specific size range for optimal performance in the bio granule production process. According to the particle size distribution of EN-196 Standard Sand (SS), which is characterized by a particle size range

of 0.08 to 2 mm, the average size distribution in standard sand falls within the range of 0.425 to 2 mm. Dry granules that were added also have sizes similar to sand particles, with dry granules ranging from 0.5 to 2 mm being used in the mortar mixture. According to a granule size study [205], it was determined that smaller-sized granules resulted in better dispersion in cement mortar, leading to a more homogeneous distribution. In the same study, when comparing granule sizes of 1-2 mm and 2-4 mm, it was found that the 1-2 mm-sized granules exhibited increased water absorption capacity due to their higher surface area.

In conclusion, all of the methods mentioned above were employed with thoroughness in preparing the granules for subsequent analysis and their integration into self-healing cementitious composites. Furthermore, the dried granules were stored at room temperature for use in the production of self-healing cementitious composites.

3.1.3. Evaluation of the Resuscitation Performances of the Dry Biogranules

The resuscitation performance of dry biogranules refers to their ability to revive and resume their metabolic activity after being stored in a dry state for a certain period of time. Dry granules have a longer shelf life and do not require any adjustments to the mix water of the mortar, making them more advantageous for use[184].

This was tested by drying the granules at 60°C for 48 hours and then resuscitating them in a nutrient medium to evaluate their activity recovery. The VSS was set to 0.5 mg. L^{1-} for the resuscitation test. The batch reactors were run in alternating anoxic and aerobic periods for 24 hours. The first 3 hours of the run were under anoxic conditions, followed by another 3 hours under aerobic conditions, and this order was repeated until the end of 24 hours. This experiment was conducted in triplicate, with three bottles prepared in an identical manner. The Figure 3.2 illustrates the appearance of the batch bottles during the application of a magnetic stirrer set to 100 rpm to establish aerobic conditions. Throughout the experiment, consistent temperature and pressure conditions were maintained within each bottle. Under anoxic conditions, the bottle caps were tightly sealed for a duration of 3 hours. Samples were taken every 3 hours to monitor the granule

activity and determine the time required for resuscitation. The urea hydrolysis activity of the dry granules after resuscitation was followed by conducting TAN.

Figure 3.2 Resuscitation experiments of dry biogranules with 3 triplicate bottles

3.1.4. Detecting the Effect of Yeast Extract on Dry Granule Activity

MICP system, yeast extract (YE) is required for spore germination[206]. The ureolytic activity of bacteria, with variations in YE concentration, plays a significant role in understanding the impact of yeast extract on the mortar.

The influence of YE on dry granule activity can be effectively assessed through the implementation of a batch test. This comprehensive batch test encompasses the following key steps: Firstly, two distinct sets of samples were meticulously prepared. One set exclusively contained dry granules, serving as the control group, while the other set was composed of an identical amount of dry granules (0.83 g of biogranules) complemented with yeast extract. Equal proportions of dry granules were introduced into both sets of samples, and to standardize the samples, they were adjusted to a uniform volume, typically 100 ml, using reactor nutrient.

Urea hydrolysis activities were monitored at 3, 6, hours during the anoxic phase. Furthermore, a Total Ammonia Nitrogen (TAN) analysis was meticulously conducted to quantitatively compare the urea hydrolysis activities between the yeast extract-containing

and yeast extract-free samples. The experimental images of two bottles, one containing yeast extract and the other without yeast extract, are depicted in the Figure 3.3 below.

Figure 3.3 Comparison of ureolytic activity in the presence and absence of YE with experimental images of 2 bottles.

3.2. Preparation of Mortar Samples

The samples were prepared in accordance with the EN 196-1 standard using a sand: cement: water ratio of 3.0: 1.0: 0.5. The basic mortar components were 1350 g of DIN EN 196-1 sand, 450 g of CEM I 42,5R cement, and 225 g of tap water were used as basic mortar components.

According to the EN 196-1 standard, in the production of cement mortar, the coarse components were added first, with cement being added initially, followed by the addition of water, and mixing at a low speed for 30 seconds. Then, sand was added within the next 30 seconds, and the mixer was operated at high speed for 30 seconds. After 90 seconds, the device was stopped, and any mortar adhering to the container was cleaned and added to the mixture. The mixing process was completed by running the device at high speed for 60 seconds. This preparation method was applied to the reference samples. However, in the abiotic samples, nutrient chemicals were included along with the cement, while in the biotic samples, both nutrient chemicals and dry granules were added, following the standard procedure. After mixing, the cement was placed into molds. After 1 day, it was removed from the molds and stored in airtight special bags for 28 days.

The bacterial content in the bio mortars was adjusted to 0.25% by weight of cement, referencing a previous thesis study. Working with this dosage within the scope of the thesis aimed to contribute significantly to time and cost savings, as minimizing the granule quantity was a key objective. This means that 0.25% of the total weight of the cement in the bio mortar mix was made up of bacteria. The harvested biogranules had a VSS:TSS ratio of 60±1%. Based on this ratio, 1.88 g of biogranules (1.13 g bacteria) were added to each bio mortar batch.

In this study, three different types of mortars were prepared and tested: (i) reference, (ii) abiotic control, (iii) biomortars. The reference, abiotic control, and bio mortar samples were each prepared with specific objectives in this study. “Reference Mortar” provided a baseline for the evaluation of the inherent behavior and properties of mortar without any additives. The "Abiotic Control Mortars" were created as control samples to evaluate the effects of added nutrients on mortar performance in the absence of biogranules. The "Biomortars" were formulated to investigate the combined impact of additional nutrients and biogranules on mortar properties. These samples allowed for an investigation of how the presence of biogranules, along with added nutrients, influenced mortar behavior and self-healing capabilities. The Table 3.2 that outlines the composition of the mortars was presented below.

Table 3.2 Composition of all mortar samples

Mortar Type	**Description**
Reference Mortar	Basic mortar mixture without additional nutrients or bio granules.
Abiotic Control	Mortars with the same additional nutrients as biomortars (2.0% Urea, 5.0% Ca-Formate, 2.0% Ca-Nitrate, and 0.1% yeast extract w/w cement), but without biogranules.
Biomortars	Mortars containing both additional nutrients and biogranules, along with the basic mortar components.

3.3.Formation of Cracks in Mortar Samples

The procedure described in the text outlines the formation of cracks in mortar samples and the subsequent determination of their self-healing performances.

The use of steel molds and the procedural details were determined based on previous thesis studies [207], [208] . First, the mortar mixtures were prepared according to a specific mix design. Then, they were poured into steel molds that have a ribbed steel reinforcement in the middle. The dimensions of the molds had a uniform shape and size of 30 mm × 30 mm × 340 mm. The ribbed steel reinforcement was 500 mm long and 6 mm in diameter. The steel reinforced mortar samples were then removed from the molds after 24 hours and cured in airtight plastic bags at room temperature for 28 days to prevent evaporation of the water content. Figure 3.4 shows moulded and demoulded mortar samples. Furthermore, detailed dimensions of the molds are also provided in Figure 3.4 to enhance understanding through drawings. This engineering drawing provides a schematic representation of the dimensions of both the mold and the steel bars used in the thesis study.

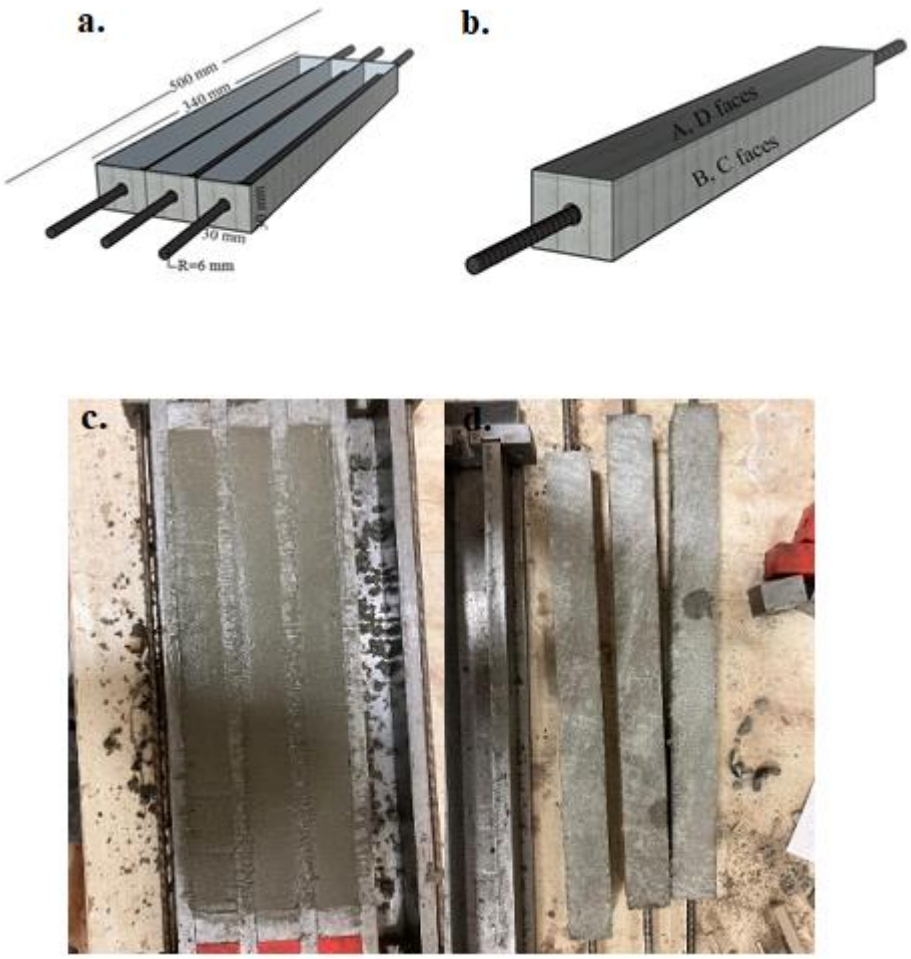

Figure 3.4 Stainless steel molds were used for preparation of all mortar batches; a) dimensions of the molds; b) naming of the faces of each specimen ‘A’ as troweled top face, ‘D’ as bottom face, ‘B’ and ‘C’ are side faces; c) mortar pouring; d) demoulded specimens.

On day 28, mortar samples underwent a uniaxial tensile test, conducted at a speed of 0.01 mm/s with stroke control. The test aimed to generate cracks of varying widths, with a targeted average crack width ranging from 100 to 800 µm. Facilitating uniaxial tension, 80 mm ribbed steel bars were positioned externally on both sides of the mortar samples and securely secured between the grips of the testing apparatus. Figure 3.6 show the uniaxial tension setup used for creation of the cracks. The setup typically involves a machine that applies a controlled tensile force to the sample along a single axis (i.e., uniaxial). The sample is typically clamped or gripped at each end and the force is applied in between those points.

During the initial stage, referred to as stage a, the applied load remained below the tensile strength of the concrete. Consequently, the concrete remained in its elastic state, preventing the formation of any cracks. It was only when the load reached the maximum tensile strength of the concrete (marked as point R) that the first crack became apparent. The number of cracks continued to increase during stage b. Transitioning from point S to Y marked the phase of crack stabilization. During this stage, the cracks that originated in stage b continued to widen, although their quantity ceased to increase. At point Y, the reinforcement material underwent plastic stage. Upon entering stage c, the number of cracks (n) could be quantified on the specimen's surface. The load was then stopped at the point determined by equation. Referencing both the eqn 2 and the Figure 3.5 adds clarity to the explanation, both of which were extracted from the thesis study from Wang[209].

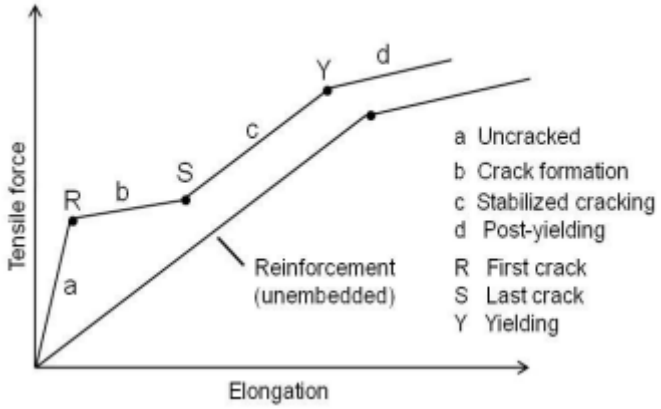

Figure 3.5 Load vs. crack development stages in concrete (Adapted from Wang's thesis study [28])

$$\delta = Wa * n + (\sigma/E) * L = Wa * n + 1.23mm \text{ [28]} \qquad \text{Equation (2)}$$

In the eqn (2):

δ ; represents the elongation (stroke in the loading program).

Wa ; stands for the average crack width, which was set at 150μm in this study.

n ; corresponds to the number of cracks observed on one surface.

Σ ; represents the average load in the plastic stage of the reinforcement, equal to 560N/mm².

E; signifies the E-modulus of the reinforcement, which is 210,000 N/mm².

L; denotes the distance between two clamps, which was 460mm in this study (360mm + 50mm * 2).

Figure 3.6 Creation of cracks with various widths via uniaxial tension.

3.4. Determination of Their Self-Healing Performances in mortar sample

Self-healing performance of the cracked mortar specimens were evaluated in three different aquatic environments: (i) tap water, (ii) rainwater, (iii) seawater. The Table 3.3 below provides detailed information on sample numbers and the range of crack widths formed.

Table 3.3 Crack width measurements for different water types.

Water Type for self-healing tests	# of Biotic Samples	Crack Width range, µm	# of Abiotic Samples	Crack Width range, µm	# of Reference Samples	Crack Width range, µm
Tap Water	3	180-575	3	30 -390	2	170 -540
Rain-water	2	75-600	2	70-420	3	60-440
Marine Water	3	124-540	3	100-485	3	130- 430

Each container used to immerse the concrete samples in water had a capacity of 3 liters of water. Separate specimens and containers were used for each test setup. One container, in which the samples were immersed in rainwater, was shown in the figure 3.7 The conductivity of tap water was approximately 20 uS/cm, while the conductivity of collected rainwater and marine water was measured as 36 uS/cm and 56013 uS/cm, respectively. Rainwater was collected from Hacettepe University's Beytepe Campus, while marine water was obtained from the coordinates provided below Didim 4th Bay (Figure 3.8).

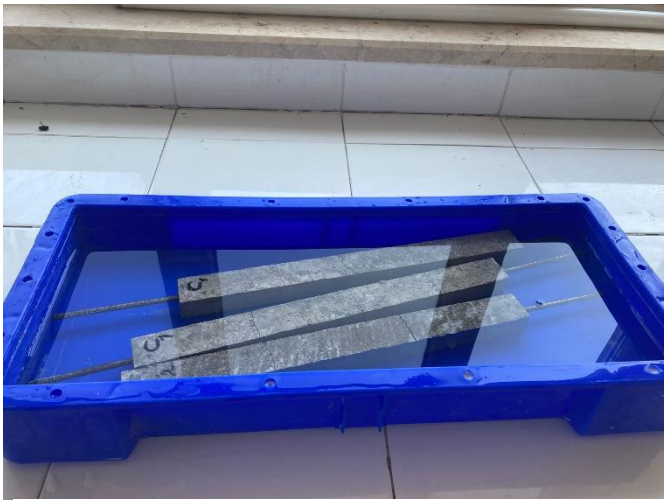

Figure 3.7 The bio-mortar samples that immersed in rainwater.

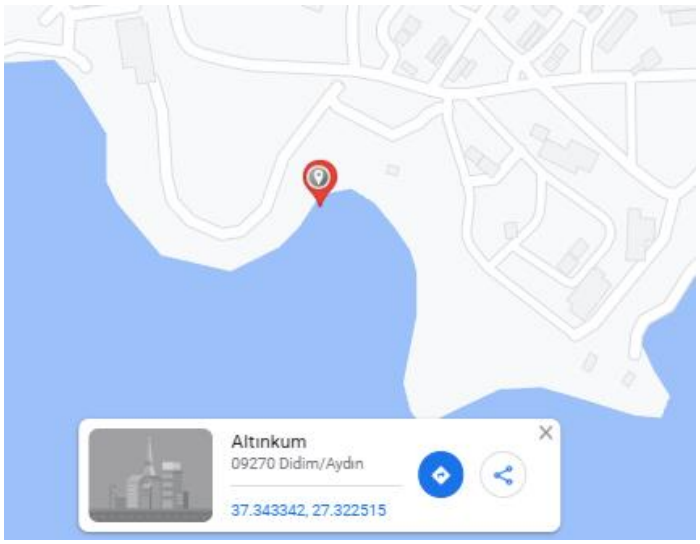

Figure 3.8 Coordinates of seawater (Didim 4th cove).

The self-healing performance of mortar samples was evaluated by tracking the evolution of crack widths over time. In this study, the width of each crack, as illustrated below figure 3.10 a with 6-8 data points, was examined on a weekly basis. Figure 3.10 b depicts a light microscope, while Figure 3.10 c displays images taken during the analysis before and after a healing process. For each crack, a total of 24 microscope images were acquired from surfaces A, B, C, and D. In cases where the concrete had three cracks, a minimum of 72 images were collected in total. In instances with four cracks, a minimum of 96 images were captured in total. The results primarily concentrated on assessing the smooth surfaces of B and C. After the initial cracks were formed and the crack widths were measured, the samples were immersed in water and monitored weekly for healing performance. Recording the crack widths at t0 (initial time point) is an important step in evaluating the self-healing performance of mortar samples.

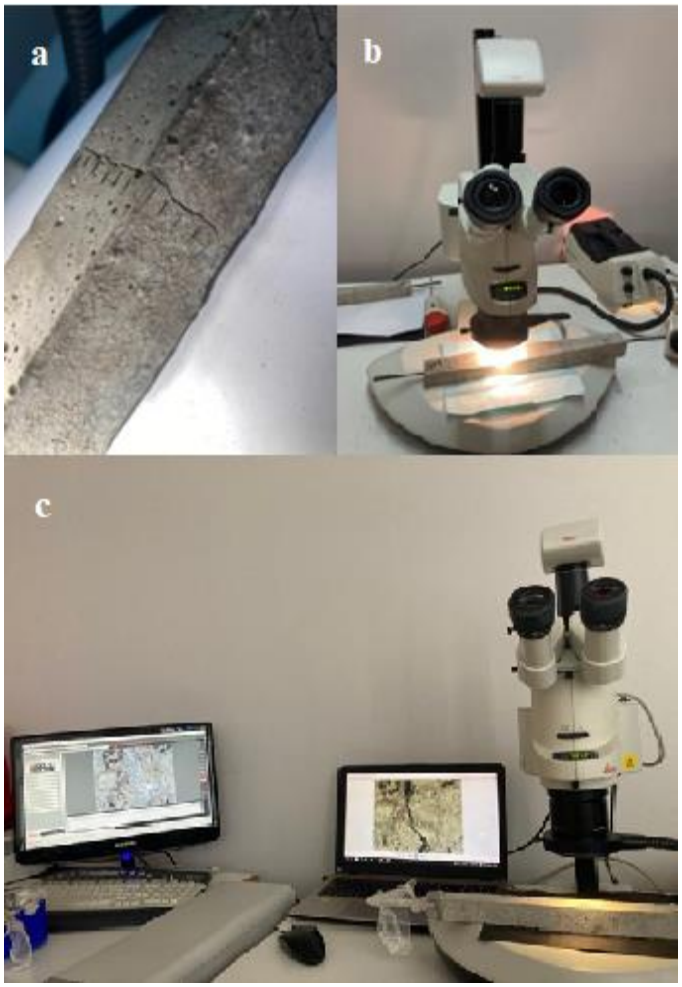

Figure 3.9 Monitoring of the changes in crack width under microscope; a) specific points on each crack, b) stereomicroscope; c) obtaining micrographs via a software for further analyses.

3.5.Data analysis

The self-healing capabilities of mortar samples were assessed by regularly measuring crack widths over several weeks. The extent of healing was determined by calculating the percentage reduction in crack width compared to the initial crack width. At least 72 data points per crack width were measured, and the results were used to compute average values and standard deviations.

The formula for quantifying crack healing percentage was:

$$\text{Crack Healing Percentage} = [1 - (w_t / w_{initial})] \times 100 \quad \text{Equation (3)}$$

Where:

- 'w_t' represented the crack width measured at different time points 't' (in days).
- '$w_{initial}$' denoted the crack width before any repairs or improvements, usually at the initial time 't_0'.

To evaluate self-healing effectiveness across various samples, both reference samples (containing basic mortar components only) and control samples (containing additional nutrients with basic mortar components) were analyzed using the same methodology as the bio granulated samples.

In this study, samples achieving a crack healing efficiency of 90% or higher, as discussed in the completed thesis, were categorized as self-healing samples. Moreover, within the self-healing category, special attention was given to the widest cracks that not only reached a healing percentage of 90% or more but also showed significant closure in narrower cracks. These criteria were employed to determine the self-healing capacity of each sample. The analysis of cracked samples involved periodic removal from water immersion, allowing them to dry for specific time intervals. Microscopic images of the cracks were likely captured using a light microscope, such as the Leica Z16 APO model, Germany, for further examination.

4. RESULTS AND DISCUSSION

4.1. Pre-Operational Assessment of Granular Reactor Performance

In this section, the results of the pre-operational assessment of the granular reactor's performance are discussed based on data extracted from a prior study of Sekercioglu (2022) entitled "Investigation of Nickel Recovery by Biogranules Tailored for Metal Recovery Through Biomineralization". The analysis aimed to evaluate the initial operating conditions of the reactor and the microbial activity of the previously developed biogranules. According to the referenced thesis study [182], the reactor had been operated for 260 days, and the kinetic analysis results for the 180th day were provided in Table 4.1 Samples were systematically collected from the reactor at 15-minute intervals, subjected to filtration, and subsequently analyzed for NH_4-N, NO_3-N, and COD concentrations.

Table 4.1 Activities of previous study's reactor operation; The activities for the 6-hour total operation [1], [2].

Treatment Phase	**Urea Hydrolysis (%)**	**Nitrate Reduction (%)**	**COD Consumption (%)**
Anoxic (3hr)	64	100	70
Aerobic(3hr)	25	-	25
Total (6hr)	89	100	95

According to the findings of the kinetic analysis, the results reveal that 64% of urea hydrolysis occurred within the first 3 hours of the anoxic period, while this percentage reached 89% during the aerobic period. Moreover, 85% of the initial concentration of 120 mg/L NO_3-N was reduced within the first 2 hours of the anoxic period. At the end of the anoxic period, microorganisms completely reduced the NO_3-N in the reactor. Additionally, approximately 70% of the initial 1200 mg/L organic carbon was oxidized by the end of the anoxic period. The substantial consumption of COD during the anoxic period facilitated the initiation of the famine period in the aerobic phase.

As the aerobic phase progressed, about 95% of the COD was removed, leaving only 50 mg/L COD remaining in the reactor by the end of the aerobic period. The results of the kinetic analysis experiment conducted by Sekercioglu (2022) also revealed a COD/N consumption ratio of 9.6 in an SBR cycle during the previous reactor operation [1], [2].

4.1.1. Microbial Composition of the Seed Biogranules

Mature biogranules developed by Sekercioglu (2022) was used as the initial seed for production of alkali resistant biogranules in this thesis study. The reactor was taken over and the operational conditions were modified as described before. The operational process began with discontinuing the nickel feed in the reactor, and after 70 days, the pH of the nutrient solution was adjusted to 9.5. Before any modifications the biogranules developed by Sekercioglu (2022) were analyzed for their microbial community by using 16s rRNA sequencing to confirm the presence of the urea hydrolyzing bacteria and the nitrate reducing bacteria in the seed bio-granules. Similar community analysis was further repeated with the biogranules produced in this thesis study to detect any community shifts occurred after the modification. Table 4.2 presents the most abundant 10 genus present in the seed mature biogranules developed by Sekercioglu (2022) and the most abundant 10 genus present in the biogranules produced this thesis study. Both analyses revealed that at least 99% of the genetic material within the bio-granules belongs to bacteria.

When evaluating the most dominant ten genera within the samples, the focus was on the presence of urea hydrolyzing and nitrate reducing bacterial community. In the mature granules developed by Sekercioglu (2022), the dominant community capable of either urea hydrolysis or nitrate reduction was determined to be at least 85.7% of the total microbial community. After the relevant modifications in the operational conditions, in this thesis study, the dominant community capable of either urea hydrolysis or nitrate reduction was determined to be at least 85.5% of the total microbial community (Table 4.2). Within the granules, bacterial species that did not rank among the top 10 dominant species during different periods were categorized as "Other" constituting less than 15% of the total abundance across all samples (Table 4.2). The results indicated that the pH modification, along with the discontinuation of nickel feeding, for the production of alkali-resistant microbial biogranules did not cause any major change in the target

community. In both cases, the overall community capable of urea hydrolysis and nitrate reduction was stable. These results showed that the modified reactor operation was suitable for transition of non-axenic mature biogranules that can hydrolyze urea and reduce nitrate under neutral pH conditions to alkali resistant biogranules that can be applied to cementitious composites without causing any significant disruption in the effective microbial community. Additionally, the increase in gram positive *Anoxybacillus* sp. abundance was considered beneficial for application in cementitious materials as they can form endospores and ensure recovery of the activity in the long term.

Table 4.2 Abundance and dominance of microbial communities in granules during various operational phases.

Bacterial Genus	**Urease**	**Nitrate Reductase**	**Pre-operation granules (%)**	**Bacterial Genus**	**Urease**	**Nitrate Reductase**	**Operation granules (%)**
Petrimonas sp.	-	+	29.6	*Hyphomicrobium* sp.	+	+	18.6
Hyphomicrobium sp.	+	+	22.1	*Anoxybacillus* sp.	+	+/-	18.6
Pseudoxanthomonas sp.	+/-*	+	12.5	*Chryseobacterium* sp.	+/-	+/-	12.5
Chryseobacterium sp.	+/-	+/-	11	*Petrimonas* sp.	-	+	7
Diaphorobacter sp.	+	+	2.9	*Propionicicclava* sp.	+	+	5.8
Enterobacteriaceae sp.	+	+	2.3	*Aquamicrobium* sp.	+/-	+	5.8

Bacterial Genus	**Urease**	**Nitrate Reductase**	**Pre-operation granules (%)**	**Bacterial Genus**	**Urease**	**Nitrate Reductase**	**Operation granules (%)**
Aquamicrobium sp.	+/-	+	2.2	*Bosea* sp.	+	+/-	5.2
Tissierella sp.	-	-	2	*Paenalcaligenes* sp.	+	+	5.2
Niabella sp.	+	-	1.8	*Brevundimonas* sp.	+	+	4.4
Ferrugini bacter sp.	+/-	-	1.3	*Pseudoxanthomonas* sp.	+/-*	+	2.4
Others			12.3				14.9

4.2.Modifications to Produce Granules Suitable for Concrete Usage (Phase I-Phase II)

As described before the biogranules used as seed were previously developed by Sekercioglu (2022) for metal recovery from metal leachate solution. After taking over the reactor, the seed was started to fed with a different nutrient solution to produce biogranules that can be incorporated into cementitious composites. The modifications to the nutrient solution and to the operational conditions can be summarized as follows: (i) nickel-free minimal nutrient solution was used, (ii) pH of the nutrient solution was set around 9.5-10. This section provides a detailed analysis of biogranules performance after the relevant modifications aimed at enhancing their suitability for integration into concrete. The primary objective of the pH adjustment was to cultivate biogranules compatible with concrete's pH requirements, optimizing their incorporation into concrete materials.

In the previous study[182], the biogranules in the reactor underwent a feeding phase with 4 mg/L nickel ion for a specific duration, and no pH adjustment was carried out during that time. In this thesis study, the activity of the seed granules was started to be fed by using a nickel-free nutrient solution for a certain period. Subsequently, on the 71st day of operation, the biogranules demonstrated favorable performance in nitrate reduction and urea hydrolysis. Upon acclimation of the nickel-free conditions, pH of the nutrient solution was set around 9.5-10. The primary objective of this adjustment was to establish an optimal environment that would promote the growth of biogranules suitable for integration into cement composites. More precisely, the pH of the reactor was elevated to a range of 9.5-10. Maintaining a high pH level of 10 indicates an alkaline environment[210], [211], which might be suitable for the desired biological or chemical processes involving these biogranules within the concrete production or application context. By implementing this pH adjustment, the intention was to foster the development of biogranules possessing characteristics compatible with the pH requirements of a concrete crack. This optimization process was undertaken to facilitate the reactivation of biogranules upon crack formation and the expected pH drop in cementitious composites.

In order to interpret the parameters responsive to the pH changes, the activities spanning up to the 120th day were subjected to analysis. Therefore, the reactor operation for the first 120 days was described in two phases: (i) encompassing the initial operational days up to the 71st day, (ii) operation under alkaline conditions from Day 71 to the Day 120. After obtaining suitable biogranules, the reactor was operated for another 60 days for regular harvesting of the produced biogranules, and this period was considered as phase 3. This approach facilitates a comprehensive assessment of the changes observed over time and provides a clear visualization of the biogranules' behavior during different operational phases.

The analyses conducted within these sub-sections collectively shed light on the biogranules' performance and structural changes during the development of appropriate biogranules that can be considered as microbial self-healing agents.

4.2.1. Evaluation of the activity of biogranules during cultivation

Regular samples were taken during the SBR operation to monitor the microbial activity of the biogranules and the granulation performance.

4.2.1.1. Evaluation of the changes in TSS, VSS, and VSS/TSS ratio during granule cultivation

Granulation is a crucial process in various biological systems, and it plays a significant role in optimizing the performance of reactors used for different applications. In monitoring and the assessment of the granule production reactor performance suspended solid content of the reactor is one of the key parameters. Total Suspended Solids (TSS) and Volatile Suspended Solids (VSS) are the common parameters to assess the reactor content. TSS includes all solid particles in the system, both organic and inorganic, while VSS specifically refers to organic matter and can also be considered as microbial mass in produced biogranules. VSS is a good indicator of the biomass content and enables to foresee the changes or disruptions in microbial activity [212].

The significance of these parameters is vividly demonstrated in Figure 4.1, which presents the dynamic fluctuations in TSS and VSS over time. Initially, VSS levels started around 4000 mg/L, rapidly increased to 5000 mg/L as the granulation process commenced, and further reached to approximately 8000 mg/L as granulation advanced, underlining a thriving granule population before harvest initiation. An interesting discovery occurred during Phase 2 on day 71 when a pH increase caused a noticeable VSS rise. Before this, VSS was about 4500 mg/L, but on day 96, it reached 7500 mg/L. Following pH increase, TSS also increased significantly from 6200 mg/L to over 12000 mg/L.

Figure 4.1 illustrates the VSS/TSS ratio, which is used to assess the bacterial composition within biogranules. The transition from Phase 1 to Phase 2, accompanied by an increase in reactor alkalinity, resulted in a decrease in the VSS/TSS ratio. This reduction can be attributed to an intensified equilibrium between CO_3^-, and HCO_3^-, triggered by the elevated pH. The increase in pH promotes the formation of CO_3^{2-} from dissolved CO_2 and HCO_3^-, subsequently supporting the formation of $CaCO_3$ [213], [214]. The increased

concentration of $CaCO_3$ and the accumulation of minerals in the system significantly increased the TSS. This increase in TSS disrupted settling in both granules and other suspended biomass to the extent that even flocculation was hindered, resulting in an increase in VSS as well, although not as increased as TSS.

The relatively higher increase in TSS compared to VSS led to a decrease in the VSS/TSS ratio. During Phase 1, this ratio was around 70%, but it stabilized at approximately 60% during Phase 2. It's worth noting that this shift in the ratio may have been influenced by the sampling process during VSS analysis, where samples collected from upper reactor levels could introduce bias towards less-settled granules, potentially leading to a relatively lower VSS value compared to the comprehensive TSS measurement. In essence, the decrease in the VSS/TSS ratio primarily resulted from increased density due to the presence of $CaCO_3$, causing the granules to settle. Additionally, the observed reduction in the ratio could be partly attributed to the practice of sampling from the upper levels during VSS analysis. This settling process might have caused an uneven distribution of solid particles within the reactor.

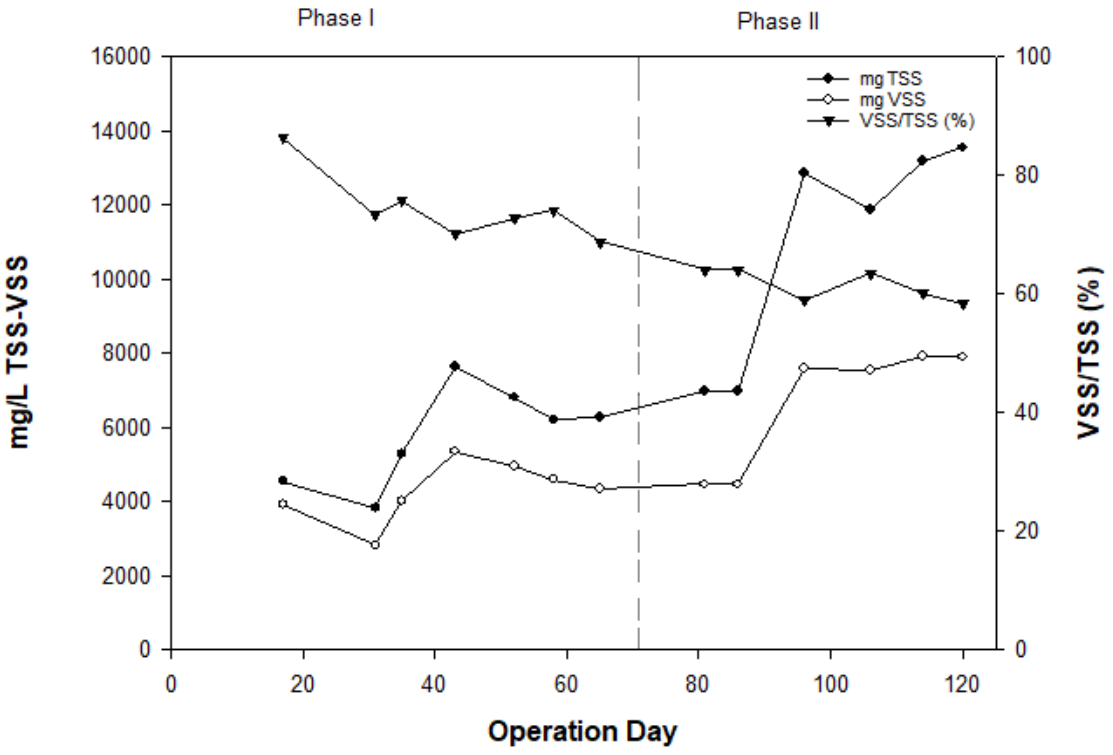

Figure 4.1 Showcases the dynamic fluctuations in TSS and VSS throughout granule cultivation.

In conclusion, the assessment of TSS and VSS has proven to be instrumental in understanding the dynamics of biogranules formation and microbial activity during cultivation. The fluctuation in TSS and VSS levels during different phases of cultivation revealed the dynamic nature of granule formation. Notably, the increase in VSS and TSS levels during Phase 2 was associated with a pH rise, resulting from changes in the carbonate balance of the aquatic environment, which further promoted the formation of minerals like $CaCO_3$. Formation of minerals around the floccular biomass increased their settling velocity and caused accumulation of floccular biomass in the bioreactor which negatively affacted the overall granule percentage. These minerals also led to a decrease in the VSS/TSS ratio.

4.2.1.2. Evaluating Urea Hydrolysis Effectiveness during granule cultivation

Figure 4.2 presents the urea hydrolysis performance of the biogranules throughout the reactor operation. In Phase 1, which entails the outcomes of urea hydrolysis conducted before any pH adjustments, a minimal nutrient medium solution was used. In contrast, Phase 2 involves the analysis of Total Ammonium Nitrogen (TAN) subsequent to a pH increase. When examining Phase 1, specifically by comparing urea hydrolysis performance across different periods within a cycle, it becomes evident that during the anoxic period, an average of 51% of the urea underwent hydrolysis, while in the aerobic period, this percentage was approximately 36%. Before the pH was raised to 9.5 on Day 71, the total n reached an approximate value of 87%.

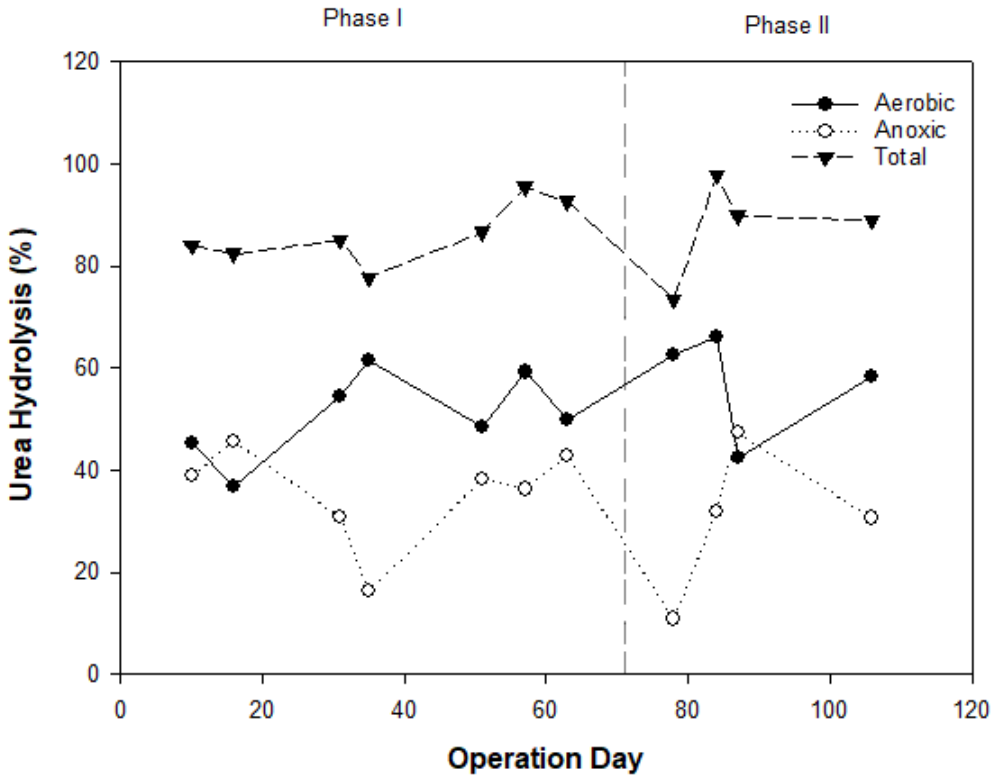

Figure 4.2 Evolution of urea hydrolysis performance throughout granule cultivation

Transitioning to Phase 2, which corresponds to the period after the pH increase, we observe that an average of 60% of the urea was hydrolyzed during the anoxic period, whereas this percentage was approximately 30% during the aerobic period. Following this pH adjustment, the total urea hydrolysis rate increased to around 87.5%. Notably, when considering the reactor's urea hydrolysis performance across both Phase 1 and Phase 2, the data consistently reveal that the obtained performances were similar. During the initial 71 days, there was an average urea hydrolysis efficiency of 86% and from day 71 to 120, the average urea hydrolysis percentage was found as 89%.

This finding emphasizes that the reactor maintains a stable and reliable urea hydrolysis performance under various conditions. This stability is crucial for the practical application of processes that rely on urea hydrolysis, demonstrating that consistent results can be achieved even when environmental conditions change. Remarkably, when considering both phases, the data consistently showed similar urea hydrolysis performances, with an average rate of 86% during the initial 71 days and 89% from day 71 to 120.

4.2.1.3. Evaluating Nitrate Reduction Performance During Granule Cultivation

In this study, a strategic decision was made regarding the frequency of nitrate analyses. It's worth noting that previous research has already demonstrated the nitrate reduction capabilities of these granules. Instead, periodic nitrate analyses were performed to confirm the presence of nitrate-reducing microbial groups using community analysis.

In Phase 1, a significant portion of the nitrate reduction performance was evaluated. This phase involved conducting nitrate analyses before any pH alteration took place. The results revealed a commendable nitrate reduction rate of 85%. This phase served as a crucial initial assessment of the granules' efficiency in reducing nitrate concentrations. The comprehensive evaluation of nitrate reduction performance highlights the impressive capabilities of the granules in various testing phases. The analysis conducted in Phase 1, conducted before any pH adjustments, revealed a significant nitrate reduction percentage of 85%. This phase served as a crucial initial assessment of the granules' efficiency in reducing nitrate concentrations.

Moving on to Phase 2, a notable achievement was achieved. A complete reduction of nitrate was observed. This indicates the granules' capability to significantly reduce nitrate even in relatively high nitrate loading rates, under alkaline pH environments. Under low pH (acidic) conditions, the reduction of nitrate generally slows down. Lower pH values can hinder the conversion of nitrate to ammonium ions and make the transformation of nitrate into nitrogen gas or nitrogen oxides less likely[215]. Hence, determining the optimal pH range for nitrate reduction is crucial. Generally, neutral, or slightly alkaline conditions (pH 7-8) are considered suitable for nitrate reduction, although this process can vary depending on the microbial species, reactants, and environmental factors [216], [217]. It's worth noting that the efficiency of nitrate reduction can be significantly affected by pH variations, particularly under different environmental and experimental conditions [216], [217]. Alkaline conditions promoting nitrate reduction have been documented in previous studies [86], [209], [218].

In conclusion, it was revealed that produced granules can reduce nitrate. Prior research had already demonstrated the nitrate reducing biogranules, while in this thesis we revealed that urea hydrolysis and nitrate reduction can be achieved in a single granular community. The presence of urea hydrolyzing and nitrate-reducing bacteria in granules was confirmed through community analysis. In Phase 1, the granules exhibited an impressive nitrate reduction rate of 85%, even before any pH adjustments were made. This initial assessment highlighted the efficiency of the previously cultivated granules. In Phase 2 complete nitrate reduction was observed. This suggested that the granules were capable of reducing nitrate effectively, even under conditions of relatively high nitrate loading rates and alkaline pH environments.

4.2.2. Granule Formation Characterization and Granulation Analyses

In this subsection, we explore the characterization of granule formation, a critical aspect of their integration into concrete. The following parameters were analyzed:

4.2.2.1. Settleability and Characteristics of Granular Biomass

In this study, settleability and granular biomass characteristics were assessed by monitoring the Sludge Volumetric Index (SVI) of the reactor contents. SVI values were determined at two different settling times, specifically after 5 minutes (SVI_5) and 30 minutes (SVI_{30}). The SVI_{30} analysis was conducted with the purpose of assessing the settling characteristics of the granules within the reactor[219]. The primary objective of this analysis was to understand how changes in operational conditions, particularly the increase in pH during the transition from Phase 1 to Phase 2, might impact the suspended volume index (SVI_{30}) and, consequently, the settling behavior of the biogranules.

During the shift from Phase 1 to Phase 2, the reactor experienced adjustments in pH levels. It is known that variations in pH can influence the microbial community and the physicochemical properties of the sludge. By examining SVI_{30} in the context of these observed pH fluctuations, we can gain valuable insights into how alterations in operational parameters relate to the settling characteristics of the biogranules. This

analysis plays a pivotal role in comprehending the reactor's overall performance and aids in optimizing operational strategies to ensure stability and efficiency[220].

The analysis revealed that the SVI_{30}/ SVI_5 ratio was approximately 50 mg/L, a value consistent with another study using the same reactor[182], [183]. This ratio proved to be a reliable indicator of granulation levels during the reactor's granulation phase, particularly when SVI_{30} reached or exceeded 50 ml/g. While SVI_{30} remained stable, reflecting the granular composition, SVI_5 could rapidly fluctuate due to granule fragmentation or increased flocculent biomass. These variations, however, didn't accurately represent the reactor's content. Consequently, it was determined that in fully granular systems, an SVI_{30} value below 50 ml/g sufficed.

In the aerobic phase with continuous stirring, aeration was intentionally suspended for a 30-minute period to calculate SVI_5 and SVI_{30} values[221], which were then plotted in Figure 4.3 Notably, during the granulation period, there was a further reduction in the SVI_{30} value. In Phase 1, before pH adjustments were made to the reactor's operation, minimum nutrient feeding was practiced. Starting from day 35, the SVI_{30} value consistently remained below 40 ml/g. This consistent trend suggested the presence of fully developed granular biomass within the reactor. On the 71st day, an increase in pH resulted in an SVI increase, exceeding 40 ml/g just after 83 days. However, approximately 30 days later, the SVI dropped below 20 ml/g. This observation demonstrated that in Phase 2, the reactor maintained its granular characteristics even after the pH adjustments. When examining SVI_{30} and the VSS/TSS ratio, an inverse relationship in their changes became evident. This was because a decrease in the SVI_{30} ratio indicated an increase in the granular level within the system, thus signifying an increase in biomass or VSS. This figure 4.3 presents the variations in Sludge Volume Index (SVI) at 30 minutes (SVI_{30}) and 5 minutes (SVI_5), as well as the SVI Ratio (SVI_{30}/ SVI_5) and the VSS (Volatile Suspended Solids) to TSS (Total Suspended Solids) Ratio.

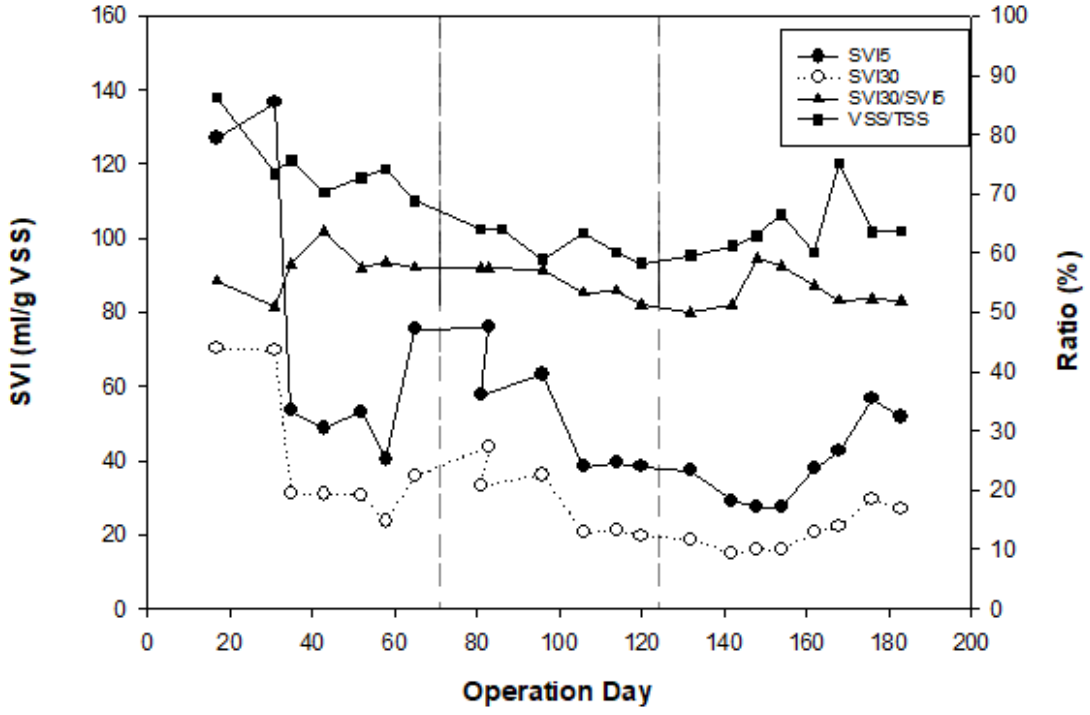

Figure 4.3 Variations in SVI_{30} and SVI_5, as well as the SVI ratio (SVI_{30}/ SVI_5) and VSS /TSS ratio throughout the reactor operation.

In conclusion, during the granulation period, it was observed that the SVI_{30} value consistently remained below 40 ml/g in Phase 1, indicating the presence of fully developed granular biomass. Even after pH adjustments in Phase 2, the reactor maintained its granular characteristics, with a temporary increase in SVI_{30} followed by a return to values below 50 ml/g. This resilience of granular characteristics in the face of pH variations is noteworthy. These findings highlight the stability and adaptability of the granular biomass within the reactor, underlining the importance of SVI measurements in assessing and optimizing the performance of biogranules-based systems.

4.2.2.2. Granular Size Distribution Analysis during granule cultivation

The size distribution of granules was compared from day 43 to 104, representing Phase I to Phase II. On the day 43, the average size of most biomass particles was less than 0.3 mm. By day 43, the majority of particles were in the range of 0.1-0.2 mm, accounting for more than 45%, and 0.0-0.1 mm, which was nearly as abundant at 40%. After 30 days, on day 70, the particle size distribution shifted to sizes larger than 0.8 mm. As depicted

in the Figure 4.4, particle size gradually increased during the development period, indicating the gradual formation of microbial sludge. By the 70th day, particles smaller than 0.1 mm had completely disappeared, and larger-sized particles were observed. On the 70th day, the majority of particles fell in the range of 0.2-0.3 mm, comprising nearly 42%, while 0.3-0.4 mm particles were nearly as abundant, at 15%, and granules larger than 0.4 mm accounted for over 10%. As previously mentioned, the pH change on the 71st day resulted in a noticeable shift in size distribution. Granules taken on the 104th day showed the reappearance of granules smaller than 0.1 mm, with the majority falling in the 0.1-0.2 mm range at around 25%. No granules larger than 0.6 mm were observed. The pH change led to the reduction in size of larger granules and the formation of new granules. Microscopic images captured during both the initial phase and Phase 2 were also provided (Figure 4.5).

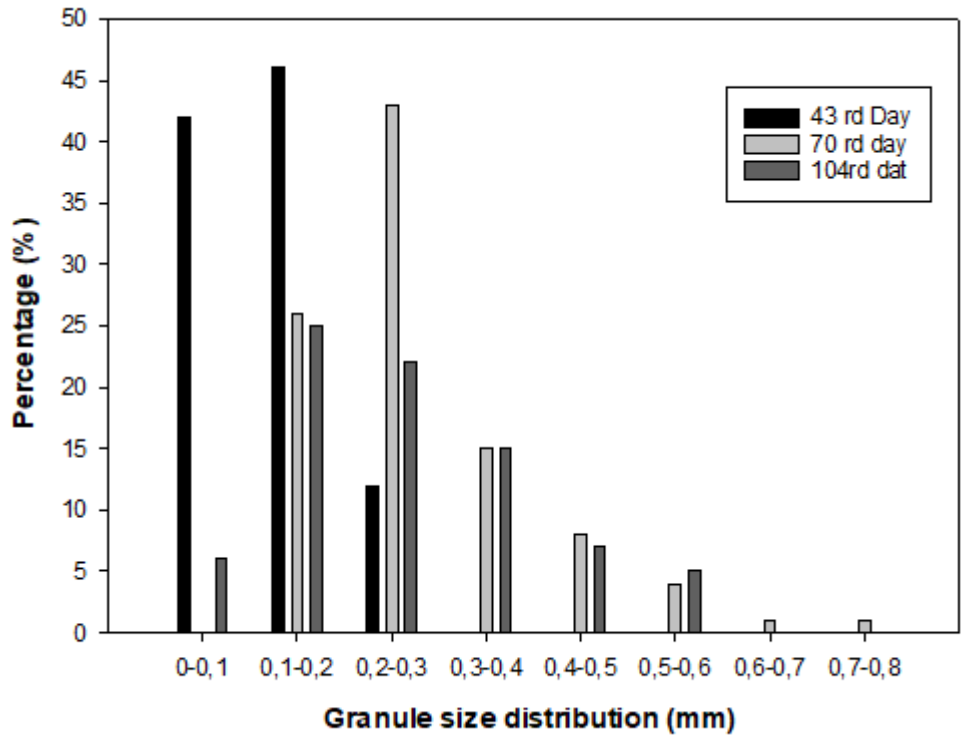

Figure 4.4 Size Distribution of granules during granule cultivation.

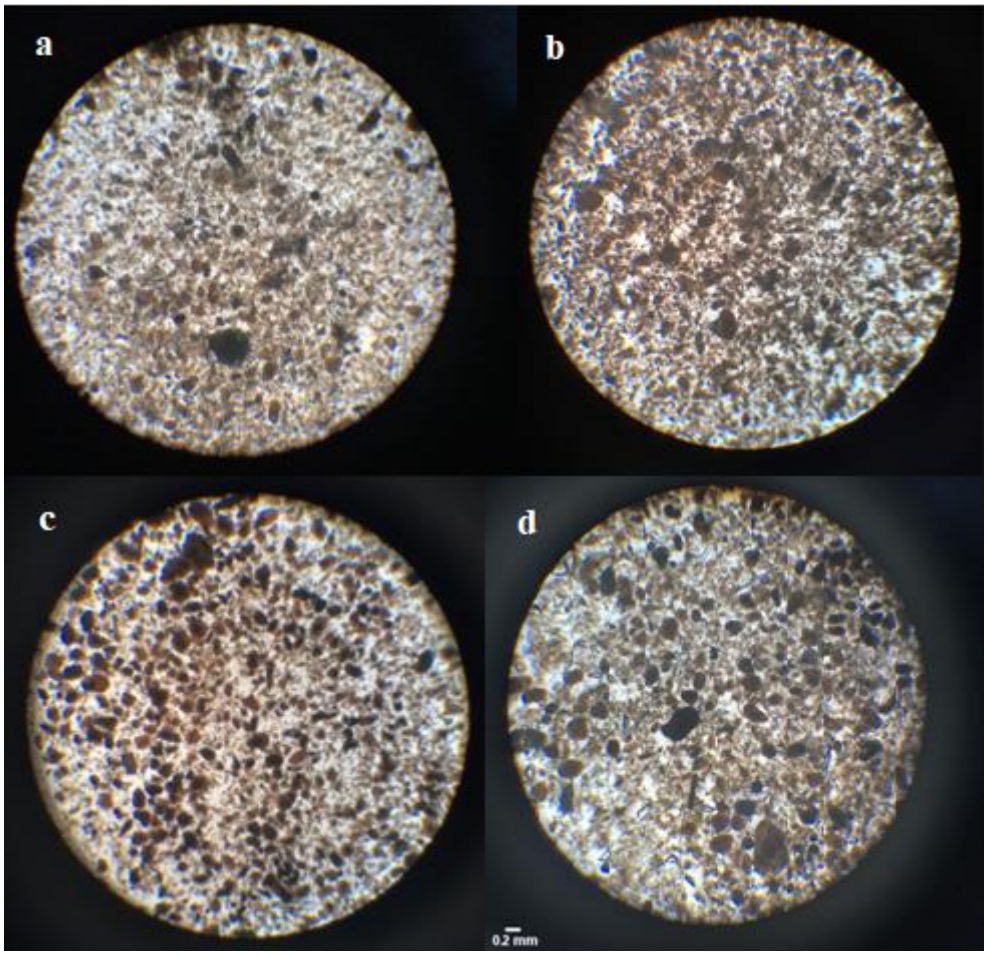

Figure 4.5 Microscopic images of granules on different days: (a)30th day; (b) 79th day; (c) 104th day; and (d)118th day during granule cultivation stage.

In summary, the analysis of granular size distribution throughout the cultivation process, spanning from day 43 to day 104, revealed dynamic changes in the composition of microbial granules. During the initial phase (Phase I), on day 43, the 85% of granules had sizes ranging from 0.1 to 0.2 mm and 0.0 to 0.1 mm, indicating the disintegration and regranulation of the microbial community. However, a significant shift occurred by day 70, with larger-sized granules (0.2-0.3 mm) becoming 70% reflecting the maturation of the granules. This period of development was characterized by the disappearance of smaller granules (<0.1 mm) and the emergence of granules larger than 0.4 mm by over than 25%. Due to the pH change introduced on the 71st day, variations in the size distribution were observed. Observed decrease in the percentage of larger granules and the reappearance of smaller granules (<0.1 mm) by day 104 indicated that the change in

operational conditions such as pH can cause disintegration and regranulation, most probably due to the changes in microbial community.

4.3. Reactor performance during granule harvesting (Phase III)

In Phase III, further analyses and evaluations were conducted to assess the continued performance and behavior of biogranules while some portions of the granules were harvested from the bioreactor. The findings from this phase also contribute to our understanding of the long-term stability and usability of the granules in cementitious composites.

4.3.1. Evaluation of the changes in TSS, VSS, and VSS/TSS Ratio during granule cultivation

After the 124th day of reactor operation, granules were regularly harvested for potential use in cementitious composites. The reactor's harvesting days and the corresponding quantities of dry biogranules were provided in Table 4.3. Initial harvest involved collecting granules from the bottom of the reactor, whereas subsequent harvests took place during well-mixed reactor contents. During the harvesting process, 200 ml samples were consistently collected from the reactor and further dried as detailed in the methods section. The dry granules were sieved through steel mesh segregating those larger than 0.45 mm and smaller than 2 mm. Dry granules out this specific size range were put back into the granule production reactor.

Table 4.3 Representation of harvest days and biogranules amounts.

Harvest Days	Dry granules
124th	5.164 g
147th	2.600 g
149th	2.100 g
175th	2.493 g
181st	2.268 g
189th	2.200 g
TOTAL	16.83 g

Additionally, a graph depicting TSS-VSS and VSS/TSS ratios is provided Figure 4.6 below. This graph offers a visual representation of the TSS-VSS relationship and the VSS/TSS ratios throughout the harvesting process, further enhancing our understanding of the granule harvesting dynamics. Notably, the lowest recorded VSS values during the harvesting process were 7764.23 and 5164.0 mg/L, while the average VSS content was approximately 6720.75 ± 950 mg/L during this period.

After collecting granules on the 149th day, the reactor's VSS analysis revealed a value of 5164 mg/L. To maintain VSS levels above 5000 mg/L, a prudent decision was made to postpone further harvesting until the 175th day. This careful approach was rooted in the consistent analyses reporting VSS values above 5000 mg throughout the reactor's operational duration, specifically when assessing microbial activity. This threshold was chosen due to the uncertainty surrounding the implications of falling below this level; there was concern that any activity loss might occur below this threshold. Therefore, harvesting was continued with a dedicated focus on keeping VSS levels above 5000 mg/L, as dropping below this level could potentially lead to a loss in microbial activity and overall reactor efficiency. Additional granule harvests occurred on the 181st and 189th days, culminating in a total yield of 16.83 g of dry biogranules. In Phase 3, the average VSS/TSS ratio was recorded at 64% ± 1.7, indicating a slight increase from the average ratio of approximately 61.5% ± 1 observed during Phase 2, prior to initiating the harvesting process.

The strategy of keeping VSS levels above 5000 mg/L underscores a cautious approach aimed at maintaining the optimal performance of the reactor. This decision was based on the consistent findings from activity analyses conducted throughout the reactor's operational period, all of which indicated VSS values exceeding 5000 mg/L. This precautionary measure was taken to avoid any potential disruptions in reactor activity.

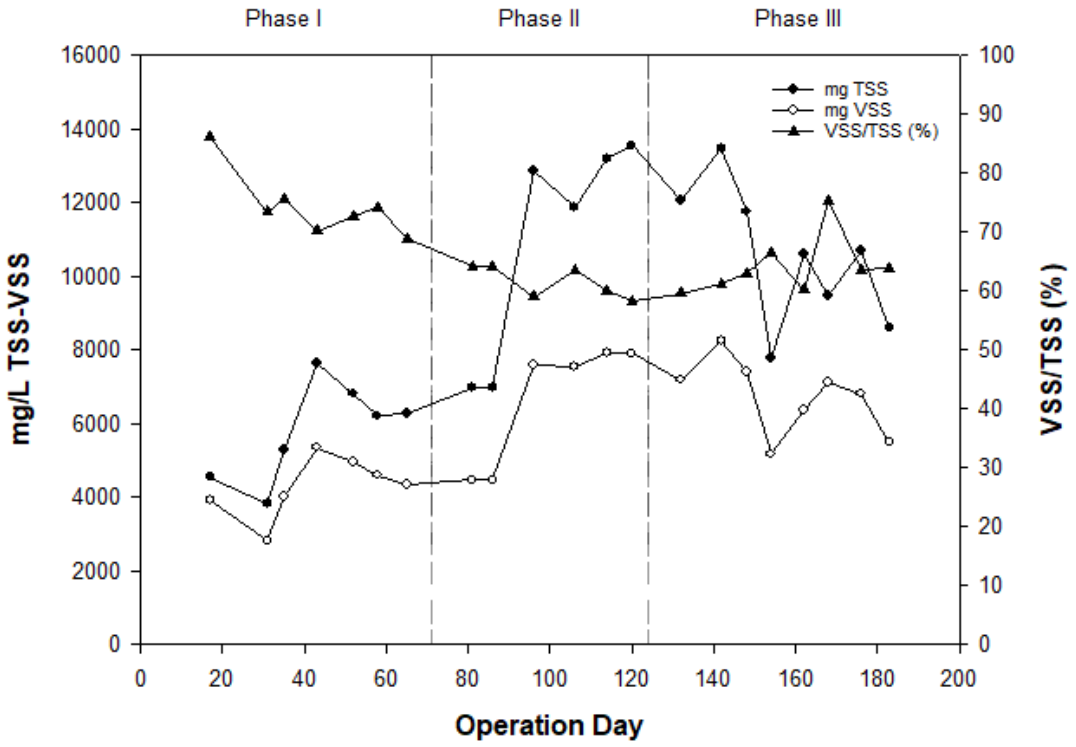

Figure 4.6 TSS-VSS and VSS/TSS ratios throughout the reactor operation.

In conclusion, the presented data outlines a comprehensive approach to granule harvesting. The harvesting process, which commenced after the 124th day of reactor operation, involved collecting dry biogranules from the reactor. Subsequent harvesting events were carried out to maintain VSS levels above 5000 mg/L, a critical threshold chosen to safeguard against potential losses in microbial activity and reactor efficiency. Total amount of dry biogranules harvested during Phase III had a dry weight of 16.83 grams, and the stability of the reactor during this period confirmed the possibility of harvesting as well as ensuring the continuity of microbial activity within the reactor. Notably, the average VSS/TSS ratio during Phase III slightly increased to 64% ± 1.7, compared to the average ratio of approximately 61.5% ± 1 observed during Phase 2 before harvesting commenced. Findings in Phase III revealed the long-term stability of biogranule production reactors designed for production of non-axenic self-healing agents for potential application in cementitious composites.

4.3.2. Urea Hydrolysis Activity of the Harvested Biogranules

In this section, an overview of the reactor's urea hydrolysis performance throughout its operation is provided. The introduction features a graph Figure 4.7 displaying urea hydrolysis across all phases of reactor operation. Phase 1 and Phase 2 illustrate the granules' activity within the reactor before the start of the harvest process. On the 124th day of reactor operation, the harvest of granules was initiated, marking the beginning of Phase 3. This phase involves interpreting urea hydrolysis outcomes through analyzing Total Ammonium Nitrogen (TAN) levels in samples collected during the harvest process. Throughout Phase 3, granule activity was carefully monitored. The analysis results indicate that activity remained consistent; in fact, during Phase 3, the total urea hydrolysis activity exceeded 90%, demonstrating its effectiveness.

In Phase 3, based on the results of reactor cycles, a urea hydrolysis efficiency of 58% in the anoxic phase, 32% in the aerobic phase, and a total 91% urea hydrolysis within the reactor were achieved. These findings further confirm that the harvest process, similar to pH regulation, did not negatively impact reactor performance. Furthermore, granules extracted from the reactor at specific intervals for potential use in concrete applications did not disrupt urea hydrolysis activity.

In summary, the presented results underscore the reactor's reliable and consistent urea hydrolysis performance across different operational phases. The consistent urea hydrolysis activities across distinct phases emphasized the stability of granule production reactor. This reinforces the reliability of utilizing reactor-derived granules for various applications, including development of microbial self-healing concrete, without compromising their urea hydrolysis efficiency.

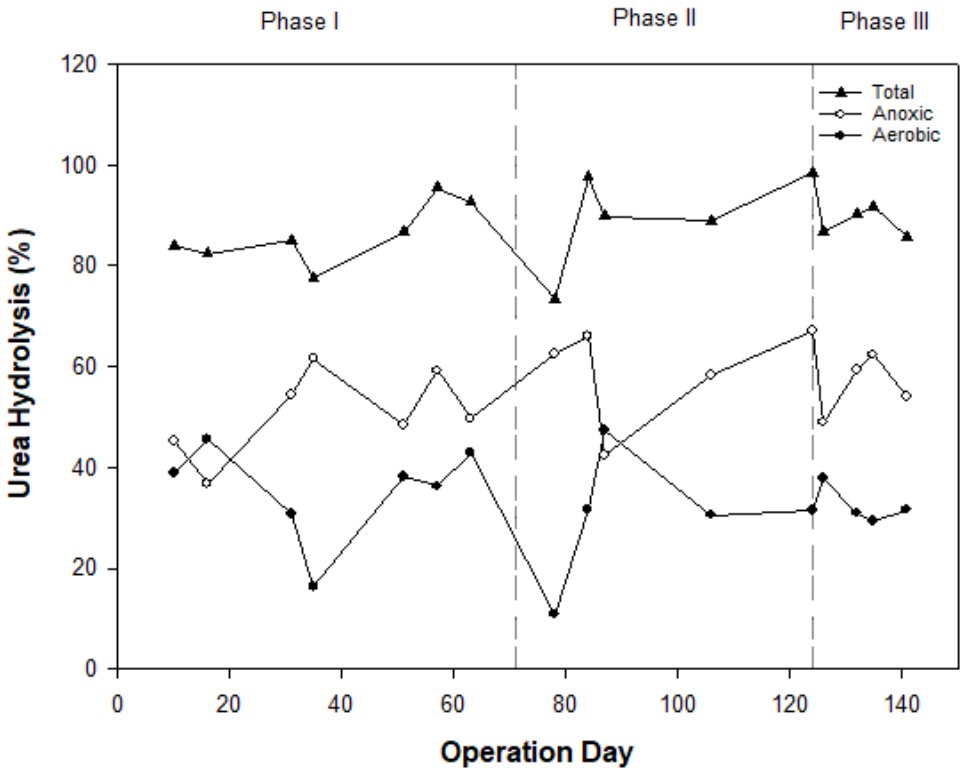

Figure 4.7 Urea hydrolysis in all operation days throughout reactor operation.

4.3.3. Nitrate Reduction Activity of the Harvested Biogranules

During Phase 3, the nitrate reduction activity of the harvested reactor was assessed. This evaluation showed that on the 124th day of reactor operation, the nitrate reduction efficiency was 98%. After three harvest cycles, which extended up to the 154th day, the nitrate reduction efficiency remained at 98%. This confirmed the sustained nitrate reduction capability of the reactor granules even after extended operational periods.

Furthermore, the nitrate reduction activities of the granules, intended to be added to concrete mixtures, were examined. According to the resuscitation tests, which will be elaborated on in subsequent sections, revealed that these granules were able to efficiently consume 200 mg/L of NO_3-N within just 3 hours. This analysis, conducted as part of pre-application testing, further validated the nitrate reduction activities of the granules.

.

In conclusion, the study conducted a comprehensive assessment of nitrate reduction activities, spanning multiple phases of reactor operation. During Phase 3, the harvested reactor consistently demonstrated an impressive nitrate reduction efficiency of 98%, both at the start of granule harvesting on the 124th day and after three extended harvest cycles, which extended up to the 154th day. These results confirm the sustained nitrate reduction capability of the reactor granules even after prolonged operational periods. In summary, the study encompassed various phases, ranging from initial assessments to extended reactor operations and pre-application tests. These phases collectively confirmed the nitrate reduction activities of the granules.

4.3.4. Assessing Settling Characteristics of Biogranules

Continuing from the previous section, Phase 3 focuses on understanding the behavior of biogranules after they have been harvested. This phase provides a unique opportunity to explore how biogranules react to changes in operational conditions following extraction. A crucial part of this analysis involves monitoring two key metrics, SVI_{30} and SVI_5, which give valuable insights into how the microbial culture settles. Similar to the significant pH adjustments during the shift from Phase 1 to Phase 2, it's reasonable to assume that comparable operational changes could impact the post-harvest qualities of the collected biogranules in Phase 3.

Following the 124th-day harvest, there was no significant increase in the reactor's SVI_{30}. However, consecutive harvests on the 147th and 149th days resulted in SVI_{30} analyses showing an increase of over 20 ml/g. After the harvest on the 175th day, the reactor's SVI_{30} reached approximately 30 ml/g. Furthermore, following weekly harvests from day 175 onwards, the reactor's SVI showed a reduction after the 181st and 189th day harvests (Figure 4.8).

Interestingly, while conducting harvests once or twice a week did not exhibit a notable increase in SVI_{30}, conducting harvests every two days resulted in a more pronounced alteration in the settling behavior of the granules. The phenomenon of more frequent harvesting, especially every two days, significantly impacting the settling behavior of the

granules can be attributed to the complex balance within the microbial community of the biogranules. Frequent harvesting disrupts the stability of the microbial ecosystem by removing a substantial portion of the biomass, including key organisms responsible for maintaining favorable settling characteristics. This disruption can lead to a temporary destabilization of the granular structure, resulting in variations in settling behavior, as observed through changes in SVI_{30} values.

Furthermore, the shortened time between harvests may not provide adequate opportunity for the microbial community to recover and adapt, leading to a more pronounced response in the granules' settling characteristics.

The same graph on Figure 4.8 has also presented a curve illustrating the VSS/TSS ratios. According to the graph, a significant shift in the ratio, reaching 66%, was noted on the 154th day, following two consecutive harvests. On the 168th day, the VSS content reached 75%. Subsequent to the harvests carried out after the 175th day, a consistently stable VSS ratio of approximately 63% was recorded on a weekly basis. These changes in the VSS/TSS ratio can be attributed to several factors. Firstly, the alterations in reactor size distribution, which occurred due to the removal of granules, can influence the distribution of granules within the reactor. Additionally, the decrease in settling velocity of the granules may lead to an increase in VSS at the analyzed points.

To integrate these findings and provide a comprehensive understanding, it can be observed that the SVI_{30} and the VSS ratio generally exhibited an inverse increase and decrease during this phase. As the settling rate of the granules decreased, an increase in VSS content was observed at the analyzed points. This suggests that the behavior of the granules, including their settling characteristics, is closely linked to the observed changes in the VSS/TSS ratio.

.

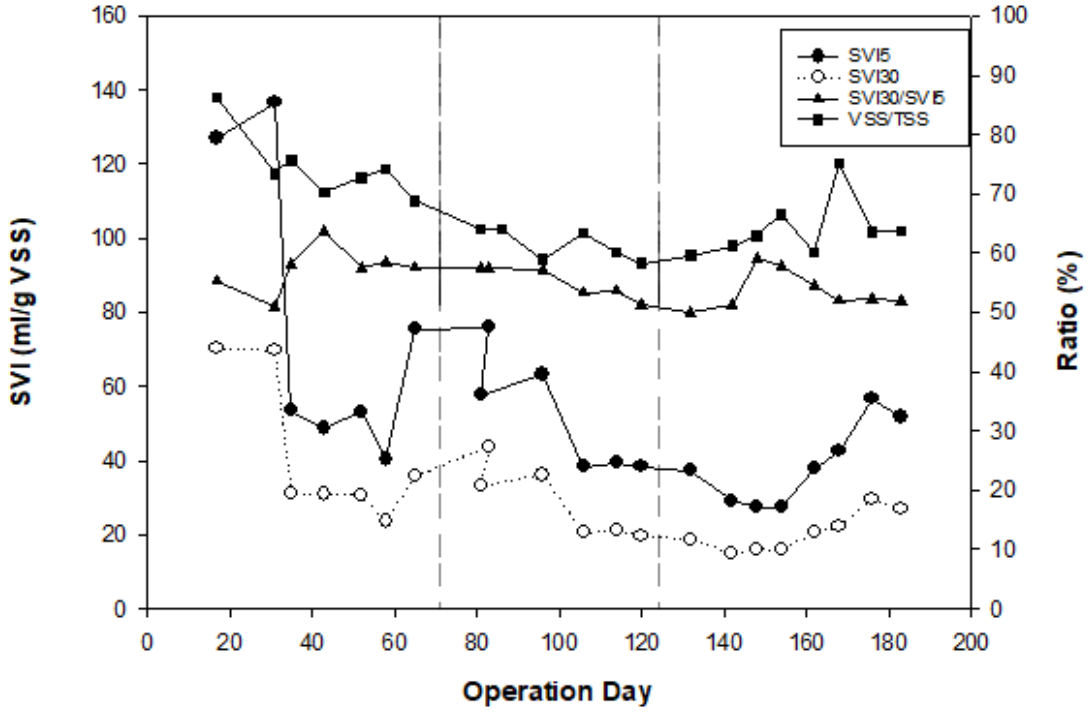

Figure 4.8 Variations in SVI_{30} and SVI_5, as well as the SVI ratio (SVI_{30}/ SVI_5) and the VSS to TSS ratio through the reactor operation.

In conclusion, with Phase 3, a detailed analysis of biogranules after their harvest enabled exploring their behavior in response to post-harvesting operational changes. Key metrics, SVI_{30} and SVI_5, were monitored to gain insights into the settling behavior of the microbial culture within the granules. While the initial harvest on the 124th day did not significantly affect SVI_{30}, consecutive harvests on the 147th and 149th days led to a notable increase. After the 175th day harvest, SVI_{30} reached approximately 30 ml/g. Interestingly, more frequent harvesting, especially every two days, had a pronounced impact on settling behavior, attributed to the disruption of the microbial ecosystem within the granules. This disruption temporarily destabilized the granular structure, resulting in variations in SVI_{30} values.

4.3.5. Granular Size Distribution through reactor operation

The size distribution of granules was compared from day 153 to 188, representing Phase III in Figure 4.9. Granules were first harvested from the reactor on day 124. By day 153, the majority of particles fell within the range of 0.2-0.3 mm, constituting nearly 40% of

the distribution, followed by the 0.3-0.4 mm range, which was almost as abundant at 17%. There were more than 20% of granules in the 0.4-0.5 mm range, and some granules had reached sizes of up to 0.8 mm. After 35 days, on day 188, the most prevalent granule size in the reactor exceeded 40% in the 0.3-0.4 mm range. The reason behind the predominance of granules in the 0.3-0.4 mm to even 0.5 mm size range in the harvested samples can be attributed to the dry granules reintroduced into the reactor during the harvest process. Additionally, microscopic images captured during both the initial phase and Phase 3 were provided in the Figure 4.10.

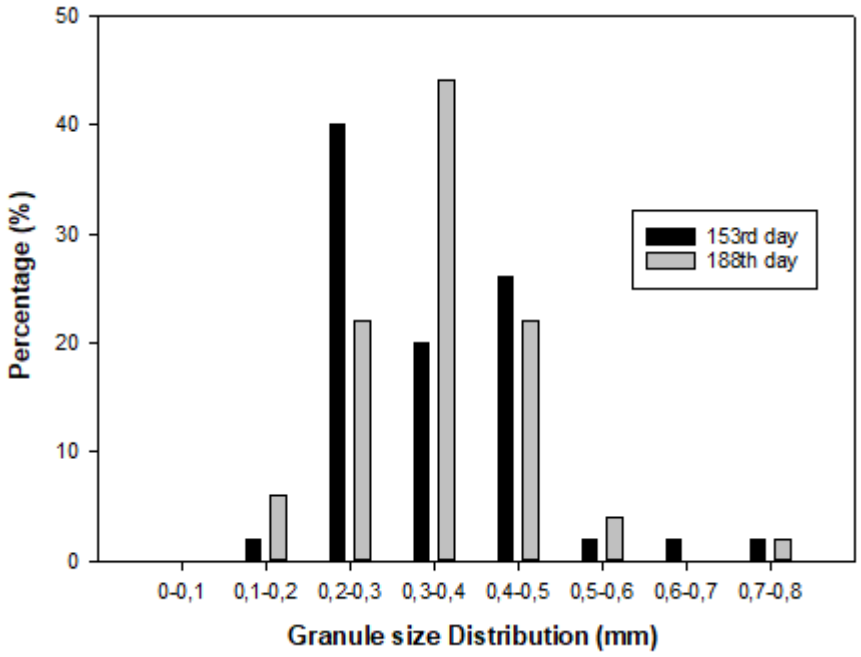

Figure 4.9 Granule size distribution during the reactor operation.

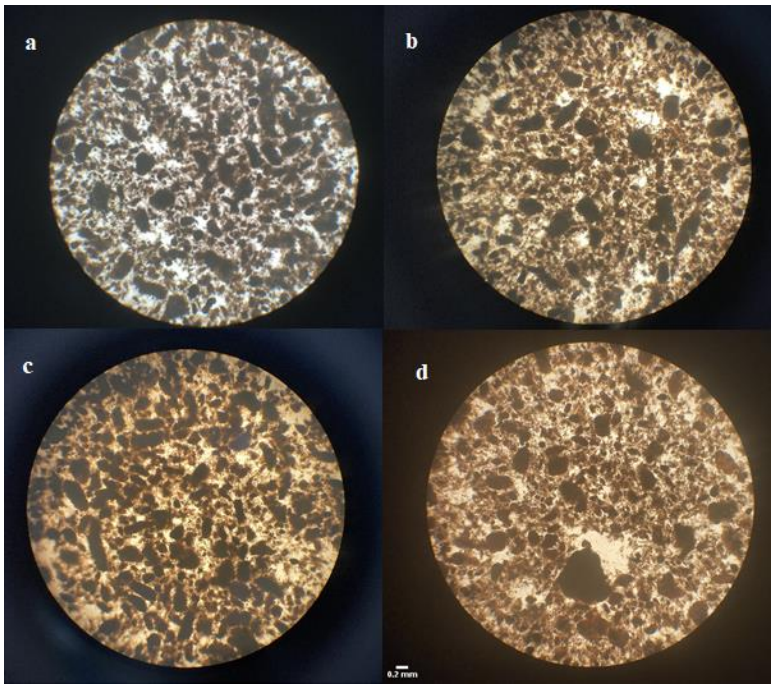

Figure 4.10 Microscopic images of granules on different days: (a)143rd day; (b)163rd day; (c)178th day; and (d)188th day through harvest processing.

In conclusion, In Phase 3, the majority of granules fell within the 0.3-0.4 mm size range, with some granules reaching sizes of up to 0.5 mm. This shift in size distribution was influenced by the reintroduction of dry granules during the harvest process.

4.3.6. Urea Hydrolysis Performance of microbial self-healing agents: Insights from Resuscitation Tests

The resuscitation performance of biogranules refers to their ability to regain activity and functionality after undergoing a period of stress or inactivity, such as drying or storage. During resuscitation, the performance of biogranules is evaluated based on various factors, including their metabolic activity, nutrient uptake, and functional capabilities. In the specific context in, the resuscitation performance of the biogranules was assessed based on their urea hydrolysis activity. The resuscitation performance of biogranules was evaluated after a drying process.

In a batch test conducted, it was observed that the dried granules exhibited urea hydrolysis activity within the initial 6-hour resuscitation period. Initial concentration of each batch was set to 1000 mg/L. During this period, the biogranules produced 240 mg/L of Total Ammoniacal Nitrogen (TAN) through urea hydrolysis, corresponding to a urea hydrolysis efficiency of 87%. By the end of the 24-hour resuscitation period, the TAN concentration reached 442 mg/L, indicating complete urea hydrolysis: 100% (Figure 4.11). The results indicated that the dried granules exhibited urea hydrolysis activity within the initial 6 hours of the resuscitation period, producing a significant amount of Total Ammoniacal Nitrogen (TAN). This suggests that the biogranules successfully recovered their urea hydrolysis capability, demonstrating a positive resuscitation performance in terms of urea hydrolysis. The TAN results obtained from the resuscitated dry biogranules are illustrated in the Figure 4.11 below representing a complete 12-hour cycle. This cycle consists of alternating 3-hour periods of anoxic and aerobic conditions.

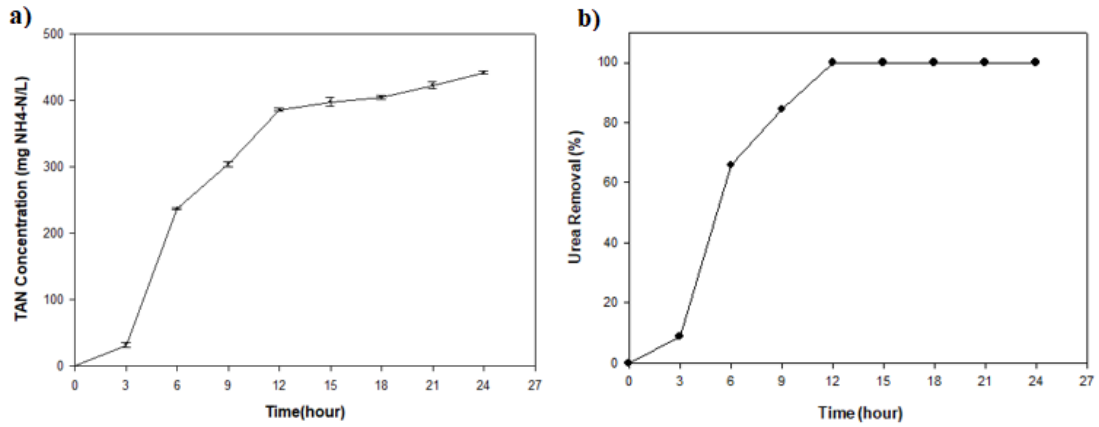

Figure 4.11 a) TAN dynamics; b) urea hydrolysis in resuscitated dry biogranules with alternating 3- hour anoxic and 3-hour aerobic periods.

4.3.7. Urea Hydrolysis Performance of Biogranules: Impact of the Presence of yeast extract

Continuing from the previous resuscitation test, this section primarily presents the outcomes of a subsequent targeted resuscitation test, specifically aimed at investigating the impact of yeast extract inclusion on urea hydrolysis activity. Similar to the preceding

test, this evaluation focused on the ability of dry granules to remove urea under anoxic conditions.

The experimental design maintained a bacterial concentration of 0.5 g/L, and the VSS:TSS ratio of the harvested biogranules was meticulously adjusted to 60±1%, resulting in a batch containing 0.83 g/L of biogranules. In this study, the central point of interest revolved around examining the potential influence of yeast extract presence on urea hydrolysis activity. To address this question, the investigation was divided into two separate batches: Yeast Extract-Containing Batch: This batch included yeast extract alongside the biogranules. Yeast extract-Absent Batch: This batch served as a control, containing biogranules without yeast extract.

The TAN analysis was conducted at the end of the 4th and 6th hours, revealing consistent findings for both batches. Initial concentration of each batch was set to 1000 mg/L. In Batch 1, which included yeast extract, TAN concentrations were 22.4 mg/L and 36.4 mg/L at the 4th and 6th hours, respectively. For Batch 2, without yeast, the corresponding TAN concentrations were 18.67 mg/L and 30.8 mg/L.

Interestingly, the comparison between the two batches yielded similar results, suggesting that the presence of YE had minimal influence on TAN outcomes (Figure 4.12). This highlights that the addition of YE, alongside urea, calcium formate, and calcium nitrate, did not lead to adverse TAN formation.

In summary, this section provides insights into the evaluation of biogranules' resuscitation performance, particularly focusing on urea hydrolysis activity. It also explores the potential impact of YE presence on biogranules' performance under anoxic conditions by comparing two batches, one with yeast and one without. Interestingly, under the specific anoxic conditions examined, the TAN analysis displayed comparable results for both batches, regardless of the presence or absence of yeast. This finding reinforces the notion that the mere presence or absence of yeast did not lead to a substantial difference in TAN generation. This observation reinforces the notion that the addition of yeast, alongside urea, calcium formate, and calcium nitrate, did not result in any adverse Total Ammonium Nitrogen (TAN) formation.

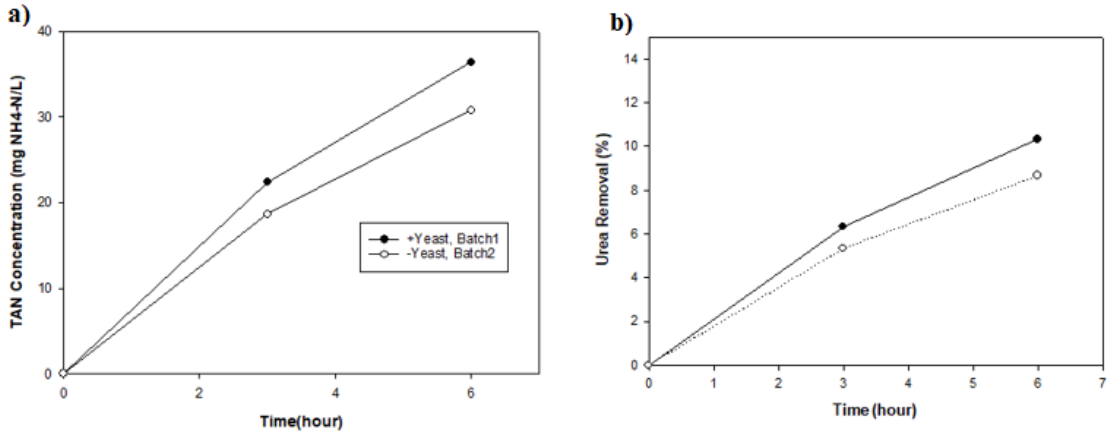

Figure 4.12 a) TAN analysis; b) urea hydrolysis results for batch 1 (with yeast extract) and batch 2 (without yeast extract) at the 4th and 6th hours.

The initial resuscitation of dried granules, conducted under alternating 3-hour anoxic and 3-hour aerobic conditions and with the presence of yeast extract, demonstrated a rapid and efficient recovery of urea hydrolysis capability within the first 6 hours, reaching 100% efficiency by the 9–12-hour mark. Furthermore, the subsequent investigation into the influence of yeast extract on urea hydrolysis activity revealed that the presence or absence of yeast had minimal effect on TAN formation under the examined anoxic conditions. These findings confirmed that the granules can be used in dry form as microbial self-healing agents, and when the environmental conditions are appropriate, they can resuscitate in hours. Their resuscitation and urea hydrolysis activity are important for achieving reliable and expectable crack healing performance.

4.4.Crack Healing Performance of Mortar Samples in Different Water Environments

Following the execution of our methods and the collection of data, the results of our study were meticulously examined and interpreted. The methodology had involved subjecting mortar samples to a uniaxial tensile test at a speed of 0.01 mm/s on day 28, which had resulted in the creation of cracks on cementitious composites with varying widths. The crack widths observed in the concrete samples had ranged from 100±20 µm to 600±30 µm. A comprehensive analysis of healing capacities had been conducted across distinct

sample categories, including reference samples, abiotic control samples, and bio mortar samples. Importantly, this analysis had taken into consideration similar crack intervals among the samples.

Throughout the study, a consistent single bacterial dosage had been employed. This particular dosage had been determined with reference to a 2021 thesis [181], which had investigated the effectiveness of various bacterial concentrations in a bio concrete mixture for crack healing. Among the different mixtures studied, the "BioC-0.25%" mixture contained a bacterial concentration equivalent to 0.25% of the cement's weight, in the form of biogranules. This specific dose was chosen for use in current research. It's worth noting that this particular mixture represented the lowest bacterial dose tested in both fresh and hardened mortar experiments in cited research [181]. As outlined in the methodology section, 1.88 grams of biogranules were introduced into the dry mortar mixture across all batches. The procedure for casting mortar into the concrete molds, referencing thesis studies[181], [208] and the method for creating cracks, referencing another thesis [222], were detailed extensively in the methodology section. Subsequently, these mixtures were exposed to realistic water conditions.

In summary, the environmental impact of incorporating biogranules capable of urea hydrolysis and nitrate reduction into the mortar mixture at a consistent dosage had been evaluated in thesis study. Detailed examinations had been conducted separately for tap water, marine water, and rainwater, followed by a collective comparison of all three environments in the subsequent sections.

4.4.1. Healing Performance in a Tap Water Environment

The evaluation of crack healing performance in a tap water environment provides valuable insights into the ability of mortar samples to self-heal under common water conditions.

In Figure 4.13 below depicts the crack healing performance of the reference samples over a 4-week period in a single graph. Notably, there is an approximate 15% increase in the healing percentage from the first to the second week. However, as the third week is entered, there is no statistically significant change observed in the percentage of crack closure. Even during the fourth week, notable healing progress for cracks up to 300 µm in width is not observed. Only a marginal improvement of approximately 5% is noted for larger crack widths. This suggests that the autogenous healing process primarily concludes within the initial two weeks.

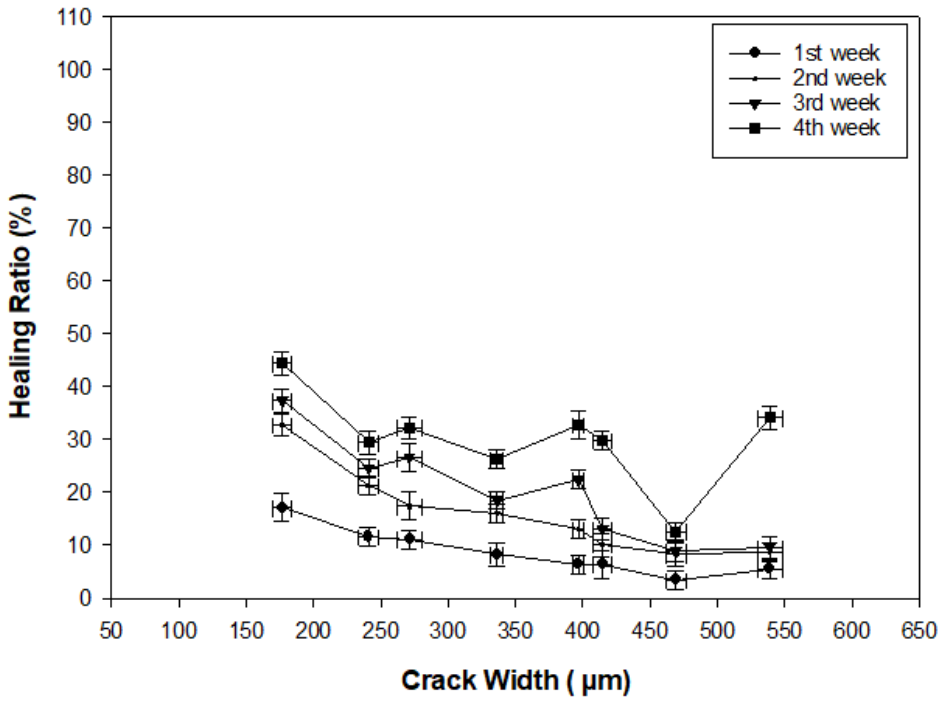

Figure 4.13 Crack self-healing performance of reference mortar samples under tap water at the end of 4 weeks of immersion treatment.

Progressing to the evaluation of autogenous healing, abiotic control samples were employed alongside the reference samples, following the detailed methodology with specified proportions of basic mortar materials and nutrients. These control samples exhibited crack widths ranging from 60 µm to 430 µm (Figure 4.14), displaying a trend similar to the reference samples. There was an increase in the healing percentage during the second week.

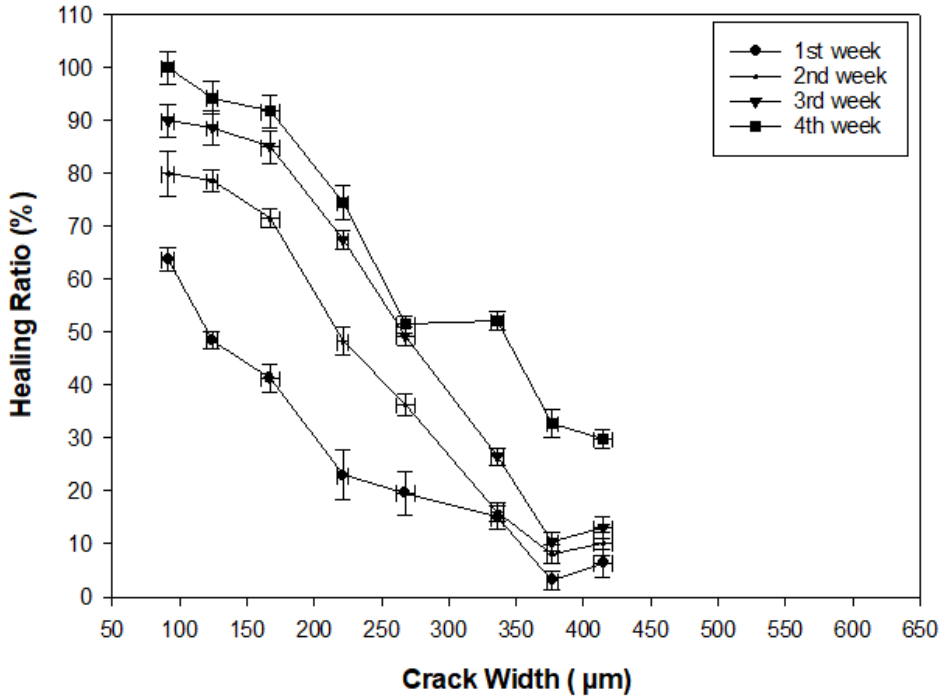

Figure 4.14 Crack self-healing performance of abiotic mortar samples under tap water at the end of 4 weeks of immersion treatment.

Turning the attention to the crack widths observed in bio mortar samples submerged in tap water, a range of 180 µm to 575 µm was noted. In the biotic mortar samples, during the first week, the healing performance varied between 30% and 54% for cracks with widths up to 300 µm, whereas for cracks wider than 300 µm, healing ranged from 10% to 30%. By the end of the second week, the two-week crack healing performance was determined to be between 50% to 65% for cracks narrower than 300 µm (Figure 4.15). Towards the end of the third week, healing performance between 65% to 75% was achieved for all observed crack widths, but for larger crack widths, only 15% to 30% healing was observed. By the conclusion of the fourth week, crack closure percentages of 90% and above were achieved for crack widths ranging from 218-240 µm.

Figure 4.15 illustrates the 4-week crack healing performance and self-healing capacity observed in the Bio mortar samples. The increase in crack healing performance noted in the first week showed a slower pace in the second and third weeks, with the progress over time aligning with different crack widths. It is worth mentioning that the healing rate of cracks was higher in the fourth week compared to the preceding weeks. Considering that

autogenous healing dominated the first two weeks, it can be stated that the period when microbial healing became more dominant was in the fourth week. The self-healing threshold of the cement composite repaired through microbial means was determined to be 230 ± 10 µm after four weeks.

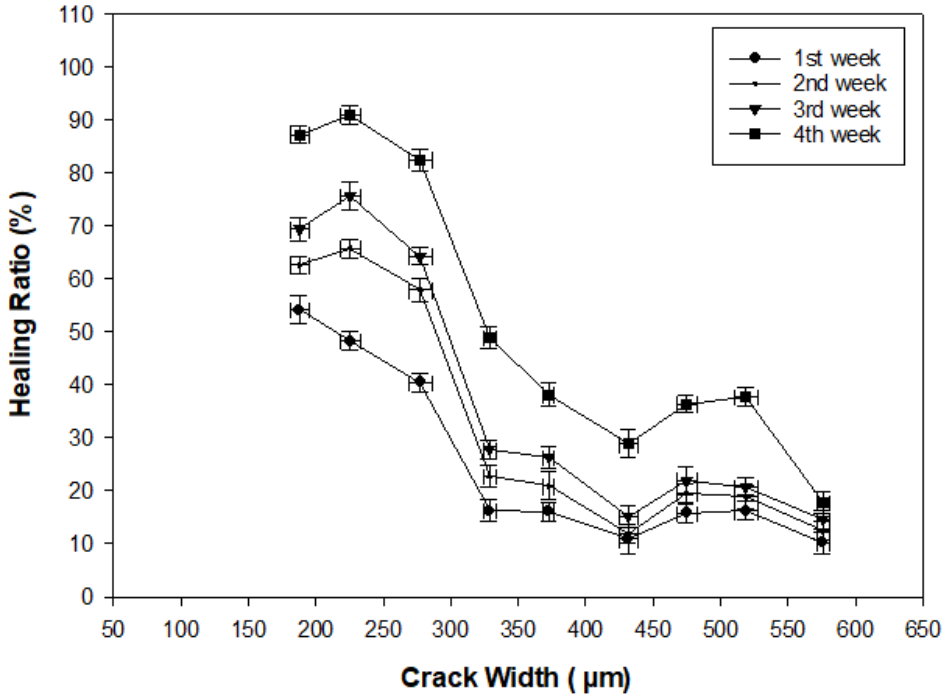

Figure 4.15 Crack self-healing performance of biotic mortar samples under tap water at the end of 4 weeks of immersion treatment.

The final Figure 4.16 and Figure 4.17 offers a concise summary. In the realm of self-healing research, it's established that the maximum crack width achieving healing in 90% of cases serves as a self-healing threshold for cementitious composites. In alignment with this principle, this study has identified and marked the maximum crack width achieving 90% healing on the graphs, enabling a comparison based on this criterion.

In Figure 4.16, there is no crack width for the reference sample that meets the 90% threshold. However, for the abiotic samples, the self-healing limit lies at 176 µm, while for the biotic samples, it extends to 240 µm as the self-healing threshold in terms of crack width. In terms of crack width, there exists a common range of 200-300 µm across graph. The corresponding healing percentages are as follows: for the reference sample, it ranges

from 38% to 30%; for the abiotic samples, it varies from 80% to 52%; and for the biotic samples, it falls between 89% and 66%. This analysis enables a clear understanding of the performance of each sample type concerning self-healing capacity.

A comparison of healing capacities was conducted among the reference samples, control samples, and bio mortar samples, all of which were subjected to similar crack intervals, as illustrated in Figure 4.16. Over the course of four weeks, it was observed that the reference mortar exhibited minimal healing, whereas the abiotic mortar showed partial closure of cracks, as depicted in Figure 4.16. Microscopic images (Fig 4.17) were taken as outlined in the procedure, employing a light microscope, and the healing efficiencies were computed using the formula detailed in the methodology section.

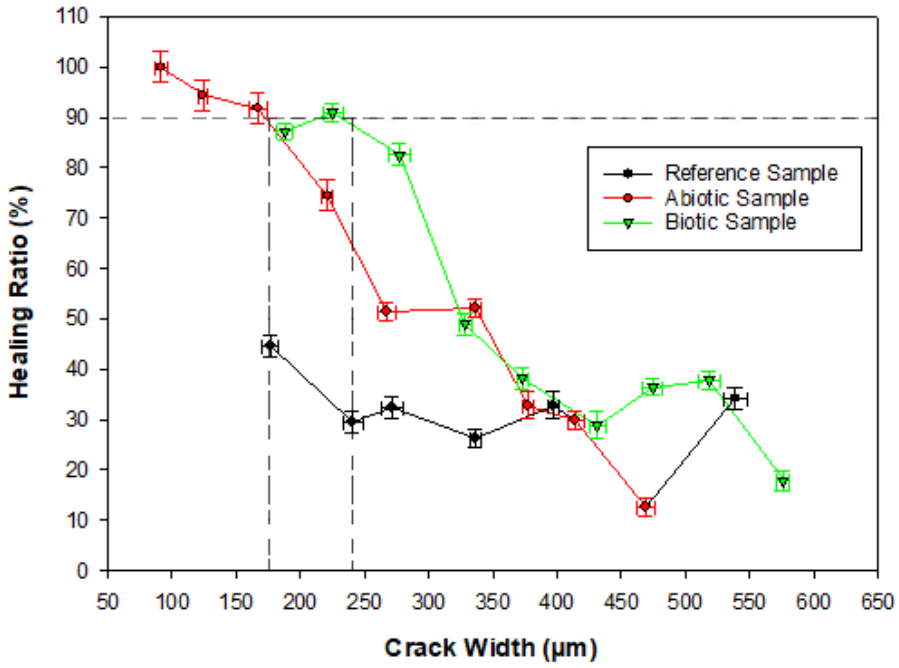

Figure 4.16 Crack self-healing performance under tap water conditions at the end of 4 weeks of immersion treatment.

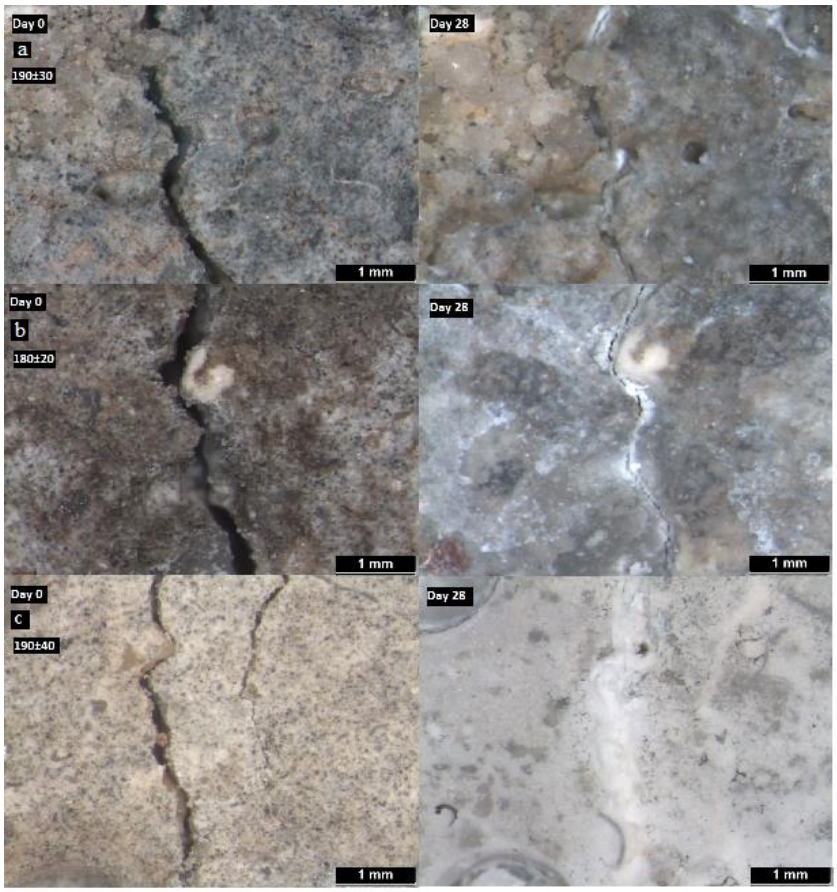

Figure 4.17 Crack healing in a) reference mortar; b) abiotic mortar; c) bio mortar containing biogranules under tap water immersion condition.

In conclusion, the evaluation of crack healing performance in a tap water environment has provided valuable insights into the self-healing capabilities of mortar samples under typical water conditions. Within the common crack width range of 200-300 µm, the analysis revealed distinctive healing percentages for each sample type: the reference sample ranged from 30% to 38%, the abiotic samples varied from 52% to 80%, and the biotic samples consistently fell between 66% and 89%. These findings offer a clear understanding of each sample's self-healing capacity.

Furthermore, the results indicated that the reference mortar displayed minimal healing, failing to meet the 90% self-healing threshold for any cracks. In contrast, the abiotic mortar exhibited partial closure of cracks, with a self-healing limit of 176 µm. The biotic mortar samples, enriched with biogranules, demonstrated a more promising performance, achieving a self-healing threshold of 240 µm, marking a significant advancement. This

suggests that cracks as wide as approximately 55 μm could be effectively healed through microbial means.

4.4.2. Healing Performance in a Rainwater Environment

Assessing healing performance in a Rainwater environment extends our understanding of the self-healing potential of mortar samples under conditions more representative of real-world exposure.

Figure 4.18 presents the crack healing performance of reference samples over a span of 4 weeks in a single graph. As seen in healing garph, there is a notable increase in the healing percentage after the second week. This indicates the completion of autogenous healing within the initial two weeks. By the end of the second week, there is healing ranging from 40% to 66% for crack widths up to 175 μm. In the same crack width range, the healing in the third week shows a slight increase, reaching 45% to 70%. For reference samples, where healing exceeding 90% is absent, the most favorable healing percentage is observed during the fourth week. Here in 4th week, healing rates range from 60% to 75% for crack widths smaller than 140 μm. In the range of 200-250 μm, healing percentages range from 30% to 45%.

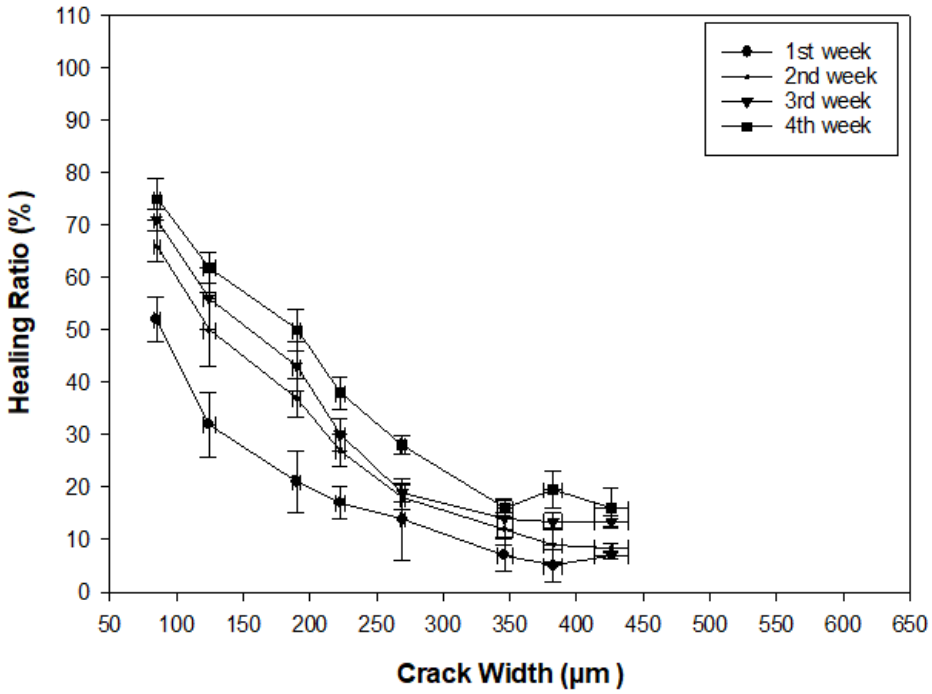

Figure 4.18 Crack self-healing performance of reference mortar samples under rainwater at the end of 4 weeks of immersion treatment.

In the abiotic mortar samples, crack widths ranged from 70 µm to 420 µm (Figure 4.19). Approximately 40% closure was observed in the control samples for crack widths narrow than 170 µm, and also up to 200 µm, with a 30% closure rate, and for cracks up to 300 µm, an around 20% closure rate was achieved in the first week. The same crack width ranges exhibited closure performances of 60%, 50%, and 30% respectively in the second week. After three weeks, crack widths between 70 µm and 170 µm showed an improvement of approximately 72% ± 6, and crack widths up to 200 µm exhibited a nearly 65% closure rate. Furthermore, based on the results of the third week, crack widths between 200 µm and 250 µm achieved closures ranging from 65% to 50%, while crack widths between 250 µm and 350 µm improved between 50% and 30% ±2. A representative visual of cracks healing autogenously in the abiotic samples is provided in Figure 4.19. Consistent trends in crack healing rates and closure rates were not observed in the control samples. However, after four weeks, it was found that cracks smaller than 142 µm exhibited the highest healing performance at 80%, cracks narrower than 200 µm showed a healing performance of around 70% and cracks up to 250 µm exhibited a healing rate of about 50%. For some larger cracks, healing ranged from 28% to 50%.

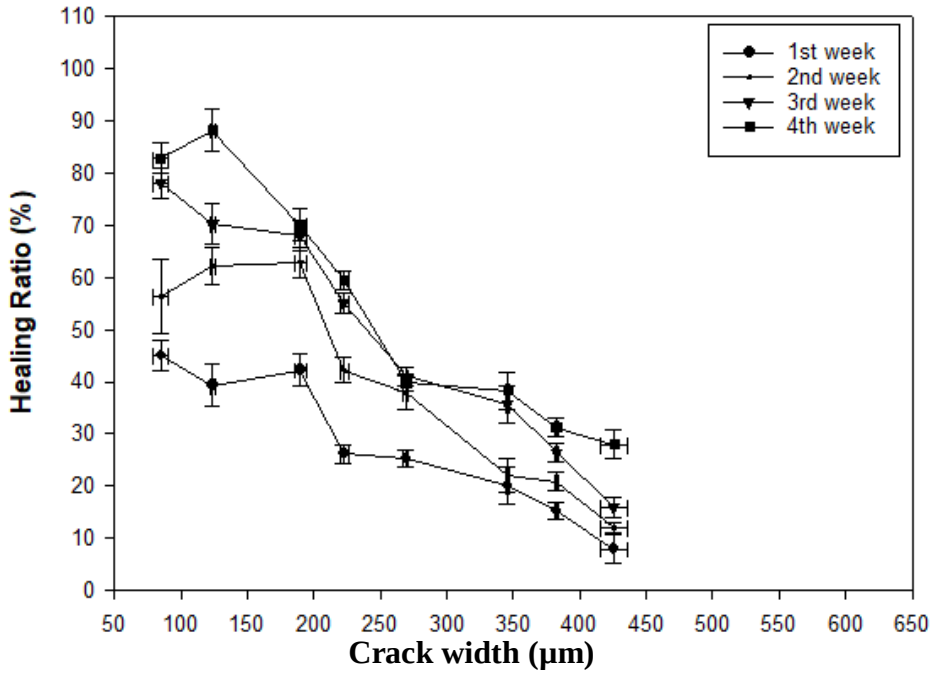

Figure 4.19 Crack self-healing performance of abiotic mortar samples under rainwater at the end of 4 weeks of immersion treatment.

In rainwater, the crack widths obtained from the Bio-0.25% samples ranged between 75 µm and 600 µm. During the first week, cracks with widths smaller than 220 µm exhibited healing ranging from 40% to 50. In the second week, within the same crack width range, cracks exhibited healing that varied around 55% ± 5. At the end of the third week, within the same crack width range, the closure percentage ranged between 65% and 84. For larger cracks measuring up to 250 µm, healing reached levels as high as 55%±5, whereas for cracks exceeding 400 µm in width, the healing rates dipped below 40%. According to the graph, the growth slope between the first and second weeks and the growth slope between the third and fourth weeks are parallel. The initial two weeks demonstrate autogenous healing dominance, while the latter two weeks indicate microbial healing predominance.

Looking at the 4-week period, it was determined that the widest crack width showing over 90% healing was 156 µm. Cracks ranging from 157 to 210 exhibited approximately 85% ± 5% healing after 4 weeks. Cracks within the range of 210 to 250 showed about 75% ± 5% healing, while cracks with widths of 250-300 µm achieved around 60% ± 10 healing.

The 4-week microbial healing progress in Bio-0.25% samples in rainwater is depicted in the Figure 20.

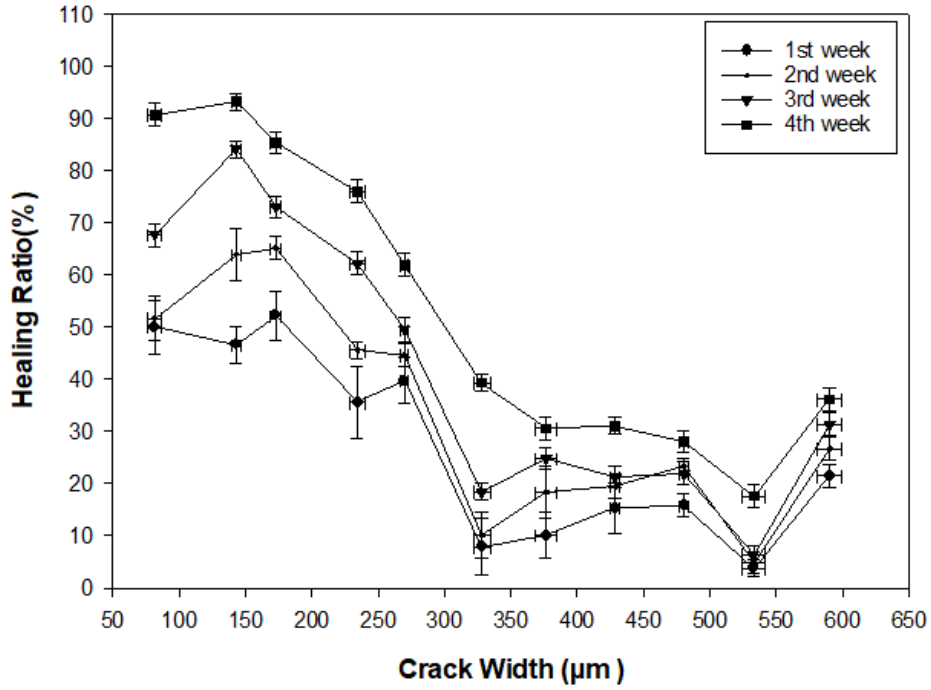

Figure 4.20 Crack self-healing performance of biotic mortar samples under rainwater at the end of 4 weeks of immersion treatment.

A comprehensive visual comparison is shown in combined graphs depicted in Figure 4.21. Considering concrete samples exposed to rainwater, graphs indicate that neither the reference nor abiotic samples meet the 90% self-healing threshold with any crack width. In contrast, biotic samples reveal a self-healing limit at 156 µm. In Figure 4.21, for crack widths between 200-250 µm, the corresponding healing percentages are as follows: reference sample, 45% to 32%; abiotic samples, 65% to 48%; and biotic samples, 81% to 70%. Similarly, for crack widths between 150-200 µm, healing percentages are: reference sample, 57% to 46%; abiotic samples, 80% to 66%; and biotic samples, 91% to 81%. This comprehensive analysis offers clear insight into the self-healing abilities of each sample type. For 300- µm -wide cracks, biotic samples achieve around 50% healing, while abiotic samples reach roughly 40%. In contrast, reference samples show only up to 22% healing. This data provides valuable understanding of the self-healing potential for each sample type. The maximum crack width exceeding 80% healing in abiotic samples is

approximately 150 µm, while in biotic samples, the crack width is around 220 µm. This indicates that the 70- µm difference represents microbial healing in rainwater.

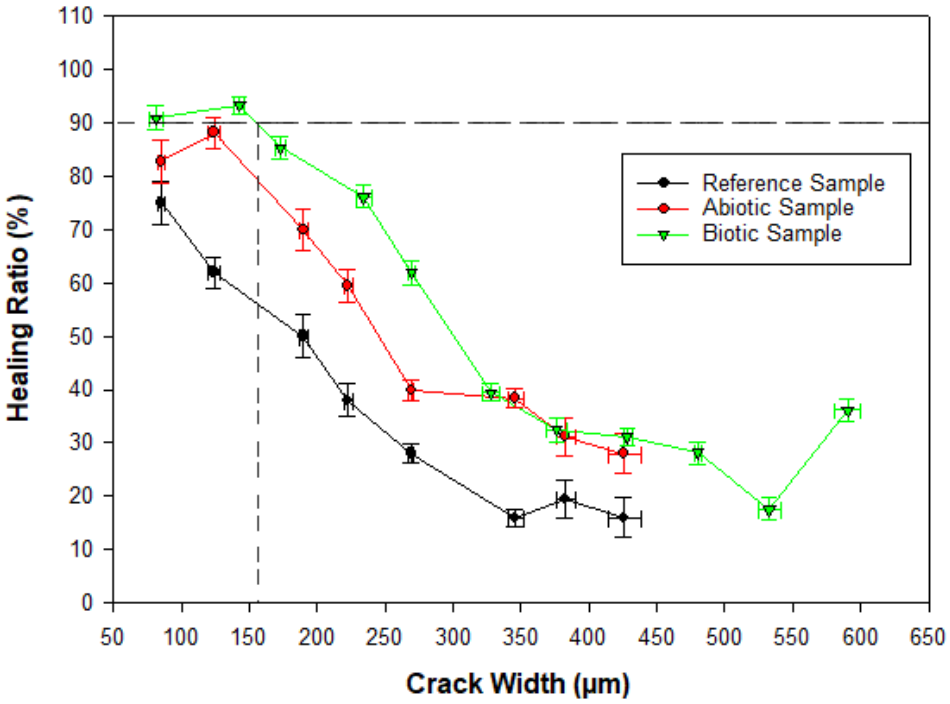

Figure 4.21 Crack self-healing performance under rainwater conditions at the end of 4 weeks of immersion treatment.

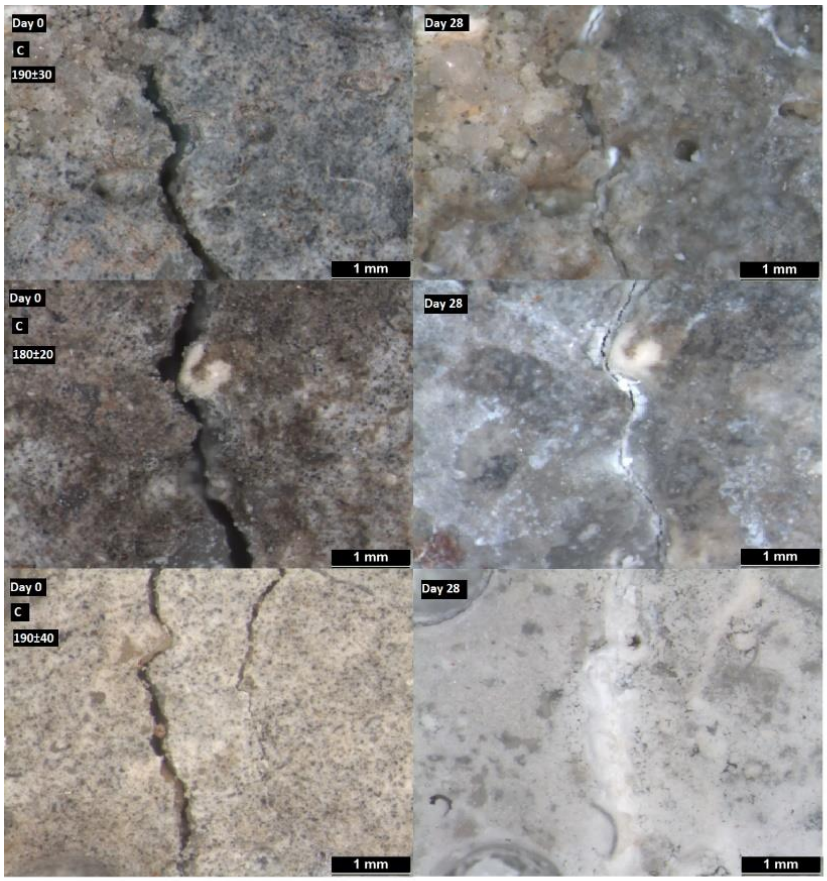

Figure 4.22 Crack healing in a) reference mortar; b) abiotic mortar; c) bio mortar containing biogranules under rainwater immersion conditions.

Biotic samples surpass both reference and abiotic samples in terms of self-healing in this specific range. These results underline the superior self-healing potential of biotic mortar samples, followed by abiotic samples, while reference samples exhibit the lowest healing performance for cracks within the 200-300 µm width range. In evaluating the self-healing performance of mortar samples under rainwater conditions, several key findings emerge. The reference and abiotic mortar samples, when subjected to rainwater exposure, do not achieve the 90% self-healing threshold across any crack width range. In contrast, the biotic samples display a clear self-healing limit at approximately 156 µm in terms of crack width. It is important to note that, in this research study, the 90% healing limit, which signifies the microbial healing threshold, µm could not be determined in abiotic mortar samples due to their lower healing capacity. Therefore, when the maximum crack widths exceeding 80% self-healing are considered, it was found that in the limit for abiotic samples is approximately 150 µm, whereas in biotic samples, this threshold extends to

around 220 µm. This distinction suggests that microbial activity plays a significant role in achieving self-healing in rainwater conditions, contributing to the observed differences.

4.4.3. Healing Performance in a Marine Water Environment

Investigating the healing performance in a marine water environment adds to our comprehension of the self-healing capabilities of mortar samples under conditions that simulate real-world exposure.

Figure 4.23 presents the weekly improvement graphs of reference samples. The crack widths in the reference samples ranged from 130 µm to 430 µm. Notably, the highest crack healing performance during the first week was achieved in cracks ranging from 130 µm to 250 µm, with a healing percentage of 60% to 35%. By the end of the second week, the same range of crack widths had improved to around 56% to 82%, and the closure percentage for cracks with a width of 180 ± 10 µm had surpassed 80%. During the third week, there was no significant change in the healing percentage. Healing percentages were approximately 77 ± 7% for cracks narrower than 225 µm, around 65% for 250 µm cracks, and around 50% for 300 µm cracks. By the end of the fourth week, the healing percentage for cracks narrower than 250 µm was recorded as 80 ± 10% (Figure 4.23). Throughout this process, the largest crack healing percentage exceeding 90% for the reference mortar sample was achieved for cracks with a width of 170 µm.

In the study, the rate of crack closure was examined, and it is stated that there was no statistically significant change in this rate after the second week. This indicates that the rate of crack closure does not significantly change after the second week, suggesting that autogenous healing is predominantly completed within the first two weeks. Therefore, referenced study's authors interpret this as evidence that autogenous healing is generally completed within the first two weeks when cracks initially form, and the healing process occurs rapidly during that period.

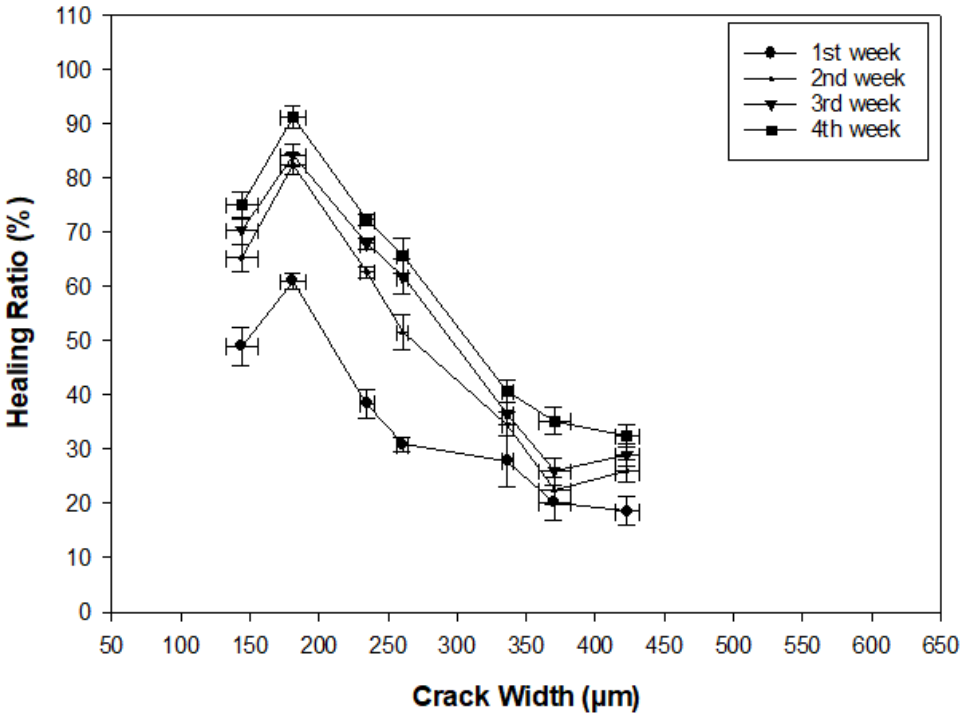

Figure 4.23 Crack self-healing performance of reference mortar samples under marine water at the end of 4 weeks of immersion treatment.

The abiotic mortar samples exhibited crack widths ranging from 100 µm to 485 µm, as depicted in Figure 4.24 Remarkably, these samples displayed a notable closure rate of around 40% for cracks within the range of 105 µm to 230 µm during the first week. This trend persisted into the second week, with these particular crack widths showing a healing performance of approximately 50%. Moreover, even for cracks up to 300 µm in width, healing percentages as low as 32% were achieved. Progressing to the third week, the healing performance increased to around 60% for crack widths up to 230 µm. Notably, for cracks ranging from 100 µm to 200 µm, an even higher healing percentage of over 70% was achieved. As the fourth week concluded, crack widths up to 200 µm provided healing percentages exceeding 85%, while widths up to 230 µm exhibited a healing rate of about 75%. For cracks up to 300 µm in width, the abiotic healing reached approximately 60%. A visual representation of autogenously healing cracks in the control samples is provided in Figure 4.24.

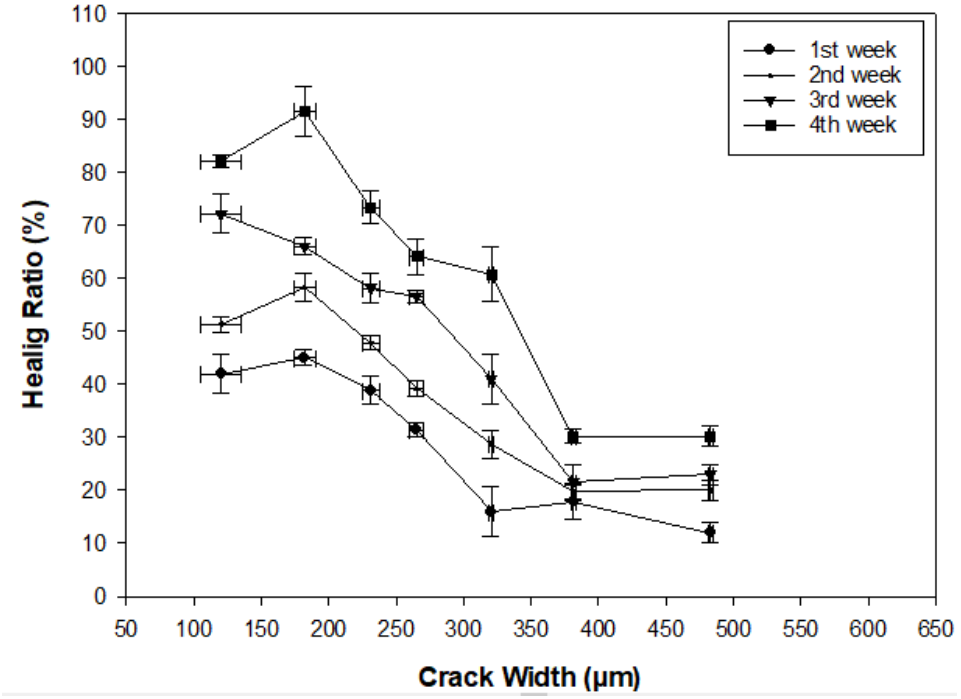

Figure 4.24 Crack self-healing performance of abiotic mortar samples under marine water at the end of 4 weeks of immersion treatment.

In Bio mortar samples immersed in marine water, crack widths ranged from 124 µm to 540 µm. Regarding the biotic mortar samples, in the first week, the healing performance exhibited variation, approximately at 30 ± 2%, for cracks with widths up to 250 µm. Subsequently, in the second week, the healing rate for cracks up to 250 µm widened to 55 ± 5%. Upon reaching the conclusion of the third week, cracks up to 250 µm in width showed a healing percentage ranging around 78 ± 3%, while cracks with a width of 300 µm exhibited a healing performance of 56% during the same week. However, larger crack widths displayed healing percentages ranging from only 20% to 55%.

Remarkably, by the fourth week's end, crack closure percentages of 90% and above were accomplished for crack widths between 215-253 µm and 125-150 µm. It's worth noting that the healing percentage for wider cracks that closed during the fourth week exhibited a range of 30% to 82% in total. Cracks up to 300 µm in width achieved 76% or higher healing, while cracks exceeding 400 µm in width experienced healing rates below 40%. Figure 4.25 vividly illustrates the 4-week crack healing performance and the self-healing capacity attained in the Bio mortar samples. With the prevalence of autogenous healing

during the initial two weeks, it becomes evident that the third week marked a heightened prevalence of microbial healing. This substantial improvement persisted into the fourth week.

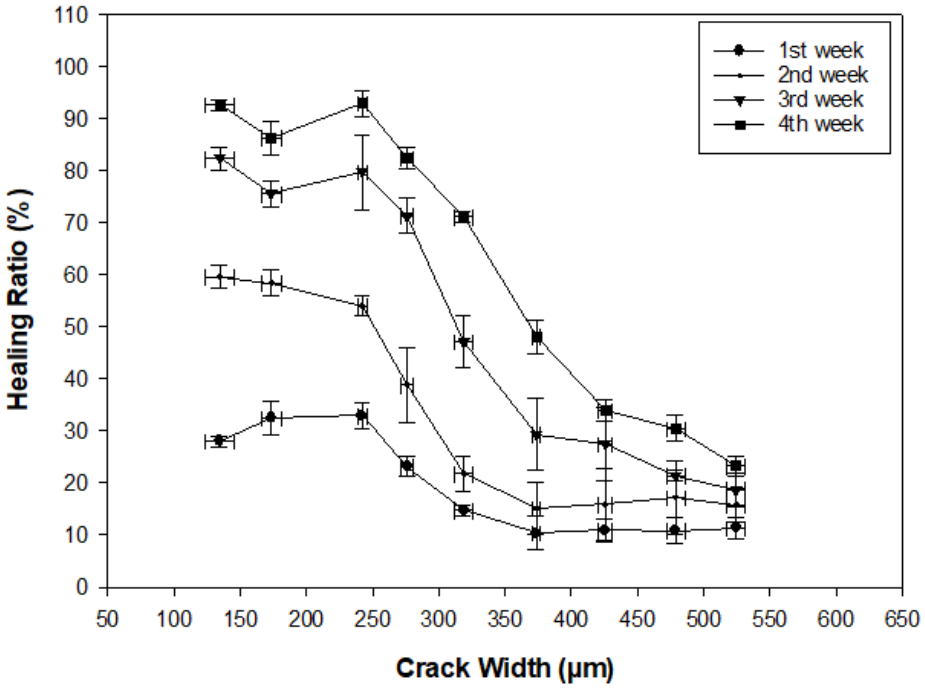

Figure 4.25: Crack self-healing performance of biotic mortar samples under marine water at the end of 4 weeks of immersion treatment.

Similar to tap water and rainwater, the healing graphs obtained for the reference, abiotic, and biotic samples at the 4th week are presented in the Figure 4.26 to facilitate a comparative analysis. Maximum crack widths achieving the 90% threshold for the reference and control samples are 170 µm and 182 µm, respectively, with their healing curves appearing similar. However, for biotic samples, the self-healing limit has been determined as 253 µm. To further elaborate, when considering concrete samples exposed to seawater, the combined data reflecting healing progress at the end of the fourth week are collectively depicted in Figure 4.26 and Figure 4.27. This inclusion enables a more encompassing visual comparison of the healing trends across the different sample types under the influence of seawater exposure.

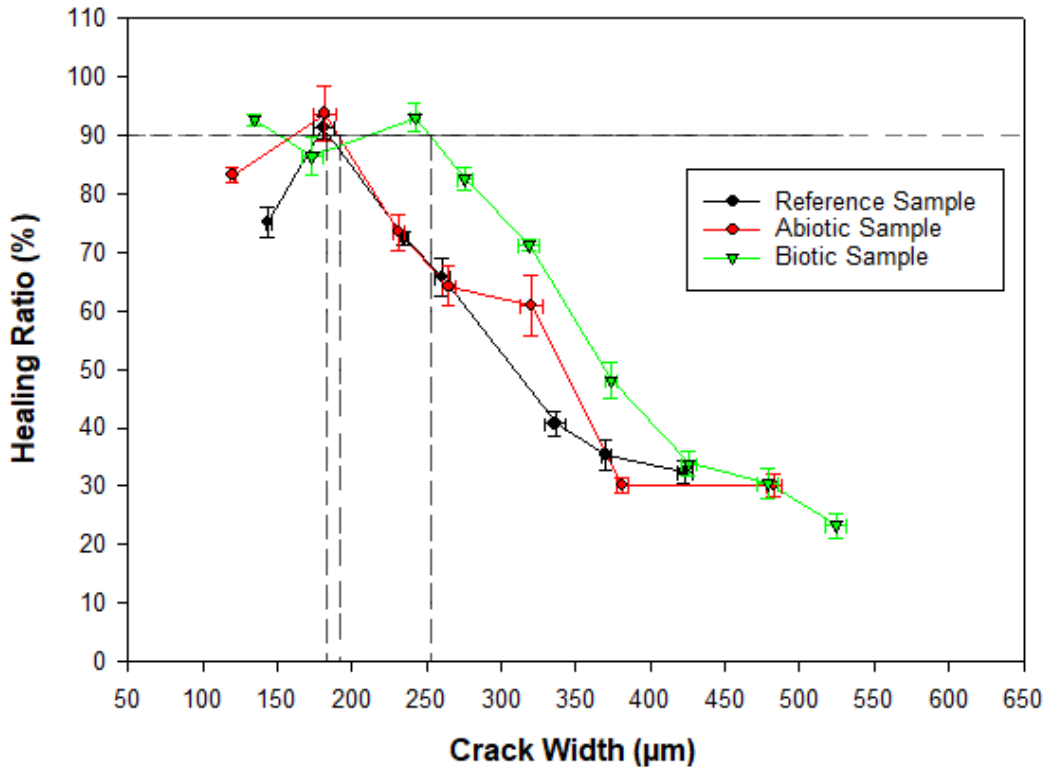

Figure 4.26 Crack self-healing performance under marine conditions at the end of 4 weeks of immersion treatment.

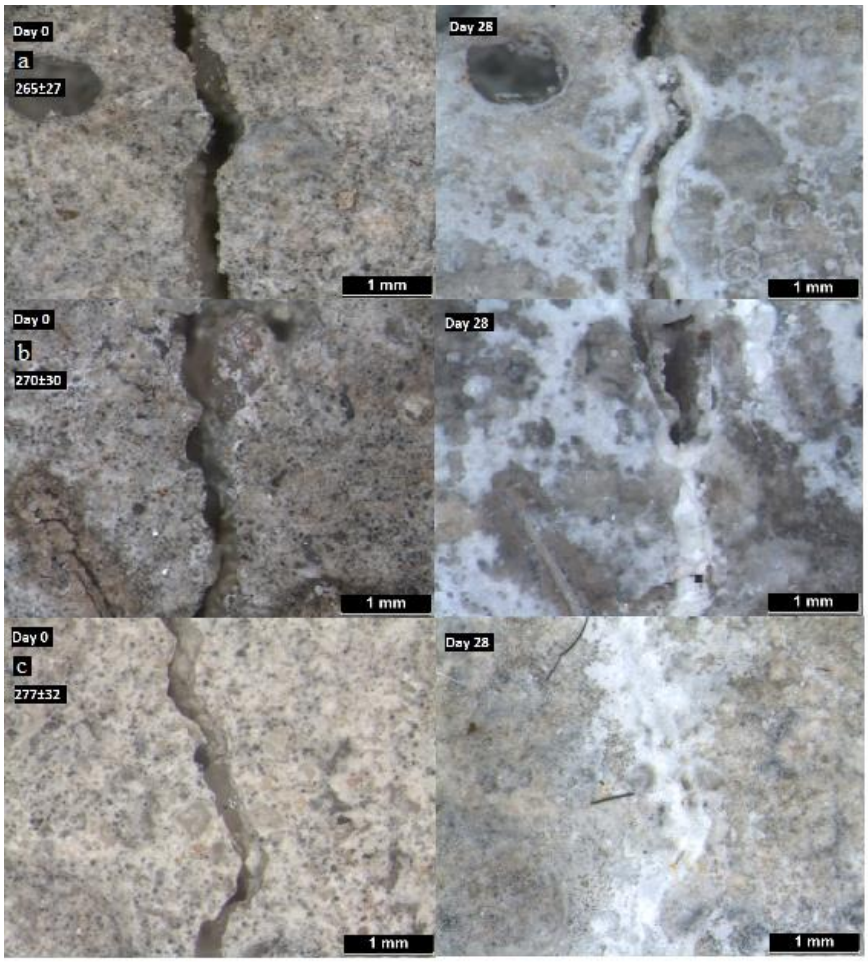

Figure 4.27 Crack healing in a) reference mortar; b) abiotic mortar; c) bio mortar containing biogranules under marine water immersion condition.

In summary, the analysis has shown that reference, abiotic, and biotic mortar samples exhibit distinct responses to seawater exposure in terms of crack healing., At the end of the fourth week, reference and abiotic samples showed self-healing limits at approximately 170 µm and 182 µm, respectively, with similar healing curves. In contrast, biotic samples displayed a self-healing limit at 253 µm under seawater conditions. This indicates an approximately 70 µm crack width could be healed by microbial means. These findings highlight the superior self-healing potential of biotic mortar samples in a marine water environment.

In a study involving the immersion of mortar samples in tap water for healing purposes, drawing upon the research of Wang et al.[222], it was established that the maximum crack width healed in the bacterial series reached a measurement of 970 μm at a single location along the crack. This signifies an approximately fourfold increase in healing width when compared to the maximum of 250 μm observed in the non-bacterial series. This difference actually indicates the importance of defining crack healing limits based on the overall crack width closure along the crack rather than extreme closures observed at a small section along the crack line. Otherwise, overestimations might occur. In a separate investigation by Erşan et al.[86] it was reported that within biotic mortars, following 28 days of healing, the threshold for effective crack closure was documented at 400 μm. Subsequently, after 56 days of healing, the microbial-induced crack closure limit extended to a width of 500 μm. Conversely, control specimens lacking bacterial intervention exhibited a self-healing capacity for cracks up to 300 μm in width after 28 days. These findings underscore the favorable influence of microbial activity on crack healing and imply a potential advantage in the treatment of larger cracks. Based on the findings from another study[183] involving tap water, it was determined that, after four weeks, the highest crack closure rate was achieved in reference and control samples for cracks smaller than 50 μm and 40 μm, reaching a rate of 69 ± 5%. Furthermore, at the end of the fourth week, biotic mortar samples containing a bacterial dosage of 0.25%, which was consistent with the granule dosage used in this thesis study, exhibited an impressive 98 ± 2% crack closure, with cracks healing up to 830 μm wide. These variations in self-healing limits reveal the importance of autogenous healing limit on the overall healing limit achieved in biotic mortars. In our study, reference and abiotic mortars did not reveal significant healing which limited the overall microbial self-healing limit at around 300 μm, while in the reported studies the limits were higher due to the higher autogenous healing performances.

The performance of bacteria-based concrete has been closely monitored in various studies conducted under freshwater conditions [127]. In the broader context of the literature, tap water categorized as freshwater. Yet, the results in this thesis study revealed that self-healing behaviors of the specimens under tap water and rainwater conditions are significantly different. Therefore, for future investigations it will be better to group the fresh water sources and link the obtained healing performances with the corresponding

fresh water source rather than generalizing all as fresh water. The pH, conductivity, mineral content and even the bacteria content may vary from source to source which may have a significant influence on the overall microbial self-healing limit.

Studies conducted under marine water conditions have demonstrated significant benefits of bacteria-based mortars. Cracks up to 0.4 mm in width can be healed under marine condition[137]. Furthermore, when subjected to turbulent marine conditions and varying crack widths ranging from 0.07 to 0.875 mm, the specimens revealed a notable 17% enhancement in overall crack healing compared to exposure to still water[223]. Recent research, as demonstrated in the articles [139], [141], highlights increased autogenous healing in marine water environments, which impacting bacteria-based healing potential. Enhanced autogenous healing, coupled with microbial activity, facilitates wider crack closure. Comparatively, in our study, cracks in marine environments show a higher healing rate under abiotic conditions. This effect, attributed to the aquatic environment rather than bacterial activity, is consistent across biotic samples.

4.4.4. The Ultimate Crack Healing Performance Limit of Bio mortars in Different Environments

To provide a comprehensive understanding of how biotic samples responded across various environments following the fourth week, the subsequent graph was generated. According to the visual representation in Figure 4.28, the crack healing thresholds reaching 90% recovery exhibited their highest Crack width values in rainwater, tap water, and seawater conditions, measuring at 156, 230, and 253 µm, respectively.

Expanding further, when analyzing cracks spanning the width range of 200 to 250 µm, the observed closure percentages were found to be 69%-80% for rainwater, 86%-89% for tap water, and 89%-90% for seawater, respectively. Within the scope of cracks ranging from 250 to 300 µm, the corresponding closure percentages were approximately 50% for rainwater, 67% for tap water, and 76% for seawater.

Similarly, for cracks extending between 300 to 350 µm, the closure percentages were noted as approximately 36% for rainwater, 43% for tap water, and 57% for seawater. Transitioning to the crack width range of 350 to 400 µm, the closure percentages stood at around 31% for rainwater, 34% for tap water, and 40% for seawater.

Addressing cracks that fell between the width span of 400 to 450 µm, each environment yielded an approximately 30% enhancement in healing performance. However, for cracks surpassing the 450- µm mark, a consistent interpretation couldn't be established. This inconsistency was attributed to the varying formation of $CaCO_3$ bridges within specific larger cracks, which did not uniformly achieve sufficient development.

The difference of approximately 70 µm in crack healing between bio mortar samples in seawater, with 253 µm of healing, and abiotic samples, with 182 µm of healing, represents the extent of microbial healing. In rainwater, microbial healing at the 80% healing threshold is approximately 70 µm. However, at 90%, microbial healing was not achieved for rainwater. In tap water, microbial healing at the 90% healing threshold is 55 µm. Microbial healing was determined by subtracting the crack healing values of abiotic and biotic samples for all environmental samples.

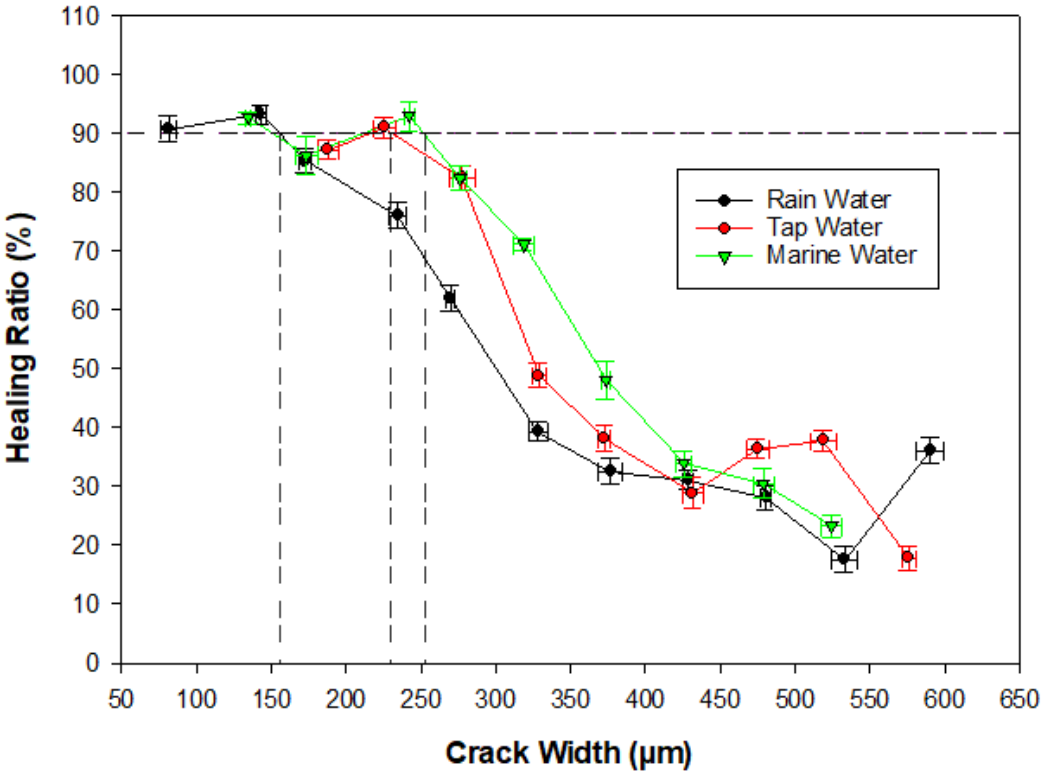

Figure 4.28 Comparative healing performances cross different environments.

Most address the potential for self-healing under ideal conditions, while only a few take into account real or challenging environments [223]–[227]. As indicated by the thesis findings, bio mortars experienced notably enhanced support in terms of mineral formation on cracks, especially in marine environments, in comparison to other water conditions. Further in-depth analysis provided valuable insights into mechanisms that prominently contributed to advanced crack healing in bio mortars submerged in seawater. The exceptional properties of seawater, such as its role as a natural habitat for diverse organisms, along with its rich mineral and ion content, significantly amplify its effectiveness in facilitating crack healing in bio mortars. Moreover, the comparatively lower ion content in rainwater compared to tap water further highlights the positive influence of ion presence on self-bacterial healing.

In conclusion, comprehensive thesis work consistently demonstrates that bio mortars achieve their highest crack healing performance in the following order: primarily in Marine water, followed by tap water, and finally in rainwater.

5. CONCLUSION

In conclusion, this comprehensive study demonstrates the outstanding performance and adaptability of the biogranules within the reactor across three distinct phases. Key findings include:

The reactor consistently achieved high urea hydrolysis efficiencies, with an average of 86% during the initial 71 days and an impressive urea hydrolysis percentage of 89% from day 71 to 120. Furthermore, notable nitrate reduction was observed, starting with an 85% reduction in Phase 1 and achieving complete nitrate reduction in Phase 2, even under alkaline pH conditions. The study also assesses the granulation performance of the reactor under varying harvest conditions, demonstrating its adaptability. During Phase 3, The sustained nitrate reduction capability persisted at 98% through Phase 3, while the urea hydrolysis efficiency was 91%.

The study also explored the impact of pH adjustments on the microbial community and the settling behavior of biogranules. The results showed that granular characteristics were maintained even after pH alterations. Frequent harvesting led to transient variations in settling behavior, underscoring the complexity of the microbial ecosystem within the biogranules. In Phase 1 of the study, where minimal nutrient feeding and stable conditions prevailed, the SVI_{30} value consistently remained below 40 ml/g. This persistent trend strongly indicated the presence of fully developed granular biomass within the reactor. However, an intriguing development occurred on the 71st day when a pH increase led to a subsequent rise in SVI, surpassing 40 after 83 days. Significantly, approximately 30 days later, the SVI dropped below 20, firmly establishing that in Phase 2, the reactor retained its granular characteristics even following the pH adjustments.

The size distribution analysis across all phases of the study demonstrates dynamic changes in granule sizes. In Phase 1, the granule size distribution ranged from particles smaller than 0.1 mm to particles between 0.2-0.3 mm, with a shift towards larger sizes

over the 70-day period. In alkalinity condition, In Phase 2, particle sizes varied from less than 0.1 mm to over 0.6 mm, with noticeable changes in size distribution due to a pH shift on the 71st day. In Phase 3, the majority of granules fell within the 0.3-0.4 mm size range, with some granules reaching sizes of up to 0.5 mm. This shift in size distribution was influenced by the reintroduction of dry granules during the harvest process.

Furthermore, additional granule harvests were carried out on the 124th and 189th days, yielding a total of 16.83 g of dry biogranules ranging in size from 0.5 to 2 mm. The data obtained from this study highlight a comprehensive approach to granule harvesting. It is noteworthy that the reactor's volatile suspended solids (VSS) levels were carefully maintained above 5000 mg/L throughout the harvesting process. This approach effectively ensured the uninterrupted performance of the reactor's granules and prevented any potential disruptions in their activity.

These laboratory-produced biogranules have demonstrated the remarkable capability to be stored in a dried form and reactivated as needed. Their efficient utilization for urea and NO_3-N removal has been quantified, yielding impressive results. The results demonstrated that the dried granules exhibited substantial urea hydrolysis activity within the initial 6 hours of the resuscitation period and efficiently consumed all the urea within a 12-hour cycle. This also includes the rapid consumption of removal of 200 mg/L of NO_3-N in a mere 3 hours. In another separate batch test, this highlights that the addition of yeast, alongside urea, calcium formate, and calcium nitrate, did not lead to adverse urea hydrolysis.

Following the resuscitation and confirmation of the dried biogranules' activity, their application in cementitious composites has been successfully demonstrated. The addition of 0.25 % of cement weight (1.88 g) biogranules has enabled the healing of these cracks, particularly those measuring between 250-300 µm wide, even in changing environments. The visual evidence further confirmed that these biogranules efficiently consumed nutrients entering the cracks with water, such as urea and nitrate, and produced $CaCO_3$, a natural mineral that effectively fills and repairs cracks.

It reveals that crack healing thresholds reaching 90% recovery were most pronounced in rainwater (156 µm), tap water (240 µm), and seawater (253 µm). Further analysis unveiled varying closure percentages within specific crack width ranges, with rainwater, tap water, and seawater exhibiting distinct behaviors. With a 90% healing threshold, microbial healing in seawater achieved a remarkable 70 µm improvement compared to abiotic samples. Conversely, in rainwater with an 90% healing threshold, a 70 µm microbial healing effect was observed. In tap water, microbial healing reaching the 90% threshold resulted in a 55 µm improvement. These microbial healing results were made from by comparing the healing differences between abiotic and biotic mortar samples.

After the fourth week, biotic samples in various environments showed their highest crack healing thresholds at 90% recovery in rainwater, tap water, and seawater conditions, measuring at 156, 240, and 253 µm, respectively. When analyzing cracks ranging from 200 to 250 µm in width, closure percentages were approximately 80%-69% for rainwater, 89%-86% for tap water, and 89%-90% for seawater. In the case of cracks between 250 and 300 µm wide, closure percentages were approximately 50% for rainwater, 67% for tap water, and 76% for marine water. The second parts of results highlight the potential of bio mortars, particularly in marine environments, for promoting crack healing due to the presence of diverse organisms, minerals, and ions.

6. REFERENCES

[1] L. Basheer, J. Kropp, and D. J. Cleland, “Assessment of the durability of concrete from its permeation properties: a review,” 2001.

[2] I. Fernandes and M. A. T. M. Broekmans, “Alkali-Silica Reactions: An Overview. Part I,” *Metallography, Microstructure, and Analysis*, vol. 2, no. 4, pp. 257–267, Aug. 2013, doi: 10.1007/s13632-013-0085-5.

[3] X. Li, D. Li, and Y. Xu, “Modeling the effects of microcracks on water permeability of concrete using 3D discrete crack network,” *Compos Struct*, vol. 210, pp. 262–273, Feb. 2019, doi: 10.1016/j.compstruct.2018.11.034.

[4] F. Hammes, A. " Ene Seka, S. De Knijf, and W. Verstraete, “A novel approach to calcium removal from calcium-rich industrial wastewater,” 2003. [Online]. Available: http://welcome.to/labmet.

[5] X. Zhang, X. Fan, M. Li, A. Samia, and X. (Bill) Yu, “Study on the behaviors of fungi-concrete surface interactions and theoretical assessment of its potentials for durable concrete with fungal-mediated self-healing,” *J Clean Prod*, vol. 292, Apr. 2021, doi: 10.1016/j.jclepro.2021.125870.

[6] “978-1-4020-6250-6”.

[7] Y. Ersan, E. Gruyaert, G. Louis, C. Lors, N. De Belie, and N. Boon, “Self-protected nitrate reducing culture for intrinsic repair of concrete cracks,” *Front Microbiol*, vol. 6, no. NOV, 2015, doi: 10.3389/fmicb.2015.01228.

[8] H. Kim, H. M. Son, J. Seo, and H. K. Lee, “Recent advances in microbial viability and self-healing performance in bacterial-based cementitious materials: A review,” *Constr Build Mater*, vol. 274, Mar. 2021, doi: 10.1016/j.conbuildmat.2020.122094.

[9] J. Wang, K. Van Tittelboom, N. De Belie, and W. Verstraete, “Use of silica gel or polyurethane immobilized bacteria for self-healing concrete,” *Constr Build Mater*, vol. 26, no. 1, pp. 532–540, Jan. 2012, doi: 10.1016/j.conbuildmat.2011.06.054.

[10] V. Wiktor and H. M. Jonkers, “Quantification of crack-healing in novel bacteria-based self-healing concrete,” *Cem Concr Compos*, vol. 33, no. 7, pp. 763–770, Aug. 2011, doi: 10.1016/j.cemconcomp.2011.03.012.

[11] R. Roy, E. Rossi, J. Silfwerbrand, and H. Jonkers, “Self-healing capacity of mortars with added-in bio-plastic bacteria-based agents: Characterization and quantification through micro-scale techniques,” *Constr Build Mater*, vol. 297, Aug. 2021, doi: 10.1016/j.conbuildmat.2021.123793.

[12] J. Chen, B. Liu, M. Zhong, C. Jing, and B. Guo, “Research status and development of microbial induced calcium carbonate mineralization technology,” *PLoS One*, vol. 17, no. 7 July, Jul. 2022, doi: 10.1371/journal.pone.0271761.

[13] X. Zhu, J. Wang, N. De Belie, and N. Boon, “Complementing urea hydrolysis and nitrate reduction for improved microbially induced calcium carbonate precipitation,” *Appl Microbiol Biotechnol*, vol. 103, no. 21–22, pp. 8825–8838, Nov. 2019, doi: 10.1007/s00253-019-10128-2.

[14] N. De Belie, “Application of bacteria in concrete: A critical review,” *RILEM Technical Letters*, vol. 1, pp. 56–61, 2016, doi: 10.21809/rilemtechlett.2016.14.

[15] N. K. Dhami, M. S. Reddy, and M. S. Mukherjee, “Biomineralization of calcium carbonates and their engineered applications: A review,” *Frontiers in Microbiology*, vol. 4, no. OCT. Frontiers Media S.A., 2013. doi: 10.3389/fmicb.2013.00314.

[16] S. Al-Thawadi, S. M. Al-Thawadi, and A. Info, “Ureolytic Bacteria and Calcium Carbonate Formation as a Mechanism of Strength Enhancement of Sand Biosynthesis of nanoparticles View project Ureolytic Bacteria and Calcium Carbonate Formation as a Mechanism of Strength Enhancement of Sand,” 2011. [Online]. Available: https://www.researchgate.net/publication/230603500

[17] R. Garg, R. Garg, and N. O. Eddy, “Microbial induced calcite precipitation for self-healing of concrete: a review,” *Journal of Sustainable Cement-Based Materials*, vol. 12, no. 3. Taylor and Francis Ltd., pp. 317–330, 2023. doi: 10.1080/21650373.2022.2054477.

[18] Y. Ç. Erşan, N. de Belie, and N. Boon, “Microbially induced CaCO3 precipitation through denitrification: An optimization study in minimal nutrient environment,” *Biochem Eng J*, vol. 101, pp. 108–118, Sep. 2015, doi: 10.1016/j.bej.2015.05.006.

[19] J. T. DeJong, B. M. Mortensen, B. C. Martinez, and D. C. Nelson, “Bio-mediated soil improvement,” *Ecol Eng*, vol. 36, no. 2, pp. 197–210, Feb. 2010, doi: 10.1016/j.ecoleng.2008.12.029.

[20] L. A. van Paassen, C. M. Daza, M. Staal, D. Y. Sorokin, W. van der Zon, and M. C. M. van Loosdrecht, “Potential soil reinforcement by biological denitrification,” *Ecol Eng*, vol. 36, no. 2, pp. 168–175, Feb. 2010, doi: 10.1016/j.ecoleng.2009.03.026.

[21] E. Kavazanjian Jr, I. Karatas, E. Kavazanjian, and J. Ismail Karatas, “10 Part of the Geotechnical Engineering Commons Recommended Citation Recommended Citation Kavazanjian,” 2008. [Online]. Available: https://scholarsmine.mst.edu/icchgehttps://scholarsmine.mst.edu/icchge/6icchge/session14/1

[22] W. De Muynck, K. Verbeken, N. De Belie, and W. Verstraete, “Influence of temperature on the effectiveness of a biogenic carbonate surface treatment for limestone conservation,” *Appl Microbiol Biotechnol*, vol. 97, no. 3, pp. 1335–1347, Feb. 2013, doi: 10.1007/s00253-012-3997-0.

[23] W. Lin, W. Lin, X. Cheng, G. Chen, and Y. C. Ersan, “Microbially induced desaturation and carbonate precipitation through denitrification: A review,” *Applied Sciences (Switzerland)*, vol. 11, no. 17. MDPI, Sep. 01, 2021. doi: 10.3390/app11177842.

[24] D. Martin, K. Dodds, I. B. Butler, and B. T. Ngwenya, “Carbonate precipitation under pressure for bioengineering in the anaerobic subsurface via denitrification,” *Environ Sci Technol*, vol. 47, no. 15, pp. 8692–8699, Aug. 2013, doi: 10.1021/es401270q.

[25] Y. Ç. Erşan, K. Van Tittelboom, N. Boon, and N. De Belie, “Nitrite producing bacteria inhibit reinforcement bar corrosion in cementitious materials,” *Sci Rep*, vol. 8, no. 1, Dec. 2018, doi: 10.1038/s41598-018-32463-6.

[26] D. Martin, K. Dodds, I. B. Butler, and B. T. Ngwenya, “Carbonate precipitation under pressure for bioengineering in the anaerobic subsurface via denitrification,” *Environ Sci Technol*, vol. 47, no. 15, pp. 8692–8699, Aug. 2013, doi: 10.1021/es401270q.

[27] V. P. Pham, A. Nakano, W. R. L. Van Der Star, T. J. Heimovaara, and L. A. Van Paassen, “Applying MICP by denitrification in soils: A process analysis,” *Environmental Geotechnics*, vol. 5, no. 2, pp. 79–93, Apr. 2018, doi: 10.1680/jenge.15.00078.

[28] Z. Yang and X. Cheng, “A performance study of high-strength microbial mortar produced by low pressure grouting for the reinforcement of deteriorated masonry structures,” *Constr Build Mater*, vol. 41, pp. 505–515, 2013, doi: 10.1016/j.conbuildmat.2012.12.055.

[29] J. He, J. Chu, and V. Ivanov, “Mitigation of liquefaction of saturated sand using biogas,” *Geotechnique*, vol. 63, no. 4, pp. 267–275, Mar. 2013, doi: 10.1680/geot.SIP13.P.004.

[30] S. T. O’donnell *et al.*, “A Stoichiometric Model for Biogeotechnical Soil Improvement.”

[31] Y. C. Ersan *et al.*, “Volume fraction, thickness, and permeability of the sealing layer in microbial self-healing concrete containing biogranules,” *Front Built Environ*, vol. 4, Nov. 2018, doi: 10.3389/fbuil.2018.00070.

[32] Y. Ç. Erşan, E. Hernandez-Sanabria, N. Boon, and N. De Belie, “Enhanced crack closure performance of microbial mortar through nitrate reduction,” *Cem Concr Compos*, vol. 70, pp. 159–170, Jul. 2016, doi: 10.1016/j.cemconcomp.2016.04.001.

[33] Y. Ç. Erşan, F. B. Da Silva, N. Boon, W. Verstraete, and N. De Belie, “Screening of bacteria and concrete compatible protection materials,” *Constr Build Mater*, vol. 88, pp. 196–203, Jul. 2015, doi: 10.1016/j.conbuildmat.2015.04.027.

[34] F. Hammes, N. Boon, J. De Villiers, W. Verstraete, and S. D. Siciliano, “Strain-specific ureolytic microbial calcium carbonate precipitation,” *Appl Environ Microbiol*, vol. 69, no. 8, pp. 4901–4909, Aug. 2003, doi: 10.1128/AEM.69.8.4901-4909.2003.

[35] F. B. Silva, N. Boon, N. De Belie, and W. Verstraete, “Industrial application of biological self-healing concrete: Challenges and economical feasibility,” *J Commer Biotechnol*, vol. 21, no. 1, pp. 31–38, Jan. 2015, doi: 10.5912/jcb662.

[36] F. B. Da Silva, N. De Belie, N. Boon, and W. Verstraete, “Production of non-axenic ureolytic spores for self-healing concrete applications,” *Constr Build Mater*, vol. 93, pp. 1034–1041, Jul. 2015, doi: 10.1016/j.conbuildmat.2015.05.049.

[37] M. Getnet Meharie, “Factors Affecting the Self-Healing Efficiency of Cracked Concrete Structures,” *American Journal of Applied Scientific Research*, vol. 3, no. 6, p. 80, 2017, doi: 10.11648/j.ajasr.20170306.12.

[38] M. R. Hossain, R. Sultana, M. M. Patwary, N. Khunga, P. Sharma, and S. J. Shaker, “Self-healing concrete for sustainable buildings. A review,” *Environmental Chemistry Letters*, vol. 20, no. 2. Springer Science and Business Media Deutschland GmbH, pp. 1265–1273, Apr. 01, 2022. doi: 10.1007/s10311-021-01375-9.

[39] T. H. Nguyen, E. Ghorbel, H. Fares, and A. Cousture, “Bacterial self-healing of concrete and durability assessment,” *Cem Concr Compos*, vol. 104, Nov. 2019, doi: 10.1016/j.cemconcomp.2019.103340.

[40] P. Dinarvand and A. Rashno, “Review of the potential application of bacteria in self-healing and the improving properties of concrete/mortar,” *Journal of Sustainable Cement-Based Materials*, vol. 11, no. 4. Taylor and Francis Ltd., pp. 250–271, 2022. doi: 10.1080/21650373.2021.1936268.

[41] N. B. R. Monteiro, J. M. Moita Neto, and E. A. da Silva, “Environmental assessment in concrete industries,” *J Clean Prod*, vol. 327, Dec. 2021, doi: 10.1016/j.jclepro.2021.129516.

[42] A. Hasanbeigi, L. Price, and E. Lin, “Emerging energy-efficiency and CO 2 emission-reduction technologies for cement and concrete production: A technical review,” *Renewable and Sustainable Energy Reviews*, vol. 16, no. 8. pp. 6220–6238, Oct. 2012. doi: 10.1016/j.rser.2012.07.019.

[43] S. Mishra and N. Anwar Siddiqui, “A Review On Environmental and Health Impacts Of Cement Manufacturing Emissions”, [Online]. Available: www.woarjournals.org/IJGAES

[44] N. Mohamad, K. Muthusamy, R. Embong, A. Kusbiantoro, and M. H. Hashim, "Environmental impact of cement production and Solutions: A review," in *Materials Today: Proceedings*, Elsevier Ltd, 2021, pp. 741–746. doi: 10.1016/j.matpr.2021.02.212.

[45] D. R. Morgan, "Compatibility of concrete repair materials systems," 1996.

[46] T. S. Wong *et al.*, "Bioinspired self-repairing slippery surfaces with pressure-stable omniphobicity," *Nature*, vol. 477, no. 7365, pp. 443–447, Sep. 2011, doi: 10.1038/nature10447.

[47] M. Nodehi, T. Ozbakkaloglu, and A. Gholampour, "A systematic review of bacteria-based self-healing concrete: Biomineralization, mechanical, and durability properties," *Journal of Building Engineering*, vol. 49. Elsevier Ltd, May 15, 2022. doi: 10.1016/j.jobe.2022.104038.

[48] E. Stanaszek-Tomal, "Bacterial concrete as a sustainable building material?," *Sustainability (Switzerland)*, vol. 12, no. 2. MDPI, Jan. 01, 2020. doi: 10.3390/su12020696.

[49] I. Mohammad, A. Khattab, H. Shekha, and M. A. Abdi, "Study on Self-healing Concrete types-A review," vol. 2, no. 1, pp. 76–87, 2019, doi: 10.26392/SSM.2019.02.01.076.

[50] E. Tziviloglou *et al.*, "Bio-based self-healing concrete: From research to field application," in *Advances in Polymer Science*, vol. 273, Springer New York LLC, 2016, pp. 345–386. doi: 10.1007/12_2015_332.

[51] M. V. S. Rao, V. S. Reddy, M. Hafsa, P. Veena, and P. Anusha, "Bioengineered Concrete-A Sustainable Self-Healing Construction Material," 2013. [Online]. Available: www.isca.in

[52] M. De, R. Kim, and V. Tittelboom, "RILEM State-of-the-Art Reports Self-Healing Phenomena in Cement-Based Materials State-of-the-Art Report of RILEM Technical Committee 221-SHC: Self-Healing Phenomena in Cement-Based Materials." [Online]. Available: http://www.springer.com/series/8780

[53] M. N. Uddin, T. Tafsirojjaman, N. Shanmugasundaram, S. Praveenkumar, and L. zhi Li, "Smart self-healing bacterial concrete for sustainable goal," *Innovative*

Infrastructure Solutions, vol. 8, no. 1. Springer Science and Business Media Deutschland GmbH, Jan. 01, 2023. doi: 10.1007/s41062-022-01020-6.

[54] I. Mohammad, A. Khattab, H. Shekha, and M. A. Abdi, "Study on Self-healing Concrete types-A review," vol. 2, no. 1, pp. 76–87, 2019, doi: 10.26392/SSM.2019.02.01.076.

[55] K. Van Tittelboom and N. De Belie, "Self-healing in cementitious materials-a review," *Materials*, vol. 6, no. 6, pp. 2182–2217, 2013, doi: 10.3390/ma6062182.

[56] A. Raza *et al.*, "Sustainability assessment, structural performance and challenges of self-healing bio-mineralized concrete: A systematic review for built environment applications," *Journal of Building Engineering*, vol. 66. Elsevier Ltd, May 01, 2023. doi: 10.1016/j.jobe.2023.105839.

[57] B. Zhang, Q. Li, X. Niu, L. Yang, Y. Hu, and J. Zhang, "Influence of a novel hydrophobic agent on freeze–thaw resistance and microstructure of concrete," *Constr Build Mater*, vol. 269, Feb. 2021, doi: 10.1016/j.conbuildmat.2020.121294.

[58] J. Y. Wang, H. Soens, W. Verstraete, and N. De Belie, "Self-healing concrete by use of microencapsulated bacterial spores," *Cem Concr Res*, vol. 56, pp. 139–152, 2014, doi: 10.1016/j.cemconres.2013.11.009.

[59] J. Xu, X. Wang, and B. Wang, "Biochemical process of ureolysis-based microbial CaCO3 precipitation and its application in self-healing concrete," *Appl Microbiol Biotechnol*, vol. 102, no. 7, pp. 3121–3132, Apr. 2018, doi: 10.1007/s00253-018-8779-x.

[60] M. Gao *et al.*, "Immobilized bacteria with pH-response hydrogel for self-healing of concrete," *J Environ Manage*, vol. 261, May 2020, doi: 10.1016/j.jenvman.2020.110225.

[61] H. M. Jonkers, A. Thijssen, G. Muyzer, O. Copuroglu, and E. Schlangen, "Application of bacteria as self-healing agent for the development of sustainable concrete," *Ecol Eng*, vol. 36, no. 2, pp. 230–235, Feb. 2010, doi: 10.1016/j.ecoleng.2008.12.036.

[62] M. Seifan and A. Berenjian, "Microbially induced calcium carbonate precipitation: a widespread phenomenon in the biological world," *Applied Microbiology and*

Biotechnology, vol. 103, no. 12. Springer Verlag, pp. 4693–4708, Jun. 18, 2019. doi: 10.1007/s00253-019-09861-5.

[63] K. H. Caesar, J. R. Kyle, T. W. Lyons, A. Tripati, and S. J. Loyd, "Carbonate formation in salt dome cap rocks by microbial anaerobic oxidation of methane," *Nat Commun*, vol. 10, no. 1, Dec. 2019, doi: 10.1038/s41467-019-08687-z.

[64] V. Achal, A. Mukherjee, D. Kumari, and Q. Zhang, "Biomineralization for sustainable construction - A review of processes and applications," *Earth-Science Reviews*, vol. 148. Elsevier, pp. 1–17, Sep. 01, 2015. doi: 10.1016/j.earscirev.2015.05.008.

[65] S. Castanier, G. Le Metayer-Levrel, and J.-P. Perthuisot, "Bacterial Roles in the Precipitation of Carbonate Minerals."

[66] F. Martirena *et al.*, "Microorganism-based bioplasticizer for cementitious materials," in *Biopolymers and Biotech Admixtures for Eco-Efficient Construction Materials*, Elsevier Inc., 2016, pp. 151–171. doi: 10.1016/B978-0-08-100214-8.00008-7.

[67] A. F. Alshalif, J. M. Irwan, N. Othman, and L. H. Anneza, "Isolation of Sulphate Reduction Bacteria (SRB) to Improve Compress Strength and Water Penetration of Bio-Concrete", doi: 10.1051/C.

[68] T. Tambunan, M. Irwan Juki, and N. Othman, "Mechanical properties of sulphate reduction bacteria on the durability of concrete in chloride condition", doi: 10.1051/matecconf/20192.

[69] Y. Ç. Erşan, "Granules with activated compact denitrifying core (ACDC) for self-healing concrete with corrosion protection functionality," 2018. [Online]. Available: https://www.researchgate.net/publication/326191349

[70] W. E. G. Müller, P. Jeanteur, R. E. Rhoads, Đ. Ugarkovic´, U. Márcio, and R. Custódio, "Progress in Molecular and Subcellular Biology."

[71] M. E. Espitia-Nery, D. E. Corredor-Pulido, P. A. Castaño-Oliveros, J. A. Rodríguez-Medina, Q. Y. Ordoñez-Bello, and M. S. Pérez-Fuentes, "Mechanisms of encapsulation of bacteria in self-healing concrete: Review," *DYNA (Colombia)*, vol. 86, no. 210. Universidad Nacional de Colombia, pp. 17–22, Jul. 01, 2019. doi: 10.15446/dyna.v86n210.75343.

[72] T. Zhu, C. Paulo, M. L. Merroun, and M. Dittrich, “Potential application of biomineralization by Synechococcus PCC8806 for concrete restoration,” *Ecol Eng*, vol. 82, pp. 459–468, Sep. 2015, doi: 10.1016/j.ecoleng.2015.05.017.

[73] M. Nodehi, T. Ozbakkaloglu, and A. Gholampour, “A systematic review of bacteria-based self-healing concrete: Biomineralization, mechanical, and durability properties,” *Journal of Building Engineering*, vol. 49. Elsevier Ltd, May 15, 2022. doi: 10.1016/j.jobe.2022.104038.

[74] M. Seifan and A. Berenjian, “Microbially induced calcium carbonate precipitation: a widespread phenomenon in the biological world,” *Applied Microbiology and Biotechnology*, vol. 103, no. 12. Springer Verlag, pp. 4693–4708, Jun. 18, 2019. doi: 10.1007/s00253-019-09861-5.

[75] M. Seifan, A. K. Samani, and A. Berenjian, “Bioconcrete: next generation of self-healing concrete,” *Applied Microbiology and Biotechnology*, vol. 100, no. 6. Springer Verlag, pp. 2591–2602, Mar. 01, 2016. doi: 10.1007/s00253-016-7316-z.

[76] F. Martirena *et al.*, “Microorganism-based bioplasticizer for cementitious materials,” in *Biopolymers and Biotech Admixtures for Eco-Efficient Construction Materials*, Elsevier Inc., 2016, pp. 151–171. doi: 10.1016/B978-0-08-100214-8.00008-7.

[77] “Concrete remediation with B. pasteurii”.

[78] C. C. Gavimath *et al.*, “POTENTIAL APPLICATION OF BACTERIA TO IMPROVE THE STRENGTH OF CEMENT CONCRETE,” 2012. [Online]. Available: http://www.bipublication.com

[79] N. B. R. Monteiro, J. M. Moita Neto, and E. A. da Silva, “Environmental assessment in concrete industries,” *J Clean Prod*, vol. 327, Dec. 2021, doi: 10.1016/j.jclepro.2021.129516.

[80] R. Pei, J. Liu, S. Wang, and M. Yang, “Use of bacterial cell walls to improve the mechanical performance of concrete,” *Cem Concr Compos*, vol. 39, pp. 122–130, 2013, doi: 10.1016/j.cemconcomp.2013.03.024.

[81] V. Achal, X. Pan, and N. Özyurt, "Improved strength and durability of fly ash-amended concrete by microbial calcite precipitation," *Ecol Eng*, vol. 37, no. 4, pp. 554–559, Apr. 2011, doi: 10.1016/j.ecoleng.2010.11.009.

[82] R. Andalib *et al.*, "Optimum concentration of Bacillus megaterium for strengthening structural concrete," *Constr Build Mater*, vol. 118, pp. 180–193, Aug. 2016, doi: 10.1016/j.conbuildmat.2016.04.142.

[83] Y. Ç. Erşan, F. B. Da Silva, N. Boon, W. Verstraete, and N. De Belie, "Screening of bacteria and concrete compatible protection materials," *Constr Build Mater*, vol. 88, pp. 196–203, Jul. 2015, doi: 10.1016/j.conbuildmat.2015.04.027.

[84] G. Miirsdorf and H. Kaltwasser, "Ammonium assimilation in Proteus vulgaris, Bacillus pasteurii, and Sporosarcina ureae," 1989.

[85] R. Siddique and N. K. Chahal, "Effect of ureolytic bacteria on concrete properties," *Construction and Building Materials*, vol. 25, no. 10. pp. 3791–3801, Oct. 10, 2011. doi: 10.1016/j.conbuildmat.2011.04.010.

[86] Y. Ç. Erşan, H. Verbruggen, I. De Graeve, W. Verstraete, N. De Belie, and N. Boon, "Nitrate reducing CaCO3 precipitating bacteria survive in mortar and inhibit steel corrosion," *Cem Concr Res*, vol. 83, pp. 19–30, May 2016, doi: 10.1016/j.cemconres.2016.01.009.

[87] J. Wang, J. Dewanckele, V. Cnudde, S. Van Vlierberghe, W. Verstraete, and N. De Belie, "X-ray computed tomography proof of bacterial-based self-healing in concrete," *Cem Concr Compos*, vol. 53, pp. 289–304, 2014, doi: 10.1016/j.cemconcomp.2014.07.014.

[88] M. Wu, X. Hu, Q. Zhang, D. Xue, and Y. Zhao, "Growth environment optimization for inducing bacterial mineralization and its application in concrete healing," *Constr Build Mater*, vol. 209, pp. 631–643, Jun. 2019, doi: 10.1016/j.conbuildmat.2019.03.181.

[89] S. Krishnapriya, D. L. Venkatesh Babu, and P. A. G., "Isolation and identification of bacteria to improve the strength of concrete," *Microbiol Res*, vol. 174, pp. 48–55, May 2015, doi: 10.1016/j.micres.2015.03.009.

[90] M. B. Arthi and K. Dhaarani, “A study on strength and self-healing characteristics of Bacterial concrete,” *International Journal of Engineering Trends and Technology*, vol. 38, 2016, [Online]. Available: http://www.ijettjournal.org

[91] B. M. Mortensen, M. J. Haber, J. T. Dejong, L. F. Caslake, and D. C. Nelson, “Effects of environmental factors on microbial induced calcium carbonate precipitation,” *J Appl Microbiol*, vol. 111, no. 2, pp. 338–349, Aug. 2011, doi: 10.1111/j.1365-2672.2011.05065.x.

[92] D. J. Tobler *et al.*, “Comparison of rates of ureolysis between Sporosarcina pasteurii and an indigenous groundwater community under conditions required to precipitate large volumes of calcite,” *Geochim Cosmochim Acta*, vol. 75, no. 11, pp. 3290–3301, Jun. 2011, doi: 10.1016/j.gca.2011.03.023.

[93] D. Martin, K. Dodds, B. T. Ngwenya, I. B. Butler, and S. C. Elphick, “Inhibition of sporosarcina pasteurii under anoxic conditions: Implications for subsurface carbonate precipitation and remediation via ureolysis,” *Environ Sci Technol*, vol. 46, no. 15, pp. 8351–8355, Aug. 2012, doi: 10.1021/es3015875.

[94] A. C. Mitchell, E. J. Espinosa-Ortiz, S. L. Parks, A. J. Phillips, A. B. Cunningham, and R. Gerlach, “Kinetics of calcite precipitation by ureolytic bacteria under aerobic and anaerobic conditions,” *Biogeosciences*, vol. 16, no. 10, pp. 2147–2161, May 2019, doi: 10.5194/bg-16-2147-2019.

[95] D. J. Skorupa, A. Akyel, M. W. Fields, and R. Gerlach, “Facultative and anaerobic consortia of haloalkaliphilic ureolytic micro-organisms capable of precipitating calcium carbonate,” *J Appl Microbiol*, vol. 127, no. 5, pp. 1479–1489, Nov. 2019, doi: 10.1111/jam.14384.

[96] S. Jain and D. N. Arnepalli, “Biochemically Induced Carbonate Precipitation in Aerobic and Anaerobic Environments by Sporosarcina pasteurii,” *Geomicrobiol J*, vol. 36, no. 5, pp. 443–451, May 2019, doi: 10.1080/01490451.2019.1569180.

[97] J. Y. Wang, D. Snoeck, S. Van Vlierberghe, W. Verstraete, and N. De Belie, “Application of hydrogel encapsulated carbonate precipitating bacteria for approaching a realistic self-healing in concrete,” *Constr Build Mater*, vol. 68, pp. 110–119, Oct. 2014, doi: 10.1016/j.conbuildmat.2014.06.018.

[98] M. Seifan, A. K. Sarmah, A. K. Samani, A. Ebrahiminezhad, Y. Ghasemi, and A. Berenjian, "Mechanical properties of bio self-healing concrete containing immobilized bacteria with iron oxide nanoparticles," *Appl Microbiol Biotechnol*, vol. 102, no. 10, pp. 4489–4498, May 2018, doi: 10.1007/s00253-018-8913-9.

[99] N. Shaheen, R. A. Khushnood, W. Khaliq, H. Murtaza, R. Iqbal, and M. H. Khan, "Synthesis and characterization of bio-immobilized nano/micro inert and reactive additives for feasibility investigation in self-healing concrete," *Constr Build Mater*, vol. 226, pp. 492–506, Nov. 2019, doi: 10.1016/j.conbuildmat.2019.07.202.

[100] J. Y. Wang, N. De Belie, and W. Verstraete, "Diatomaceous earth as a protective vehicle for bacteria applied for self-healing concrete," *J Ind Microbiol Biotechnol*, vol. 39, no. 4, pp. 567–577, Apr. 2012, doi: 10.1007/s10295-011-1037-1.

[101] S. Han, E. K. Choi, W. Park, C. Yi, and N. Chung, "Effectiveness of expanded clay as a bacteria carrier for self-healing concrete," *Appl Biol Chem*, vol. 62, no. 1, Dec. 2019, doi: 10.1186/s13765-019-0426-4.

[102] S. C. Chuo *et al.*, "Insights into the current trends in the utilization of bacteria for microbially induced calcium carbonate precipitation," *Materials*, vol. 13, no. 21. MDPI AG, pp. 1–28, Nov. 01, 2020. doi: 10.3390/ma13214993.

[103] C. Liu, Z. Lv, J. Xiao, X. Xu, X. Nong, and H. Liu, "On the mechanism of Cl− diffusion transport in self-healing concrete based on recycled coarse aggregates as microbial carriers," *Cem Concr Compos*, vol. 124, Nov. 2021, doi: 10.1016/j.cemconcomp.2021.104232.

[104] M. Alazhari, T. Sharma, A. Heath, R. Cooper, and K. Paine, "Application of expanded perlite encapsulated bacteria and growth media for self-healing concrete," *Constr Build Mater*, vol. 160, pp. 610–619, Jan. 2018, doi: 10.1016/j.conbuildmat.2017.11.086.

[105] L. Jiang, G. Jia, C. Jiang, and Z. Li, "Sugar-coated expanded perlite as a bacterial carrier for crack-healing concrete applications," *Constr Build Mater*, vol. 232, Jan. 2020, doi: 10.1016/j.conbuildmat.2019.117222.

[106] L. Rosso, J. R. Lobry, S. Bajard, and J. P. Flandrois, “Convenient Model To Describe the Combined Effects of Temperature and pH on Microbial Growth,” 1995. [Online]. Available: https://journals.asm.org/journal/aem

[107] J. Wang, H. M. Jonkers, N. Boon, and N. De Belie, “Bacillus sphaericus LMG 22257 is physiologically suitable for self-healing concrete,” *Appl Microbiol Biotechnol*, vol. 101, no. 12, pp. 5101–5114, Jun. 2017, doi: 10.1007/s00253-017-8260-2.

[108] G. Kim, J. Kim, and H. Youn, “Effect of temperature, pH, and reaction duration on microbially induced calcite precipitation,” *Applied Sciences (Switzerland)*, vol. 8, no. 8, Aug. 2018, doi: 10.3390/app8081277.

[109] R. Ferrer, J. Quevedo-Sarmiento, A. Rivadeneyra, V. Bejar, R. Delgado, and A. Ramos-Cormenzana, “Calcium Carbonate Precipitation by Two Groups of Moderately Halophilic Microorganisms at Different Temperatures and Salt Concentrations,” 1988.

[110] B. M. Mortensen, M. J. Haber, J. T. Dejong, L. F. Caslake, and D. C. Nelson, “Effects of environmental factors on microbial induced calcium carbonate precipitation,” *J Appl Microbiol*, vol. 111, no. 2, pp. 338–349, Aug. 2011, doi: 10.1111/j.1365-2672.2011.05065.x.

[111] J. Zhang *et al.*, “Microbial network of the carbonate precipitation process induced by microbial consortia and the potential application to crack healing in concrete,” *Sci Rep*, vol. 7, no. 1, Dec. 2017, doi: 10.1038/s41598-017-15177-z.

[112] H. M. Jonkers, A. Thijssen, G. Muyzer, O. Copuroglu, and E. Schlangen, “Application of bacteria as self-healing agent for the development of sustainable concrete,” *Ecol Eng*, vol. 36, no. 2, pp. 230–235, Feb. 2010, doi: 10.1016/j.ecoleng.2008.12.036.

[113] M. M. Tezer and Z. B. Bundur, “Development of a 2-phase bio-additive for self-healing cement-based materials,” *Journal of the Faculty of Engineering and Architecture of Gazi University*, vol. 36, no. 3, pp. 1171–1184, 2021, doi: 10.17341/gazimmfd.695637.

[114] Z. B. Bundur, A. Amiri, Y. C. Ersan, N. Boon, and N. De Belie, “Impact of air entraining admixtures on biogenic calcium carbonate precipitation and bacterial

viability," *Cem Concr Res*, vol. 98, pp. 44–49, Aug. 2017, doi: 10.1016/j.cemconres.2017.04.005.

[115] J. Y. Wang, D. Snoeck, S. Van Vlierberghe, W. Verstraete, and N. De Belie, "Application of hydrogel encapsulated carbonate precipitating bacteria for approaching a realistic self-healing in concrete," *Constr Build Mater*, vol. 68, pp. 110–119, Oct. 2014, doi: 10.1016/j.conbuildmat.2014.06.018.

[116] S. Gupta, H. W. Kua, and H. J. Koh, "Application of biochar from food and wood waste as green admixture for cement mortar," *Science of the Total Environment*, vol. 619–620, pp. 419–435, Apr. 2018, doi: 10.1016/j.scitotenv.2017.11.044.

[117] N. Shaheen, R. A. Khushnood, S. Ud Din, and A. Khalid, "Influence of bio-immobilized lime stone powder on self-healing behaviour of cementitious composites," in *IOP Conference Series: Materials Science and Engineering*, Institute of Physics Publishing, Nov. 2018. doi: 10.1088/1757-899X/431/6/062002.

[118] J. Y. Wang, N. De Belie, and W. Verstraete, "Diatomaceous earth as a protective vehicle for bacteria applied for self-healing concrete," *J Ind Microbiol Biotechnol*, vol. 39, no. 4, pp. 567–577, Apr. 2012, doi: 10.1007/s10295-011-1037-1.

[119] J. Zhang *et al.*, "Immobilizing bacteria in expanded perlite for the crack self-healing in concrete," *Constr Build Mater*, vol. 148, pp. 610–617, Sep. 2017, doi: 10.1016/j.conbuildmat.2017.05.021.

[120] H. W. Kua, S. Gupta, A. N. Aday, and W. V. Srubar, "Biochar-immobilized bacteria and superabsorbent polymers enable self-healing of fiber-reinforced concrete after multiple damage cycles," *Cem Concr Compos*, vol. 100, pp. 35–52, Jul. 2019, doi: 10.1016/j.cemconcomp.2019.03.017.

[121] J. Wang, A. Mignon, G. Trenson, S. Van Vlierberghe, N. Boon, and N. De Belie, "A chitosan based pH-responsive hydrogel for encapsulation of bacteria for self-sealing concrete," *Cem Concr Compos*, vol. 93, pp. 309–322, Oct. 2018, doi: 10.1016/j.cemconcomp.2018.08.007.

[122] J. Y. Wang, N. De Belie, and W. Verstraete, "Diatomaceous earth as a protective vehicle for bacteria applied for self-healing concrete," *J Ind Microbiol Biotechnol*, vol. 39, no. 4, pp. 567–577, Apr. 2012, doi: 10.1007/s10295-011-1037-1.

[123] J. Xu and X. Wang, “Self-healing of concrete cracks by use of bacteria-containing low alkali cementitious material,” *Constr Build Mater*, vol. 167, pp. 1–14, Apr. 2018, doi: 10.1016/j.conbuildmat.2018.02.020.

[124] C. Liu, X. Xu, Z. Lv, and L. Xing, “Self-healing of concrete cracks by immobilizing microorganisms in recycled aggregate,” *Journal of Advanced Concrete Technology*, vol. 18, no. 4, pp. 168–178, Apr. 2020, doi: 10.3151/jact.18.168.

[125] H. Chen, C. Qian, and H. Huang, “Self-healing cementitious materials based on bacteria and nutrients immobilized respectively,” *Constr Build Mater*, vol. 126, pp. 297–303, Nov. 2016, doi: 10.1016/j.conbuildmat.2016.09.023.

[126] C. Qian, H. Chen, L. Ren, and M. Luo, “Self-healing of early age cracks in cement-based materials by mineralization of carbonic anhydrase microorganism,” *Front Microbiol*, vol. 6, no. NOV, 2015, doi: 10.3389/fmicb.2015.01225.

[127] W. Khaliq and M. B. Ehsan, “Crack healing in concrete using various bio influenced self-healing techniques,” *Constr Build Mater*, vol. 102, pp. 349–357, Jan. 2016, doi: 10.1016/j.conbuildmat.2015.11.006.

[128] R. A. Khushnood, Z. A. Qureshi, N. Shaheen, and S. Ali, “Bio-mineralized self-healing recycled aggregate concrete for sustainable infrastructure,” *Science of the Total Environment*, vol. 703, Feb. 2020, doi: 10.1016/j.scitotenv.2019.135007.

[129] S. Mondal and A. (Dey) Ghosh, “Investigation into the optimal bacterial concentration for compressive strength enhancement of microbial concrete,” *Constr Build Mater*, vol. 183, pp. 202–214, Sep. 2018, doi: 10.1016/j.conbuildmat.2018.06.176.

[130] S. Mondal, P. Das, P. Datta, and A. (Dey) Ghosh, “Deinococcus radiodurans: A novel bacterium for crack remediation of concrete with special applicability to low-temperature conditions,” *Cem Concr Compos*, vol. 108, Apr. 2020, doi: 10.1016/j.cemconcomp.2020.103523.

[131] Zhang, Weng, Ding, and Qian, “Use of Genetically Modified Bacteria to Repair Cracks in Concrete,” *Materials*, vol. 12, no. 23, p. 3912, Nov. 2019, doi: 10.3390/ma12233912.

[132] K. Chetty *et al.*, “Self-healing bioconcrete based on non-axenic granules: A potential solution for concrete wastewater infrastructure,” *Journal of Water Process Engineering*, vol. 42. Elsevier Ltd, Aug. 01, 2021. doi: 10.1016/j.jwpe.2021.102139.

[133] V. Cappellesso *et al.*, “A review of the efficiency of self-healing concrete technologies for durable and sustainable concrete under realistic conditions,” *International Materials Reviews*, 2023, doi: 10.1080/09506608.2022.2145747.

[134] “Bacteria-based self-healing concrete,” 2011.

[135] H. F. Li, Q. Q. Yu, K. Zhang, X. Y. Wang, Y. Liu, and G. Z. Zhang, “Effect of types of curing environments on the self-healing capacity of mortars incorporating crystalline admixture,” *Case Studies in Construction Materials*, vol. 18, Jul. 2023, doi: 10.1016/j.cscm.2022.e01713.

[136] “RM4L2020 Conference Proceedings - Online Version”.

[137] D. Palin, V. Wiktor, and H. M. Jonkers, “A bacteria-based self-healing cementitious composite for application in low-temperature marine environments,” *Biomimetics*, vol. 2, no. 3, Sep. 2017, doi: 10.3390/biomimetics2030013.

[138] Y. Zhang, R. Wang, and Z. Ding, “Influence of Crystalline Admixtures and Their Synergetic Combinations with Other Constituents on Autonomous Healing in Cracked Concrete—A Review,” *Materials*, vol. 15, no. 2. MDPI, Jan. 01, 2022. doi: 10.3390/ma15020440.

[139] D. Palin, V. Wiktor, and H. M. Jonkers, “Autogenous healing of marine exposed concrete: Characterization and quantification through visual crack closure,” *Cem Concr Res*, vol. 73, pp. 17–24, 2015, doi: 10.1016/j.cemconres.2015.02.021.

[140] H. Liu *et al.*, “Effects of external multi-ions and wet-dry cycles in a marine environment on autogenous self-healing of cracks in cement paste,” *Cem Concr Res*, vol. 120, pp. 198–206, Jun. 2019, doi: 10.1016/j.cemconres.2019.03.014.

[141] D. Palin, H. M. Jonkers, and V. Wiktor, “Autogenous healing of sea-water exposed mortar: Quantification through a simple and rapid permeability test,” *Cem Concr Res*, vol. 84, pp. 1–7, Jun. 2016, doi: 10.1016/j.cemconres.2016.02.011.

[142] V. Cappellesso, T. Van Mullem, and K. Van Tittelboom, “Self-healing bacterial concrete exposed to freezing and thawing associated with chlorides Sulfuric acid

corrosion in sewers View project Self-healing cracks in cementitious materials View project", doi: 10.5281/zenodo.6324948.

[143] M. Maes, D. Snoeck, and N. De Belie, "Chloride penetration in cracked mortar and the influence of autogenous crack healing," *Constr Build Mater*, vol. 115, pp. 114–124, Jul. 2016, doi: 10.1016/j.conbuildmat.2016.03.180.

[144] C. C. Hung and H. H. Hung, "Potential of sodium sulfate solution for promoting the crack-healing performance for strain-hardening cementitious composites," *Cem Concr Compos*, vol. 106, Feb. 2020, doi: 10.1016/j.cemconcomp.2019.103461.

[145] H. Liu, Q. Zhang, C. Gu, H. Su, and V. Li, "Self-healing of microcracks in Engineered Cementitious Composites under sulfate and chloride environment," *Constr Build Mater*, vol. 153, pp. 948–956, Oct. 2017, doi: 10.1016/j.conbuildmat.2017.07.126.

[146] C. Xue, W. Li, Z. Luo, K. Wang, and A. Castel, "Effect of chloride ingress on self-healing recovery of smart cementitious composite incorporating crystalline admixture and MgO expansive agent," *Cem Concr Res*, vol. 139, Jan. 2021, doi: 10.1016/j.cemconres.2020.106252.

[147] Y. Qin, Q. Wang, D. Xu, and W. Chen, "Mechanical behavior and healing efficiency of microcapsule-based cemented coral sand under various water environments," *Materials*, vol. 14, no. 19, Oct. 2021, doi: 10.3390/ma14195571.

[148] K. Chetty *et al.*, "Self-healing bioconcrete based on non-axenic granules: A potential solution for concrete wastewater infrastructure," *Journal of Water Process Engineering*, vol. 42. Elsevier Ltd, Aug. 01, 2021. doi: 10.1016/j.jwpe.2021.102139.

[149] D. de la Broise *et al.*, "Scale-Up to Pilot of a Non-Axenic Culture of Thraustochytrids Using Digestate from Methanization as Nitrogen Source," *Mar Drugs*, vol. 20, no. 8, Aug. 2022, doi: 10.3390/md20080499.

[150] Y. C. Ersan, "Overlooked Strategies in Exploitation of Microorganisms in the Field of Building Materials," 2019, pp. 19–45. doi: 10.1007/978-981-13-0149-0_2.

[151] M. Sonmez and Y. C. Ersan, “Production of concrete compatible biogranules for self-healing concrete applications,” *MATEC Web of Conferences*, vol. 289, p. 01002, 2019, doi: 10.1051/matecconf/201928901002.

[152] Y. Tang and J. Xu, “Application of microbial precipitation in self-healing concrete: A review on the protection strategies for bacteria,” *Construction and Building Materials*, vol. 306. Elsevier Ltd, Nov. 01, 2021. doi: 10.1016/j.conbuildmat.2021.124950.

[153] W. Tang, O. Kardani, and H. Cui, “Robust evaluation of self-healing efficiency in cementitious materials - A review,” *Construction and Building Materials*, vol. 81. Elsevier Ltd, pp. 233–247, Apr. 15, 2015. doi: 10.1016/j.conbuildmat.2015.02.054.

[154] D. Snoeck and N. De Belie, “Mechanical and self-healing properties of cementitious composites reinforced with flax and cottonised flax, and compared with polyvinyl alcohol fibres,” *Biosyst Eng*, vol. 111, no. 4, pp. 325–335, 2012, doi: 10.1016/j.biosystemseng.2011.12.005.

[155] K. Van Tittelboom, N. De Belie, W. De Muynck, and W. Verstraete, “Use of bacteria to repair cracks in concrete,” *Cem Concr Res*, vol. 40, no. 1, pp. 157–166, Jan. 2010, doi: 10.1016/j.cemconres.2009.08.025.

[156] K. Van Tittelboom, E. Gruyaert, H. Rahier, and N. De Belie, “Influence of mix composition on the extent of autogenous crack healing by continued hydration or calcium carbonate formation,” *Constr Build Mater*, vol. 37, pp. 349–359, Dec. 2012, doi: 10.1016/j.conbuildmat.2012.07.026.

[157] V. Li, “Tensile strain-hardening behavior or polyvinyl alcohol engineered cementitious composite (PVA-ECC),” 2001. [Online]. Available: https://www.researchgate.net/publication/279888212

[158] V. Li and V. C. Li, “On Engineered Cementitious Composites (ECC) A Review of the Material and Its Applications,” 2003. [Online]. Available: https://www.researchgate.net/publication/237783722

[159] M. Koda, H. Mihashi, T. Nishiwaki, and T. Kikuta, “Experimental study on self-healing capability of frcc using synthetic fibers,” *Journal of Structural and*

Construction Engineering, vol. 76, no. 667, pp. 1547–1552, Sep. 2011, doi: 10.3130/aijs.76.1547.

[160] D. Homma, H. Mihashi, and T. Nishiwaki, "Self-healing capability of fibre reinforced cementitious composites," *Journal of Advanced Concrete Technology*, vol. 7, no. 2, pp. 217–228, 2009, doi: 10.3151/jact.7.217.

[161] V. C. Li, Y. M. Lim, and Y.-W. Chan, "Feasibility study of a passive smart self-healing cementitious composite."

[162] A. Talaiekhozani, A. Keyvanfar, A. Shafaghat, and R. Andalib, "A Review of Self-healing Concrete Research Development Removal of pollutants from air by using biological processes View project Simulation on Lighting Energy Consumption for Potential Energy Saving at Rest and Service Area Malaysia View project," 2014. [Online]. Available: http://www.jett.dormaj.com

[163] H. Mihashi, Y. Kaneko, T. Nishiwaki, and K. Otsuka, "Fundamental study on development of intelligent concrete characterized by self-healing capability for strength," *Transactions of the Japan Concrete Institute*, vol. 22, pp. 441–450, 2000, doi: 10.3151/crt1990.11.2_21.

[164] K. Van Tittelboom, N. De Belie, D. Van Loo, and P. Jacobs, "Self-healing efficiency of cementitious materials containing tubular capsules filled with healing agent," *Cem Concr Compos*, vol. 33, no. 4, pp. 497–505, Apr. 2011, doi: 10.1016/j.cemconcomp.2011.01.004.

[165] W. Zhong and W. Yao, "Influence of damage degree on self-healing of concrete," *Constr Build Mater*, vol. 22, no. 6, pp. 1137–1142, Jun. 2008, doi: 10.1016/j.conbuildmat.2007.02.006.

[166] K. Van Tittelboom, D. Snoeck, P. Vontobel, F. H. Wittmann, and N. De Belie, "Use of neutron radiography and tomography to visualize the autonomous crack sealing efficiency in cementitious materials," *Materials and Structures/Materiaux et Constructions*, vol. 46, no. 1–2, pp. 105–121, Jan. 2013, doi: 10.1617/s11527-012-9887-1.

[167] D. G. Bekas, K. Tsirka, D. Baltzis, and A. S. Paipetis, "Self-healing materials: A review of advances in materials, evaluation, characterization and monitoring

techniques," *Composites Part B: Engineering*, vol. 87. Elsevier Ltd, pp. 92–119, Feb. 15, 2016. doi: 10.1016/j.compositesb.2015.09.057.

[168] D. Ramachandran, F. Liu, and M. W. Urban, "Self-repairable copolymers that change color," *RSC Adv*, vol. 2, no. 1, pp. 135–143, Jan. 2012, doi: 10.1039/c1ra00137j.

[169] D. M. Chipara, M. Flores, A. Perez, N. Puente, K. Lozano, and M. Chipara, "Adding autonomic healing capabilities to polyethylene oxide," *Advances in Polymer Technology*, vol. 32, no. SUPPL.1, Mar. 2013, doi: 10.1002/adv.21296.

[170] Y. C. Yuan *et al.*, "Self-healing of low-velocity impact damage in glass fabric/epoxy composites using an epoxy-mercaptan healing agent," *Smart Mater Struct*, vol. 20, no. 1, Jan. 2011, doi: 10.1088/0964-1726/20/1/015024.

[171] J. Ling, M. Z. Rong, and M. Q. Zhang, "Electronic Supplementary Information Coumarin Imparts Repeated Photochemical Remendability to Polyurethane," 2011.

[172] T.-H. Ahn and T. Kishi, "Crack Self-healing Behavior of Cementitious Composites Incorporating Various Mineral Admixtures," 2010.

[173] D. Homma, H. Mihashi, and T. Nishiwaki, "Self-healing capability of fibre reinforced cementitious composites," *Journal of Advanced Concrete Technology*, vol. 7, no. 2, pp. 217–228, 2009, doi: 10.3151/jact.7.217.

[174] "Standard Test Method for Water Permeability of Concrete."

[175] K. Sisomphon, O. Copuroglu, and A. Fraaij, "Application of encapsulated lightweight aggregate impregnated with sodium monofluorophosphate as a self-healing agent in blast furnace slag mortar," 2011.

[176] T. Nishiwaki, H. Mihashi, B. K. Jang, and K. Miura, "Development of self-healing system for concrete with selective heating around crack," *Journal of Advanced Concrete Technology*, vol. 4, no. 2, pp. 267–275, 2006, doi: 10.3151/jact.4.267.

[177] Michelle, "Self-healing concrete with a microencapsulated healing agent," 2011. [Online]. Available: https://www.researchgate.net/publication/265943003

[178] T. Diep and P. Thao, “QUASI-BRITTLE SELF-HEALING MATERIALS: NUMERICAL MODELLING AND APPLICATIONS IN CIVIL ENGINEERING,” 2011.

[179] C. Dry, “Improvement in Reinforcing Bond Strength in Reinforced Concrete with Self Repairing Chemical Adhesives.” [Online]. Available: http://spiedl.org/terms

[180] K. Van Tittelboom, N. De Belie, F. Lehmann, and C. U. Grosse, “Acoustic emission analysis for the quantification of autonomous crack healing in concrete,” *Constr Build Mater*, vol. 28, no. 1, pp. 333–341, Mar. 2012, doi: 10.1016/j.conbuildmat.2011.08.079.

[181] “INVESTIGATION OF PERFORMANCE PROPERTIES OF CEMENT-BINDER SYSTEMS WITH MICROBIAL SELF-HEALING ABILITY MİKROBİYAL KENDİLİĞİNDEN İYİLEŞME KABİLİYETİNE SAHİP ÇİMENTO BAĞLAYICILI SİSTEMLERİN PERFORMANS ÖZELLİKLERİNİN İNCELENMESİ.”

[182] K. Şekercioğlu, “ABSTRACT INVESTIGATION OF NICKEL RECOVERY BY BIOGRANULES TAILORED FOR METAL RECOVERY THROUGH BIOMINERALIZATION.”

[183] M. Sonmez and Y. Ç. Erşan, “Production and compatibility assessment of denitrifying biogranules tailored for self-healing concrete applications,” *Cem Concr Compos*, vol. 126, Feb. 2022, doi: 10.1016/j.cemconcomp.2021.104344.

[184] Y. Ç. ERŞAN, “Self-Healing Performance of Biogranule Containing Microbial Self-Healing Concrete Under Intermittent Wet/Dry Cycles,” *Politeknik Dergisi*, vol. 24, no. 1, pp. 323–332, Mar. 2021, doi: 10.2339/politeknik.742210.

[185] J. Li, L. Bin Ding, A. Cai, G. X. Huang, and H. Horn, “Aerobic sludge granulation in a full-scale sequencing batch reactor,” *Biomed Res Int*, vol. 2014, 2014, doi: 10.1155/2014/268789.

[186] E. Mekonnen, A. Kebede, A. Nigussie, G. Kebede, and M. Tafesse, “Isolation and Characterization of Urease-Producing Soil Bacteria,” *Int J Microbiol*, vol. 2021, 2021, doi: 10.1155/2021/8888641.

[187] K. Paine, “BACTERIA-BASED SELF-HEALING OF CONCRETE: EFFECTS OF ENVIRONMENT, EXPOSURE AND CRACK SIZE.”

[188] S. S. Bang, J. K. Galinat, and V. Ramakrishnan, “Calcite precipitation induced by polyurethane-immobilized Bacillus pasteurii,” 2001. [Online]. Available: www.elsevier.com/locate/enzmictec

[189] Z. Basaran Bundur, M. J. Kirisits, and R. D. Ferron, “Biomineralized cement-based materials: Impact of inoculating vegetative bacterial cells on hydration and strength,” *Cem Concr Res*, vol. 67, pp. 237–245, 2015, doi: 10.1016/j.cemconres.2014.10.002.

[190] J. A. Aguilar-Torrejón, P. Balderas-Hernández, G. Roa-Morales, C. E. Barrera-Díaz, I. Rodríguez-Torres, and T. Torres-Blancas, “Relationship, importance, and development of analytical techniques: COD, BOD, and, TOC in water—An overview through time,” *SN Applied Sciences*, vol. 5, no. 4. Springer Nature, Apr. 01, 2023. doi: 10.1007/s42452-023-05318-7.

[191] H. Ray, D. Saetta, and T. H. Boyer, “Characterization of urea hydrolysis in fresh human urine and inhibition by chemical addition,” *Environ Sci (Camb)*, vol. 4, no. 1, pp. 87–98, Jan. 2018, doi: 10.1039/c7ew00271h.

[192] J. M. Ebeling, M. B. Timmons, and J. J. Bisogni, “Engineering analysis of the stoichiometry of photoautotrophic, autotrophic, and heterotrophic removal of ammonia-nitrogen in aquaculture systems,” *Aquaculture*, vol. 257, no. 1–4, pp. 346–358, Jun. 2006, doi: 10.1016/j.aquaculture.2006.03.019.

[193] P. Zamora *et al.*, “Ammonia recovery from urine in a scaled-up Microbial Electrolysis Cell,” *J Power Sources*, vol. 356, pp. 491–499, 2017, doi: 10.1016/j.jpowsour.2017.02.089.

[194] M. N. Yahya, H. Gökçekuş, D. Orhon, B. Keskinler, A. Karagunduz, and P. I. Omwene, “A study on the hydrolysis of urea contained in wastewater and continuous recovery of ammonia by an enzymatic membrane reactor,” *Processes*, vol. 9, no. 10, Oct. 2021, doi: 10.3390/pr9101703.

[195] “14787324_DOC040.94.10015.Oct12_N-Parameter.web (1)”.

[196] R. Baird *et al., Standard Methods for the Examination of Water and Wastewater*.

[197] M. Layer *et al.*, “Organic substrate diffusibility governs microbial community composition, nutrient removal performance and kinetics of granulation of aerobic

granular sludge," *Water Res X*, vol. 4, Aug. 2019, doi: 10.1016/j.wroa.2019.100033.

[198] R. Bao, L. Xue, X. Yan, and S. Yu, "Characteristics of nitrogen removal in aerobic granular sludge reactor at low temperature," in *Applied Mechanics and Materials*, 2013, pp. 1438–1441. doi: 10.4028/www.scientific.net/AMM.295-298.1438.

[199] F. Traina, S. F. Corsino, M. Torregrossa, and G. Viviani, "Biopolymer Recovery from Aerobic Granular Sludge and Conventional Flocculent Sludge in Treating Industrial Wastewater: Preliminary Analysis of Different Carbon Routes for Organic Carbon Utilization," *Water (Switzerland)*, vol. 15, no. 1, Jan. 2023, doi: 10.3390/w15010047.

[200] S. P. Wei *et al.*, "Flocs in disguise? High granule abundance found in continuous-flow activated sludge treatment plants," *Water Res*, vol. 179, Jul. 2020, doi: 10.1016/j.watres.2020.115865.

[201] Y. Ç. Erşan and T. H. Erguder, "The effects of aerobic/anoxic period sequence on aerobic granulation and COD/N treatment efficiency," *Bioresour Technol*, vol. 148, pp. 149–156, Nov. 2013, doi: 10.1016/j.biortech.2013.08.096.

[202] Y. Ersan, E. Gruyaert, G. Louis, C. Lors, N. De Belie, and N. Boon, "Self-protected nitrate reducing culture for intrinsic repair of concrete cracks," *Front Microbiol*, vol. 6, no. NOV, 2015, doi: 10.3389/fmicb.2015.01228.

[203] N. A. Sorkhoh, A. S. Ibrahim, M. A. Ghannoum, and S. S. Radwan, "Applied Microbiology Biotechnology High-temperature hydrocarbon degradation by Bacillus stearothermophilus from oil-polluted Kuwaiti desert," 1993.

[204] D. Jafarpour, S. M. B. Hashemi, and M. Mousavifard, "Inactivation kinetics of pathogenic bacteria in persimmon using the combination of thermosonication and formic acid," *Food Science and Technology International*, vol. 29, no. 4, pp. 383–394, Jun. 2023, doi: 10.1177/10820132221095718.

[205] C. Zhang, R. Liu, M. Chen, X. Li, Z. Zhu, and J. Yan, "Effects of independently designed and prepared self-healing granules on self-healing efficiency for cement cracks," *Constr Build Mater*, vol. 347, Sep. 2022, doi: 10.1016/j.conbuildmat.2022.128626.

[206] P. Risdanareni, L. Ma, J. Wang, and N. De Belie, “Suitable yeast extract concentration for the production of self-healing mortar with expanded clay as bacterial carrier,” *Materiales de Construccion*, vol. 72, no. 348, 2022, doi: 10.3989/mc.2022.02422.

[207] “INVESTIGATION OF PERFORMANCE PROPERTIES OF CEMENT-BINDER SYSTEMS WITH MICROBIAL SELF-HEALING ABILITY MİKROBİYAL KENDİLİĞİNDEN İYİLEŞME KABİLİYETİNE SAHİP ÇİMENTO BAĞLAYICILI SİSTEMLERİN PERFORMANS ÖZELLİKLERİNİN İNCELENMESİ.”

[208] Y. Çağatay Erşan and Y. C. Çağatay Erşan, *Microbial nitrate reduction induced autonomous self-healing in concrete. Microbial nitrate reduction induced autonomous self-healing in concrete*.

[209] J. Wang, “Self-Healing Concrete by Means of Immobilized Carbonate Precipitating Bacteria Zelfhelend beton door middel van geïmmobiliseerde carbonaatprecipiterende bacteriën,” 2012.

[210] Y. Sumra, S. Payam, and I. Zainah, “The pH of Cement-based Materials: A Review,” *Journal Wuhan University of Technology, Materials Science Edition*, vol. 35, no. 5. Wuhan Ligong Daxue, pp. 908–924, Oct. 01, 2020. doi: 10.1007/s11595-020-2337-y.

[211] M. A. Rakib, A. Hossain, M. H. Rashid, and C. Dutta, *EFFECT OF MIXING WATER pH ON CONCRETE Strengthening of Reinforced Concrete Beams View project SEISMIC ANALYSIS OF MUD HOUSE View project EFFECT OF MIXING WATER pH ON CONCRETE*. 2020. [Online]. Available: https://www.researchgate.net/publication/351811543

[212] O. Monge, M. T. Certucha Barragn, and F. J. Almendariz Tapi, “Microbial Biomass in Batch and Continuous System,” in *Biomass Now - Sustainable Growth and Use*, InTech, 2013. doi: 10.5772/55303.

[213] G. H. Rau, “Electrochemical splitting of calcium carbonate to increase solution alkalinity: Implications for mitigation of carbon dioxide and ocean acidity,” *Environ Sci Technol*, vol. 42, no. 23, pp. 8935–8940, Dec. 2008, doi: 10.1021/es800366q.

[214] S. Yang, Y. He, Y. Liu, C. Chou, P. Zhang, and D. Wang, “Effect of wastewater composition on the calcium carbonate precipitation in upflow anaerobic sludge blanket reactors,” *Frontiers of Environmental Science and Engineering in China*, vol. 4, no. 2, pp. 142–149, Jun. 2010, doi: 10.1007/s11783-010-0026-3.

[215] Y. H. Huang and T. C. Zhang, “Effects of low pH on nitrate reduction by iron powder,” *Water Res*, vol. 38, no. 11, pp. 2631–2642, 2004, doi: 10.1016/j.watres.2004.03.015.

[216] K. Addy, A. J. Gold, L. E. Christianson, M. B. David, L. A. Schipper, and N. A. Ratigan, “Denitrifying Bioreactors for Nitrate Removal: A Meta-Analysis,” *J Environ Qual*, vol. 45, no. 3, pp. 873–881, May 2016, doi: 10.2134/jeq2015.07.0399.

[217] Y. F. Lin, S. R. Jing, D. Y. Lee, Y. F. Chang, and K. C. Shih, “Nitrate removal and denitrification affected by soil characteristics in nitrate treatment wetlands,” *J Environ Sci Health A Tox Hazard Subst Environ Eng*, vol. 42, no. 4, pp. 471–479, Mar. 2007, doi: 10.1080/10934520601187690.

[218] J. Peng, T. Cao, J. He, D. Dai, and Y. Tian, “Improvement of Coral Sand With MICP Using Various Calcium Sources in Sea Water Environment,” *Front Phys*, vol. 10, Mar. 2022, doi: 10.3389/fphy.2022.825409.

[219] J. Czarnota, A. Masłoń, and M. Zdeb, “Powdered keramsite as unconventional method of AGS technology support in GSBR reactor with minimum-optimum OLR,” in *E3S Web of Conferences*, EDP Sciences, Jul. 2018. doi: 10.1051/e3sconf/20184400024.

[220] S. A. Silva, A. Val del Río, A. L. Amaral, E. C. Ferreira, M. Madalena Alves, and D. P. Mesquita, “Monitoring morphological changes from activated sludge to aerobic granular sludge under distinct organic loading rates and increasing minimal imposed sludge settling velocities through quantitative image analysis,” *Chemosphere*, vol. 286, Jan. 2022, doi: 10.1016/j.chemosphere.2021.131637.

[221] J.-F. Wang, Z.-H. An, X.-Y. Zhang, B. Angelotti, M. Brooks, and Z.-W. Wang, “Effects of Nitrate Recycle on the Sludge Densification in Plug-Flow Bioreactors Fed with Real Domestic Wastewater,” *Processes*, vol. 11, no. 7, p. 1876, Jun. 2023, doi: 10.3390/pr11071876.

[222] J. Wang, “Self-Healing Concrete by Means of Immobilized Carbonate Precipitating Bacteria Zelfhelend beton door middel van geïmmobiliseerde carbonaatprecipiterende bacteriën,” 2012.

[223] M. B. E. Khan, L. Shen, and D. Dias-da-Costa, “Self-healing behaviour of bio-concrete in submerged and tidal marine environments,” *Constr Build Mater*, vol. 277, Mar. 2021, doi: 10.1016/j.conbuildmat.2021.122332.

[224] D. Palin, H. M. Jonkers, and V. Wiktor, “Autogenous healing of sea-water exposed mortar: Quantification through a simple and rapid permeability test,” *Cem Concr Res*, vol. 84, pp. 1–7, Jun. 2016, doi: 10.1016/j.cemconres.2016.02.011.

[225] C. Xue, “Performance and mechanisms of stimulated self-healing in cement-based composites exposed to saline environments,” *Cem Concr Compos*, vol. 129, May 2022, doi: 10.1016/j.cemconcomp.2022.104470.

[226] G. Anglani, J. M. Tulliani, and P. Antonaci, “Behaviour of pre-cracked self-healing cementitious materials under static and cyclic loading,” *Materials*, vol. 13, no. 5, Mar. 2020, doi: 10.3390/ma13051149.

[227] R. P. Borg, E. Cuenca, E. M. Gastaldo Brac, and L. Ferrara, “Crack sealing capacity in chloride rich environments of mortars containing different cement substitutes and crystalline admixtures.”

ANNEX

ANNEX 1 – Reactor Performance Before Take Over.

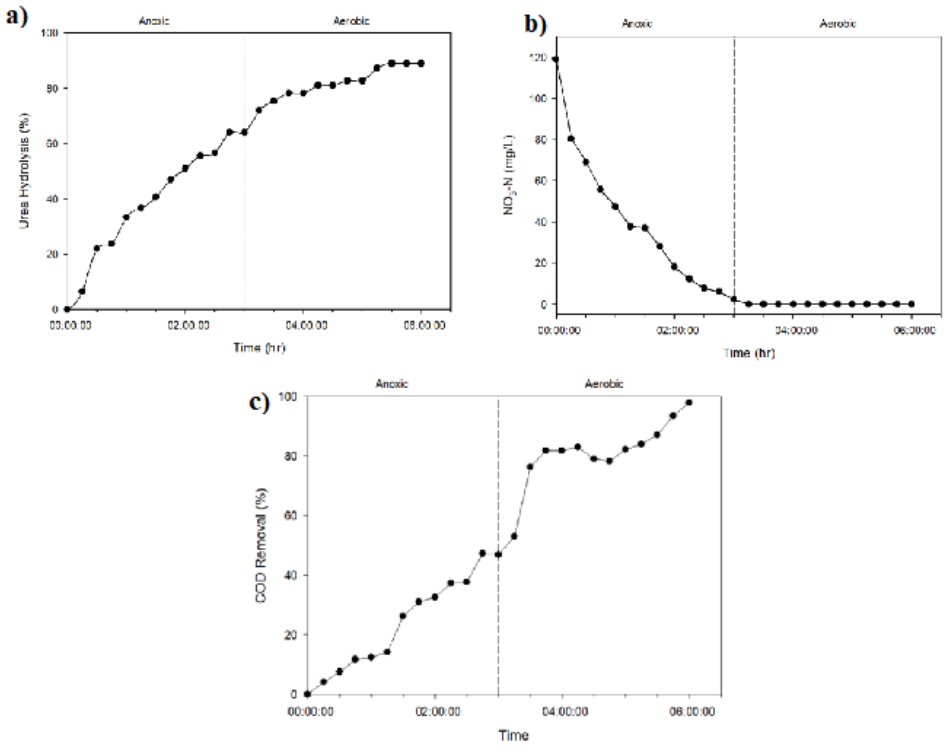

Figure Kinetic analysis results of a)Urea hydrolysis performance ;b) NO_3-N reduction; c)Oxidation of organic substrate in one cycle of pre-reactor operation

ANNEX 2 - Conference Papers Derived from Thesis

Ozbay, B., Erşan, Y.Ç. 2022. A novel non-axenic granulated culture based microbial self-healing concrete, 6th Eurasia Waste Management Symposium, 24-26 Oct, Istanbul, Turkey